Skeletal muscle pericytes as signal mediators in the vessel wall - Isolation and functional characterization in a hamster model

Aus dem Institut für Chirurgische Forschung im
Walter-Brendel-Zentrum für experimentelle Medizin (WBex)
der Ludwig-Maximilians-Universität München
Vorstand: Prof. Dr. med. Ulrich Pohl

Dissertation zur Erlangung des Doktorgrades der Humanmedizin
an der Medizinischen Fakultät der Ludwig-Maximilians-Universität, München

vorgelegt von
Stefan Wallner
aus München

2012

Mit Genehmigung der Medizinischen Fakultät
der Universität München

Berichterstatter:	Prof. Dr. med. Ulrich Pohl
Mitberichterstatter:	Priv. Doz. Dr. Sabine Krause Prof. Dr. Alexander Baethmann
Mitbetreuung durch die promovierte Mitarbeiterin:	Dr. rer. nat. Kristin Pogoda
Dekan:	Prof. Dr. med. Dr. h.c. M. Reiser, FACR, FRCR
Tag der mündlichen Prüfung:	20.12.2012

Table of Contents

I Introduction

1. Regulation of blood flow in the vascular system

The human vascular system represents a distinct organ that by containing blood and regulating its flow serves a wide range of functions: transport of blood gases and nutrients, elimination of metabolic products, pH regulation and immune function are just some examples [1]. In humans it functions as a closed system. Although the basic anatomy of this system has already been known in ancient Egypt and India [2], only in the 16th and 17th century some of the underlying mechanisms were uncovered [3].

To fulfill its multiple roles every single part is optimized for its specific function: While arteries serve as high pressure conductors away from the heart, veins conduct blood back to the heart [4]. Arteries, depending on their size, function as a conduit or resistance vessel, the latter regulating vascular diameter and therefore blood flow according to current metabolic needs (Figure I-1) [5]. Capillaries have very thin walls consisting of only a single layer of endothelial cells adapted specifically to facilitate free diffusion of oxygen and other metabolites [4].

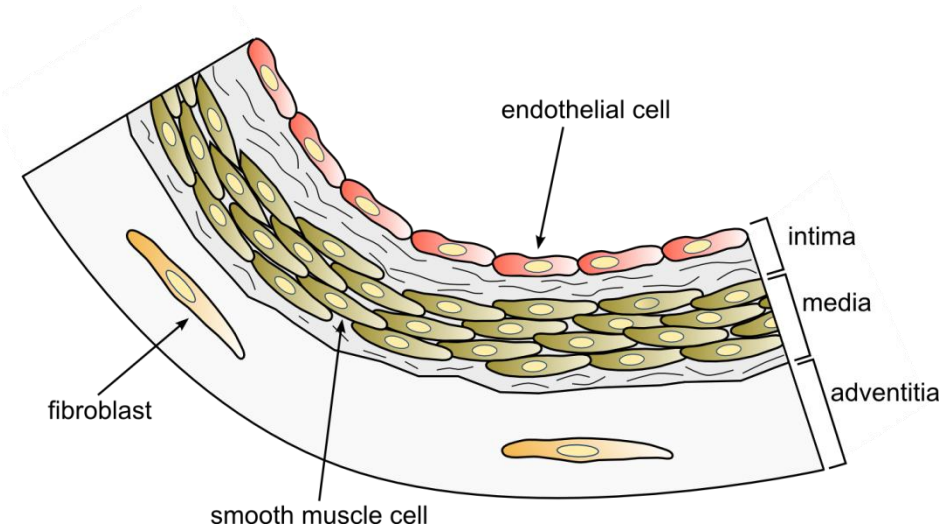

Figure I-1: Vessel wall of a small, muscular artery: The arterial wall in principle consists of three distinct layers with distinct predominating cells types. The Tunica intima is formed by a single layer of endothelial cells that function as an adaptive barrier between the blood stream and the underlying tissue. The composition of the subjacent Tunica media depends on the size of the artery. While larger vessel walls comprise a higher content of elastic fibers, smaller arteries and arterioles such as the one depicted contain mainly smooth muscle cells by which they are able regulate vascular tone by contraction or relaxation. The third layer, called Tunica adventitia is made mainly of connective tissue that supports the vessel in the surrounding tissue. (image redrawn and modified based on [1])

Fundamentally three distinct types of cells are responsible to ensure proper micro-vascular function: endothelial cells as the contact layer to the blood compartment, smooth muscle cells

[1] http://upload.wikimedia.org/wikipedia/commons/0/05/Anatomy_artery.png; Original image from Stijn A.I. Ghesquiere (www.applesnail.net) under license CC BY-NC-SA, retrieved on 10.08.2010

as regulators of vascular tone and pericytes serving as multipurpose cells coordinating and save-guarding vascular function [1].

1.1. Smooth muscle cells regulate vascular diameter

Smooth muscle cells in the wall of small arteries and in particular, arterioles represent the effector cells regulating local and, as a whole, global blood flow in every organ. Their main task is to assure an adequate distribution of nutrients and oxygen adapted to the current metabolic need of the individual tissue [6, 7] while maintaining an adequate arterial blood pressure.

Three major regulatory mechanisms exist that are differentially active in different regions of resistance arteries. Metabolic regulation adapts the tissue blood supply to the current metabolic needs by vasodilation of the supporting small arteries if products related to tissue activity accumulate [8]. Autoregulation on the other hand aims at keeping blood flow and capillary pressure stable under varying blood pressures [9, 10]. The underlying Bayliss effect has been shown among others to be mediated by diacylglycerol-sensitive canonical transient receptor potential (TRPC) subunits that lead to a depolarization of the cellular membrane upon increases of blood pressure and vice versa [11-14]. Finally, the endothelium exerts vital effects on vascular smooth muscle cells. It regulates vascular tone via the release of signaling molecules such as NO, prostacyclin and endothelin, but also by direct signal exchange via myo-endothelial junctions [15-17]. Under disease conditions some of these mechanisms become also activated by immune cells which may then lead to a stronger perfusion of the inflamed tissue [4, 18].

1.2. Endothelium is involved in blood flow regulation

The endothelium forms a thin layer lining the interior of blood vessels in the entire circulatory system. It has a pivotal function in vascular signaling: on the one hand it acts as a sensor. E.g. it is responsive to shear stress or vasoactive blood constituents such as histamine which bind to endothelial receptors. In either case endothelial mediators are released and diffuse to the underlying smooth muscle cells [15, 17].

Among these vaso-active endothelial mediators are nitric oxide (NO), lipid mediators such as prostaglandins and the endothelium derived hyperpolarizing factor (EDHF). These substances regulate vascular tone and therefore blood flow to the affected organ [15-17]. Especially by EDHF signaling, it serves a very important function in the coordination of blood flow regulation in microvascular networks [19-21].

2. Gap junctional coupling in coordinating vascular responses

2.1. Connexins connect the cytoplasm of two adjacent cells

Connexins comprise a family of transmembrane proteins in vertebrates. They are able to form so called gap junction channels connecting the cytoplasm of two adjacent cells. For this purpose six connexin proteins in a circular arrangement are necessary to form a single connexon and in turn two connexons (hemi-channels) form a functional gap junction pore as depicted in Figure I-2 [22-24].

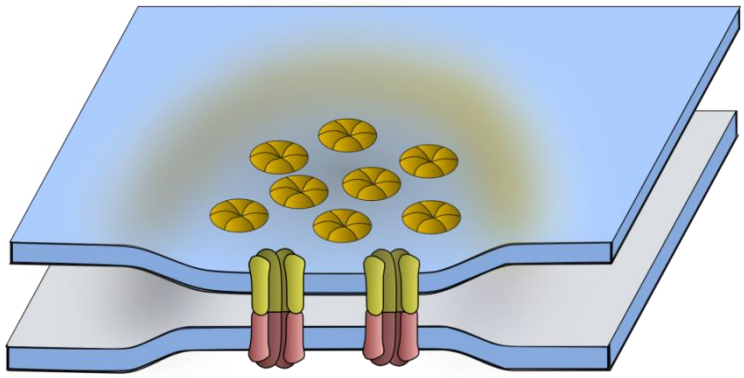

Figure I-2: Schematic representation of a section through gap junction channels in the membranes of two adjacent cells. Individual connexons in the membrane bilayer are composed of six connexin proteins each. Always two channels in adjacent cells form one functional gap junction channel (image redrawn based on a part of [2])

Cellular coupling represents a well-controlled process. Depending on their connexin expression pattern neighboring cells that both express connexins can be coupled but this is not imperative. The type of connexin expressed also has great influence on the permeability and selectivity of the gap junction channel. In humans, 21 different connexins have been discovered. Connexin proteins are commonly named by the letters “Cx” followed by their respective molecular mass in kilo-Dalton (kDa) [25]. They differ in their characteristics determining channel permeability, but also in the length and amino acid sequence of their carboxyl tail whereas the channel building N-terminal part has highly conserved regions. The C-terminal tail has many sites for posttranslational modifications and binding sites for protein interaction partners and is therefore also involved in channel independent intracellular signaling, most likely functioning as an adapter protein [26-28].

Connexins are essential in a wide spectrum of physiological processes in cardiovascular physiology. In the heart, electrical coupling of cardiomyocytes via gap junction channels formed mainly by connexin 43 (Cx43) ensures propagation of action potentials [29]. In the vascular system, the expression of connexins Cx37, Cx40, Cx43 and Cx45 has been reported [30, 31]. Interestingly, the expression of these four gap junction proteins is non-redundant,

[2] http://upload.wikimedia.org/wikipedia/commons/c/c6/Connexon_and_connexin_structure.svg; Original image is in the public domain, retrieved on 13.05.2009

meaning one connexin cannot completely take over the function of another connexin. While the expression of Cx45 seems to be restricted to smooth muscle cells [32, 33], Cx37 and Cx40 are expressed primarily in endothelial cells [34, 35]. Cx43 as one of the most abundantly expressed connexins in humans can be found in both cells types [34, 36, 37]. Depending on the connexin proteins forming the pore, gap junctions allow not only the flow of ions as an electrical current but also the exchange of small signaling molecules such as IP_3 [38-40] up to a molecular weight of around 1 kDa [41-44]. Recently also the passage of the significantly larger molecule Calmodulin with 17 kDa has been reported [45].

2.2. **The vessel wall forms a functional syncytium**

2.2.1. Coordinated regulation of blood flow

Blood flow to organs and tissues in the human body is not steady but constantly adapting to changing metabolic and functional demands. Therefore, in a wide network of resistance arteries and capillaries all vascular cells have to act together in a coordinated manner to allow proper vascular function. Local changes in vessel diameter are only of limited effect since upstream segments contribute significantly to the total flow resistance in a given section of the vascular system. To this end vascular cells, especially endothelial cells, are coupled to neighboring cells, forming a functional syncytium with the aim of concerted vascular activity first described by Duling [46] in 1970. It has been found to be related to membrane potential [47, 48] and even acts over distances of more than 2mm [19]. Potentially on such a long journey the signal is even regenerated [49, 50].

Experimentally a local application of noradrenalin near capillaries induces a bidirectional conduction of vasoconstriction to the adjacent arterioles and venules [51]. In the same way local stimulation with endothelium derived hyperpolarizing factor (EDHF) stimulating agents such as acetylcholine induces a local endothelial hyperpolarization that is conducted further along the vessel wall [52]. The primary means of conduction is gap junctional coupling between endothelial cells. This mechanism leads in the case of EDHF to a simultaneous dilation of upstream arterioles [48]. Interestingly, dilations propagate over longer distances than constrictions. In the end this process leads to an “integrated response” of large feeder arteries and their distal daughter vessels [19, 53, 54], in which the overall conductivity of the vascular bed has been shown to play a vital role [54, 55].

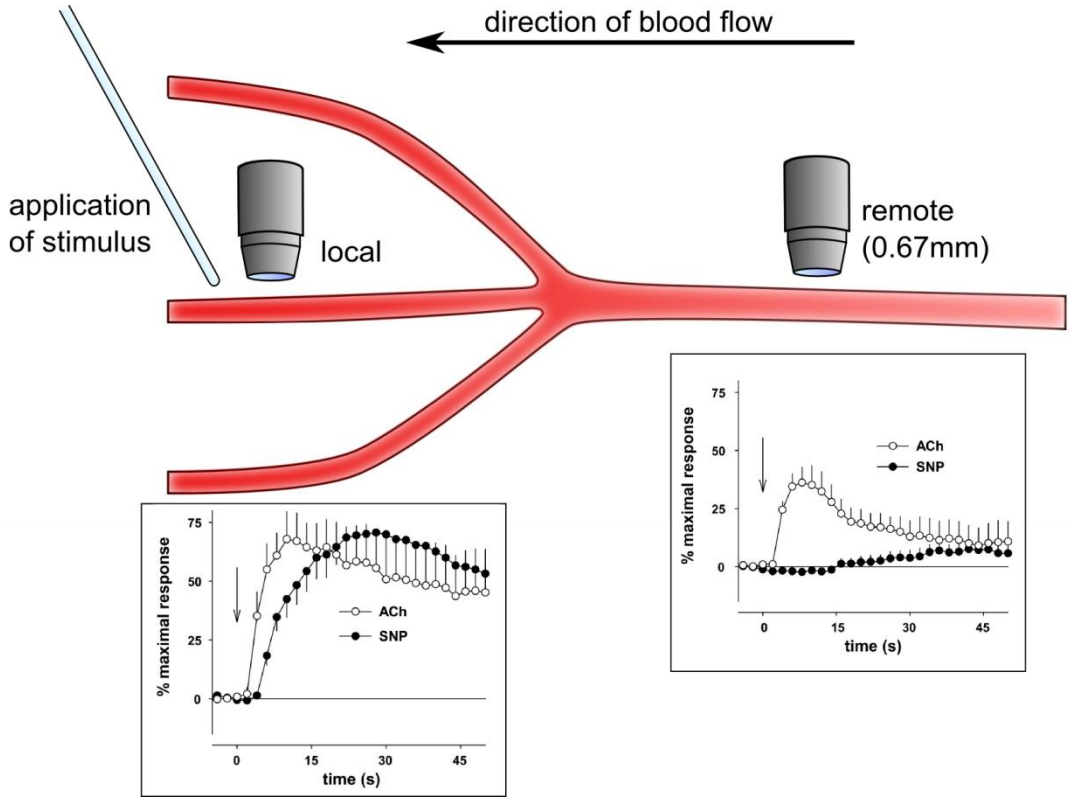

Figure I-3: Principle of conducted dilation. Local stimulation of an arteriole by application of the EDHF stimulator acetylcholine (ACh) induces a vasodilation in the vessel (left). This signal is relayed and in turn leads to a remote vasodilation in the supplying vessels (right). In contrast the local dilation by SNP which does not induce hyperpolarization is not transduced upstream. Inserted data images taken from: [20]

2.2.2. Regulation of vessel development

Proper coupling of cells in the vascular wall could be shown to be essential for proper formation and maintenance of blood vessels. In this respect, mice deficient for connexin 45 exhibited severe defects in the maturation of their vascular system [56]. Although in these animals vasculogenesis seemed to be normal, they showed an impairment of transformation into mature vessels. In coronary arteries deficiency in connexin 43 leads to malformations, while loss of connexins 37 and 40 induced cavernous hemangioma formation [57]. Functionally endothelial cells in the vessel wall signals seem to require gap junctional communication for the activation of TGF-β and terminal cell differentiation of pericytes as well as endothelial cells [58].

3. Pericytes serve as multi-purpose cells in the vessel wall

Pericytes represent a cell population in the wall of small blood vessels that is difficult to characterize. Since their initial description in 1873 by Rouget [59] only limited progress has been made for pericytes. They were further characterized by Zimmermann in 1923 [60] and subsequently referred to as "*Zimmermann's cells*". After the first electron microscopy studies had been published in 1956 [61] Kuwabara independently re-discovered pericytes as so called "intramural cells" in 1961. Finally in 1966 Ashton and Olivera proposed that these two entities might essentially be the same cells [62].

Although some amount of data has been collected on pericytes since their first discovery, only very little is known on skeletal muscle pericytes. One reason is the fact that pericytes are a heterogeneous group of cells that exhibit major differences depending on the tissue they have been isolated from [63, 64]. This is even complicated more by the fact that apparently terminal pericyte differentiation can encompass a whole spectrum of endothelial cell, SMC and fibroblast markers and characteristics that make the status of these cells rather points on a continuum than a clearly distinguishable cell population [65-67]. Therefore phenotype, expression of surface markers and respective function remain a subject of lively debate in the literature.

The great variability of pericyte phenotypes has been summarized by Shepro already in 1993 as follows: They "regulate endothelial proliferation and differentiation; contract in manners that either exacerbate or stem endothelial cell junctional inflammatory leakage; function as a progenitor cell; synthesize and secrete a wide variety of vaso-active, autoregulating agonists; synthesize and release structural constituents of the basement membrane and extracellular matrix. Pericytes are also involved in specific microvascular diseases." [68]

3.1. Morphology and localization

Pericytes are perivascular cells that can be found close to capillaries, pre-capillary arterioles, post-capillary venules and collecting venules [69]. They possess a cell body with a prominent nucleus and extend long cytoplasmic processes that encircle the vessel wall.[70] A single pericyte covers a large vascular area comprising multiple endothelial cells. Interestingly, pericyte numbers vary greatly depending on the tissue. Relatively low numbers of pericytes are found in skeletal muscle with one pericyte per every 100 endothelial cells compared to for example the retina with a one on one ratio [68, 69].

Pericytes are equally heterogeneous in their protein expression pattern as they are in their phenotypes [63-67]. Smooth muscle actin (αSMA), desmin, the proteoglycan NG2, platelet-derived growth factor receptor β (PDGFR-β) and pAPN/CD13 (aminopeptidase N) have been used and validated in previous studies as pericyte markers [63, 66, 69, 71-75]. Unfortunately, none of those molecules is expressed exclusively in pericytes and could therefore serve as an exclusive marker for the detection of pericytes in tissue sections or flow-cytometry. One of the reasons for this heterogeneity lies in the ability of pericytes to transdifferentiate into other cell types such as smooth muscle cells and fibroblasts [71]. Pericytes at any given tissue and vascular bed might therefore just represent a specific point in a continuum of pericytic phenotypes. Another factor in pericyte heterogeneity is the formation of mature pericytes and perivascular macrophages through cell fusion of bone marrow-derived cells (BMDCs) with yet unknown partner cells leading to multiple slightly different phenotypes [76].

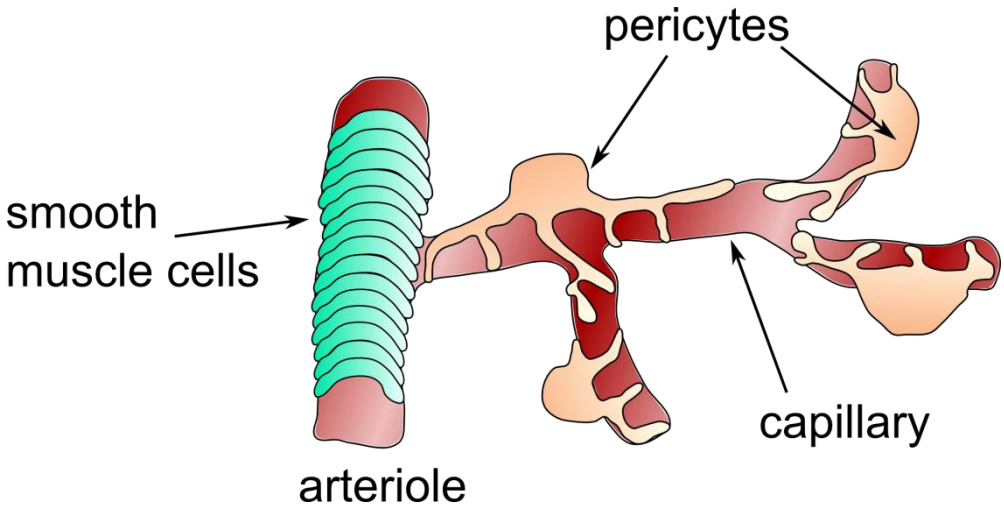

Figure I-4: Schematic representation of the localization of pericytes in the vascular system. In situ pericytes are large, flat cells with far reaching protrusions. They mainly reside around small vessels in the microcirculation, where they may provide mechanical stabilization for the vessel. Image modified after: [77]

3.2. **Physiological functions**

Pericytes reside at the interface between the endothelium and the underlying smooth muscle cells and connective tissue. They therefore are at the crossroads to actively regulate and coordinate processes such as angiogenesis and vascular tone [78, 79]. Their functions seem to be tissue specific; therefore not every item on the following listing of functions might be applicable to every pericyte in every location.

3.2.1. Mechanical stabilization and interaction with microvessels

Pericytes are producers as well as resorbers of the extracellular matrix and through this actively contribute to the connective tissue matrix surrounding blood vessels [70]. Morphologically they share a close homology to vascular smooth muscle cells and as mentioned above might even have the potential to differentiate into them. They also express some classical SMC marker proteins such as αSMA and vimentin. This function has been studied extensively in CNS capillary pericytes. Since they are essentially contractile cells, they are considered to have the ability to contribute to the regulation of blood flow and regulation of vascular permeability at the capillary level [80, 81]. This has been shown under certain experimental conditions also in the retina [81]. To fulfill their constrictive function in capillaries (the physiologic meaning of which is absolutely unclear) pericytes express the contractile proteins actin and myosin. There are however prominent differences in the expression pattern of those markers in pericyte populations originating from different tissues and vascular beds [66, 82, 83].

3.2.2. Sensing and integrating mechanical and chemical stimuli

In the control of vascular integrity and function pericytes have the ability to sense a variety of metabolic stimuli, integrate these signals and react either by sending signals to neighboring cells or by contracting or relaxing themselves, thereby directly influencing vascular tone [84-

87]. In this respect *in vitro* studies suggest a role for pericytes in oxygen and carbon dioxide sensing and thereby an involvement in the regulation of adequate tissue perfusion [88-91]. Metabolic activity also leads to characteristic physiological changes that can be sensed by pericytes. In this respect an acidic extracellular pH [92] as well as increasing levels of the ATP breakdown product adenosine induced pericyte relaxations *in vitro* [93]. Reports on a concentration dependent effect did not specifically indicate pericyte involvement although this has been speculated in kidney vessels [94, 95]. Adenosine signaling via A1 and A2A receptors also could be shown to lead to the upregulation of K_{ATP} channel activity [96]. These K_{ATP} channels are inherently metabolically regulated with an increase in activity when the intracellular ATP level decreases leading to a hyperpolarization of the cell and therefore favoring dilation [96, 97].

The endothelial relaxation signal NO also leads to a relaxation in vascular pericytes [98]. Interestingly the metabolite lactate has a constricting effect when the supply of oxygen is high but can also lead to a relaxation under hypoxic conditions [87]. This constriction is also speculated to involve communication with endothelial cells, while hypoxia closes gap junctions between pericytes and endothelial cells [87]. Furthermore a wide range of vasoactive molecules have been described to be sensed by pericytes and induce a reaction. While serotonin, histamine and noradrenaline [99, 100], as well as angiotensin II and thromboxane A2 [101, 102] induced contractions, the application of the prostacyclin PGI2 [101] and of vasoactive intestinal peptide (VIP) [100] induced a relaxation.

To relay its signals a single pericyte has up to 1000 direct contact sites with adjacent endothelial cells [103] and therefore implicitly possesses the ability to integrate signals along the length of the vessel [81]. Depending on their state, pericytes also have the ability to secrete cytokines targeted at the endothelium in a paracrine and cell-cell contact-dependent manner. For example endothelin-1 produced in endothelial cells has a potent vasoconstrictive and mitogenic effect on pericytes [104, 105], while platelet-derived growth factor (PDGF) produced in pericytes controls pericyte hyperplasia and endothelial proliferation in angiogenesis [106].

3.2.3. Control of angiogenesis and endothelial proliferation

Pericytes also play an active role in the control of angiogenesis, endothelial proliferation and the formation of new blood vessels [71, 106-108]. Unlike the original view that initial endothelial tubes form without pericyte contact, and pericytes are only recruited later during vascular remodeling, meanwhile pericytes could be shown to be also present and to play an active role in the sprouting and remodeling of blood vessels [71, 109]. In a similar way exercise is a strong inducer of angiogenesis as an early adaptive response to eccentric contractions [110]. In this model it could be shown that NF-κB is activated in human skeletal muscle shortly following a damaging exercise and its activation primarily takes place in a distinct population of pericytic cells [110]. Furthermore under hypoxic conditions vascular endothelial growth factor (VEGF) from pericytes has the ability to simulate endothelial cells as well as pericytes to proliferate and migrate [111].

3.2.4. Reservoir cells for transdifferentiation and macrophage-like activity

Pericytes are heterogeneous in respect to their origin [64]. In the retina they develop from mesoderm and neural crest, in other tissues pericytes can be recruited from bone marrow precursors or be generated by transdifferentiation of endothelial cells during postnatal

vascular repair [112-114]. Most likely all of these processes contribute to the pericyte pool, therefore under cell culture conditions proliferation of pre-existent pericytes as well as transdifferentiation from monocyte-derived macrophages are likely to contribute.

Not only the origin of pericytes is manifold, they also themselves possess the potential to further transdifferentiate into a variety of cell types such as macrophage and fibroblast like cells [115, 116]. Therefore they have been reported recently to be a potential new cell source for future efforts in skeletal regenerative medicine. For this purpose the candidate growth factor Nell-1 could be shown to be able to induce osteogenic differentiation in pericytes [117].

In the CNS and potentially also in other tissues, pericytes are very likely to be progenitor cells of (brain) macrophages [116]. But already when they still can be considered pericytes they already show a wide range of functions generally found in macrophages. For example they have pinocytic and phagocytic activity from different compartments and of different kind of fluids [118-127]. Furthermore they express a set of macrophage markers, such as CD4, CR3 complement, CD11b and Fc receptors [128] at least in animal experiments. In a reaction to *in vitro* stimulation with IFN-γ they react with an upregulation of MHC-II molecules on the cell surface [129]. They are therefore considered potential antigen presenting cells in stroke and vasculogenesis models [130, 131]. Nevertheless, some caution should be exercised in interpreting these findings since perivascular macrophages display a phenotype very similar to pericytes and can be easily mistaken.

4. microRNA can act as a fine-modulator of gene expression

4.1. Introduction

MicroRNA or, shorter, miRNA are short RNA molecules with an average length of 20 – 22 bases that are expressed in eukaryotic cells. Although they were already discovered in 1993 in the nematode C. elegans while studying the lin-14 gene [132] their function was only recognized seven years later. With let-7 in the year 2000 the second miRNA was discovered and found to be highly conserved among different species [133, 134]. A high level of conservation usually is a clear indication of vital importance for a cellular component because loss would have been fatal [135, 136].

Functionally miRNAs act as post-transcriptional regulators of gene expression by serving as recognition elements in a multi-enzyme complex [137]. Their target sequences can mostly be found in the 3' UTR of a transcribed mRNA, but this does not always have to be the case [138]. If a target mRNA has been recognized it is silenced or degraded to inhibit its translation [137]. In humans there are estimates that more than 1000 miRNAs exist [139], that may have about 60% of the whole transcriptome as a target [140, 141]. This becomes possible since one miRNA can target hundreds or thousands of different mRNAs. miRNAs therefore possess the ability to induce or fine-tune whole gene programs all at once [142].

4.2. Biogenesis and mode of action

The biogenesis and maturation of miRNAs takes place in part in the nucleus and in part in the cytosol (for an overview see: [143]). On the genomic DNA level the majority of miRNAs is intergenic and transcribed independently, up to 40% is intronic. But also localization within an exon has been described in some cases [144]. miRNA is usually transcribed by RNA polymerase II [145] under control of specific promoter elements [146] into a so-called primary miRNA (pri-miRNA). One pri-miRNA can be the precursor to up to 6 different miRNAs. It is several hundred nucleotides long and includes multiple arms with an about 80 nucleotide long RNA stem-loop on each arm [145, 147].

This molecule is recognized by the so called "microprocessor complex". This complex is formed by a protein called "DiGeorge Syndrome Critical Region 8" (DGCR8) (Pasha in invertebrates) that associates with Drosha, a nuclease. In this machinery every individual miRNA contained in the primary miRNA is cut down to a double-stranded piece of RNA with a two nucleotide overhang at one side and an hairpin at the other, this is called a pre-miRNA [148]. The pre-miRNAs are then exported from the nucleus by Exportin 5 in a GTP dependent process. Exportin 5 recognizes the pre-miRNA by their overhangs [149].

In the cytoplasm the precursor miRNA is further processed by another nuclease called Dicer. Dicer cuts the loop of the molecule leaving an RNA duplex of about 22 bases length [150]. Although theoretically both strands can be active usually one is preferred thermodynamically and the other one is degraded [151-153]. The now mature miRNA is finally incorporated into the so-called "RNA-induced silencing complex" (RISC). RISC is a multi-enzyme complex containing among others Dicer and so-called Argonaute proteins (Ago). Argonaute proteins are essential components of the RISC. They are RNA binding proteins and responsible for the

correct recognition of the target sequence. Some even can directly cleave the target mRNA [154]. The mode and mechanism of silencing is dependent on the degree of complementarity between the miRNA seed sequence and the recognized mRNA. If the complementarity is complete the target mRNA is degraded, if the complementarity is only partial it is silenced [142] and further translation is blocked.

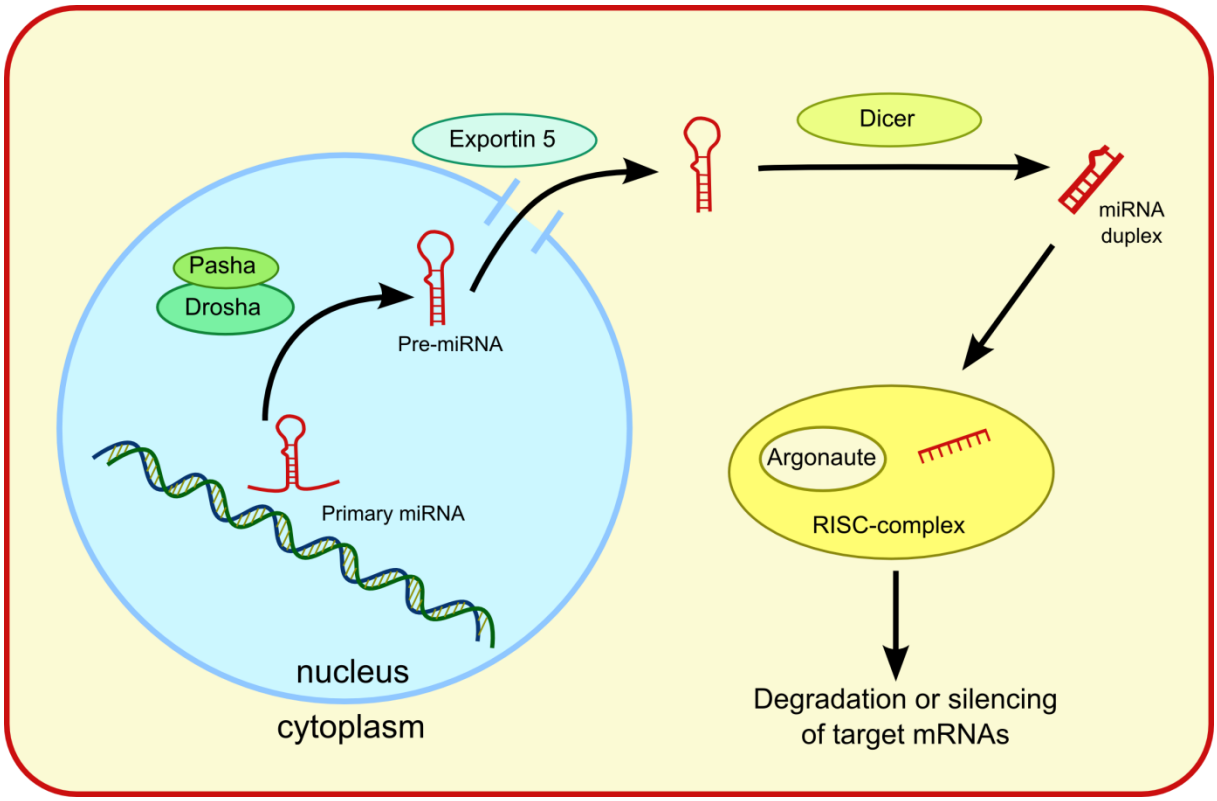

Figure I-5: Schematic mechanism of the well characterized miRNA biogenesis pathway in C. elegans. Primary miRNA is transcribed from intronic or exonic DNA and cleaved by the protease-complex Drosha/Pasha. The resulting pre-miRNA is then actively exported from the nucleus by Exportin 5 and cleaved to the characteristic mature RNA duplex by the enzyme Dicer. It is then finally integrated into the so called RISC complex and serves as the template for target mRNA recognition and silencing. Differences in the mammalian system lie mainly in the individual enzymes. Basic structure and function of the pathways are analogous. (Image rearranged based upon figure 2 from [155]).

5. Aims of the study

As has been presented in the previous chapters, studies on isolated pericytes have up to the present been mainly conducted on retinal and brain vessel pericytes. However, their role and functional characteristics in skeletal muscle are less clear. Their localization at the interface of tissue and capillaries supports the hypothesis that they play a role as sensors in the control of vascular tone. Therefore, a better understanding and analysis of skeletal muscle pericyte biology seems indispensable. Currently, this is hampered by the lack of established methods to isolate and cultivate pericytes from skeletal muscle. The primary goal of the present work was therefore to

- **establish an isolation protocol** for pericytes from skeletal muscle and to
- **characterize the obtained cells** with published pericyte markers from other tissues, but also with endothelial and smooth muscle cell markers

Furthermore pericytes might function as sensors of tissue activity and metabolism and affect the vascular tone of microvessels by generation of hyperpolarizing signals and/or calcium waves that could be transferred to the endothelium via gap junctions. For that reason we aimed to

- clarify their **potential for electrical signal generation** (hyperpolarization) as well as conduction of calcium and electrical signals in view of the fact that pericytes exert a role as sensors in the vascular wall
- investigate the **expression of connexins** and formation of **functional gap junctions** of these cells

Finally, as pericytes, by forming gap junctions with endothelial cells have been shown to be a prerequisite for the final maturation of vessels [57] we hypothesized that this process might involve gap junctional transfer of miRNA, thereby controlling the alteration of gene programs in endothelial cells. We consequently aimed to

- analyze the potential **intercellular transfer of miRNA** using connexin expressing and non-expressing HeLa cells

II Materials

1. Technical equipment

Machine	Manufacturer
3D micromanipulator	Physics Instruments, Karlsruhe
Patch-Clamp analog-digital interface Digidata 1200B	Axon Instruments / Molecular Devices, Biberach an der Riss
AxioVision software	Zeiss, Oberkochen
Axopatch 200A patch clamp amplifier	Axon Instruments / Molecular Devices, Biberach an der Riss
Bio-Photometer 6131	Eppendorf, Hamburg
Cell counter Z2	Beckman-Coulter, Krefeld
Cell culture centrifuge Megafuge 1.0R	Heraeus Instruments, Hanau
Cell separation system MiniMACS	Miltenyi Biotech, Bergisch Gladbach
Clampfit software	Axon Instruments / Molecular Devices, Biberach an der Riss
Confocal laser scanning microscope LSM-410	Carl Zeiss, Göttingen
Confocal laser scanning microscope TCS SP5	Leica Microsystems, Wetzlar
ELISA plate reader Infinite F200	Tecan, Maennedorf, Switzerland
FACS-Sort flow cytometer	Beckton Dickinson, Heidelberg
Femtojet injection system	Eppendorf, Hamburg
Floor-centrifuge RC-5B	Sorvall / Thermo Scientific, Bad Homburg
Flow workbench LaminAir HB2448	Heraeus Instruments, Hanau
Fluorescence microscope Axiovert 200M	Carl Zeiss, Göttingen
Gel documentation system Doc 1000	Bio-Rad, Munich
Gel electrophoresis apparatus Mighty Small II	Amersham Pharmacia, Freiburg
Gel system PerfectBlue Mini-L	PeqLab, Erlangen
Humidified incubator MCO-17AI	Sanyo Electric, Munich
Inverted cell culture microscope Fluovert FU	Leica Microsystems, Wetzlar
Micropipette puller P77 Flaming/Brown	Sutter Instrument, Novato, USA
Microscopy CCD-camera for dye injection experiments	Till Vision, Gräfelfing
Office 2010 Office suite	Microsoft, Unterschleißheim
Origin data analysis software	Microcal, Northhampton, USA
pH meter PHM-82 Standard	Radiometer Copenhagen, Willich
Power supply for agarose gels PS305	Life Technologies, Darmstadt
Power supply for SDS gels P25	Biometra, Göttingen
SPSS 20 statistical software package	IBM, Ehningen
Steam sterilizer	H&P Labortechnik, Oberschleißheim
Thermocycler Mastercycler ep gradient S	Eppendorf, Hamburg
Tube luminometer LB9507	Berthold, Bad Wildbad
Western Blot Imaging System ORCA-ER	Hamamatsu Photonics, Herrsching

2. Consumables

Article	Manufacturer
Borosilicate fiber glass tubing	Hilgenberg, Maldfeld
Buttoned cannula	Braun, Melsungen
Blotting paper	Whatman / Biometra, Göttingen
Cell culture dishes (dia. 3.5 and 10 cm)	Falcon/BD, Franklin Lakes, USA
Cell culture plates (6, 12 and 24 well)	Falcon/BD, Franklin Lakes, USA
Cell culture flasks T 25	Falcon/BD, Franklin Lakes, USA
Cell Scraper	Falcon/BD, Franklin Lakes, USA
Cryotubes	Biozym Scientific, Hessisch-Oldendorf
Discofix-3 (three-way stopcock)	Braun, Melsungen
Disposable pipettes (5, 10 and 25 ml)	Costar, Corning, USA
Glass capillaries (unmachined) GB 100F-10	Science Products GmbH, Hofheim
Insulin syringe BD MicroFine (U40)	Becton-Dickinson, Heidelberg
Lab-Tek chamber slides	Nunc, Wiesbaden
MiniMACS MS columns	Miltenyi Biotec, Bergisch Gladbach
Multiwell plates (24 well)	Falcon/BD, Franklin Lakes, USA
PD Tips	Eppendorf, Hamburg
96-well plates, transparent, flat bottom	Corning, Amsterdam, Netherlands
Petri dishes for bacterial culture	Greiner, Frickenhausen
Pipette tips	Sarstedt, Nümbrecht
Polystyrene round-bottom tube 5 ml	Falcon/BD, Eremdodegem, Belgien
Reaction tube 1,5 ml	Eppendorf, Hamburg
Reaction tubes 15 and 50 ml	Falcon/BD, Franklin Lakes, USA
Silicone grease, high-vacuum, heavy	Wacker Chemie GmbH, München
Silicone rubber Elastosil RT622A	Wacker Chemie GmbH, München
Slide mounts	Marienfeld, Lauda-Königshofen
Coverslips (dia. 15 mm)	Saur Laborbedarf, Reutlingen
Surgical tools (forceps, scissors)	FST fine science tools, Heidelberg

3. Reagents

Substance	Manufacturer
4-Aminopyridine (4-AP)	Sigma-Aldrich, Taufkirchen
accutase	Sigma-Aldrich, Taufkirchen
Acrylamide 30% (37.5:1)	Genaxxon Bioscience, Ulm
Agarose	AppliChem, Darmstadt
Alexa 488	Invitrogen, Karlsruhe
Ammonium persulfate (APS)	Sigma-Aldrich, Taufkirchen
Ampicillin	AppliChem, Darmstadt
Bacto-tryptone	AppliChem, Darmstadt
Bandeiraea simplecifolia lectin, TRITC conjugated	Sigma-Aldrich, Taufkirchen
BCA protein assay	Pierce /Thermo, Schwerte
Boric acid	AppliChem, Darmstadt
Bovine serum albumin	Sigma-Aldrich, Taufkirchen
Bromophenol blue	Sigma-Aldrich, Taufkirchen
BSA, fraction V, fatty acid free	Boehringer-Mannheim, Mannheim
Calcein AM	Invitrogen, Karlsruhe
Calcium-chloride, $CaCl_2$	Merck, Darmstadt
Chamber slides Lab-Tek	Nunc / Thermo, Schwerte
Chemiluminescence substrate ECL	AppliChem, Darmstadt
Collagen G	Biochrom AG, Berlin
Collagenase A	Roche, Mannheim
$DiBAC_4(3)$	Invitrogen, Karlsruhe
D-MEM (Dulbecco's modified Eagle Medium)	Invitrogen, Karlsruhe
DMSO (Dimethyl sulfoxide)	AppliChem, Darmstadt
DNA ladder, 2-log	New England Biolabs, Frankfurt/Main
Dual-Luciferase Reporter Assay System E1910	Promega, Mannheim
EDTA (Ethylenediaminetetraacetic acid)	AppliChem, Darmstadt
EGTA (Ethylene glycol tetraacetic acid)	Sigma-Aldrich, Taufkirchen
Endothelial Cell Growth Medium	Promocell, Heidelberg
Ethanol	AppliChem, Darmstadt
Ethidium bromide	Sigma-Aldrich, Taufkirchen
FACS-Flow	Becton-Dickinson, Heidelberg
FCS (Fetal Calf Serum)	Biochrom AG, Berlin
Flufenamic acid	Sigma-Aldrich, Taufkirchen
Formaldehyde 37 %	AppliChem, Darmstadt
Glucose	AppliChem, Darmstadt
Glycerol	AppliChem, Darmstadt
Glycine	AppliChem, Darmstadt
Growth factor supplement	Promocell, Heidelberg
HEPES (4-(2-hydroxyethyl)-1-piperazine-ethane-sulfonic acid)	Sigma-Aldrich, Taufkirchen
HiPerFect transfection reagent	Qiagen, Hilden
Hydrogen peroxide (H_2O_2)	AppliChem, Darmstadt
Immu-Mount mounting medium	Shandon, Pittsburg, USA
Leupeptin	AppliChem, Darmstadt
L-Glutamin	Invitrogen, Karlsruhe

Substance	Manufacturer
LNA (N^{ω}-nitro-L-arginine)	Sigma-Aldrich, Taufkirchen
Magnesium chloride, $MgCl_2$	AppliChem, Darmstadt
Medium 199	Invitrogen, Karlsruhe
Methanol	AppliChem, Darmstadt
Microbeads rat-anti-mouse IgM	Miltenyi Biotec, Bergisch-Gladbach
miRNA mimics	Dharmacon / Thermo, Schwerte
N,N,N',N'-tetramethylethylenediamine (TEMED)	AppliChem, Darmstadt
NBCS (New born calf serum)	Biochrom AG, Berlin
Nonfat dried milk powder	AppliChem, Darmstadt
NP-40	Sigma-Aldrich, Taufkirchen
Nucleotide mix	Roche, Mannheim
PageRuler electrophoresis protein standards	Fermentas, St. Leon-Rot
PBS- / PBS+	Apotheke des Klinikums Innenstadt, München
Penicillin G	Sigma-Aldrich, Taufkirchen
PKH-26 Red Fluorescent Cell Linker Kit	Sigma-Aldrich, Taufkirchen
Plasmid purification Kit NucleoBond Xtra	Macherey-Nagel, Düren
Plasmid purification Kits Mini & Maxi	Qiagen, Hilden
Potassium chloride, KCl	Merck, Darmstadt
Potassium dihydrogen phosphate, KH_2PO_4	Merck, Darmstadt
Pronase E	Merck, Darmstadt
Propodium-Iodide	Sigma-Aldrich, Schnelldorf
Puromycin	AppliChem, Darmstadt
Rapid DNA ligation Kit	Roche, Mannheim
Restriction enzymes	New England Biolabs, Frankfurt/Main
RNAse, DNAse free	Invitrogen, Karlsruhe
siRNA resuspension buffer	Qiagen, Hilden
Sodium chloride (NaCl)	AppliChem, Darmstadt
Sodium deoxylcholate	AppliChem, Darmstadt
Sodium dihydrogen phosphate (NaH_2PO_4)	AppliChem, Darmstadt
Sodium dodecylsulfate (SDS)	AppliChem, Darmstadt
Sodium fluoride	Merck, Darmstadt
Sodium hydrogen carbonate ($NaHCO_3$)	Merck, Darmstadt
Sodium hydroxide (NaOH)	AppliChem, Darmstadt
Sodium orthovanadate	Alexis / Enzo Life Sciences, Lörrach
Sodium pyrophosphate	Sigma-Aldrich, Taufkirchen
Sodium pyruvate	Sigma-Aldrich, Taufkirchen
Streptomycin	Sigma-Aldrich, Taufkirchen
SuperFect transfection reagent	Qiagen, Hilden
Superoxide dismutase (SOD)	Roche, Mannheim
Taq DNA polymerase	Roche, Mannheim
TEMED (Tetramethylethylenediamine)	AppliChem, Darmstadt
Tris Base	AppliChem, Darmstadt
Triton X-100	Sigma-Aldrich, Taufkirchen
Trypsin-EDTA	Sigma-Aldrich, Taufkirchen
Tween 20	AppliChem, Darmstadt
Western blot blocking reagent	Roche, Mannheim
Western-Blotting Membrane Hybond-P	Amersham Pharmacia, Freiburg

Substance	Manufacturer
XL-1 blue competent E. coli	Stratagene / Agilent, Waldbronn
Xylene-cyanol	AppliChem, Darmstadt
Yeast extract	AppliChem, Darmstadt
β-Glycerophosphate	Sigma-Aldrich, Taufkirchen
β-Mercapto-ethanol	AppliChem, Darmstadt

III Methods

1. Mammalian cell culture

Established cell culture techniques were used to cultivate primary hamster pericytes, endothelial cells as well as immortalized tumor cell lines. The cell lines used in this work are listed in Table III-1.

Cell line	Origin	Growth	Selection
PC	Primary hamster pericytes	adherent	-
SMC	Primary smooth muscle cells	adherent	-
3G5	Antibody producing hybridoma cell line	suspension	-
HUVEC	Primary human umbilical vein endothelial cells	adherent	-
HeLa	Human cervix carcinoma	adherent	-
HeLa40	HeLa stably transfected with connexin 40	adherent	Puromycin
HeLa43	HeLa stably transfected with connexin 43	adherent	Puromycin

Table III-1: Overview of the cell lines used in the current study. Respective growth conditions and selection antibiotics are given where applicable

Fetal calf serum (FCS) was heat inactivated prior to use by incubation for 30 minutes at 56°C and subsequent frozen for storage at -20°C. All cell culture work was performed under sterile conditions in a laminar flow workbench. Cell growth was monitored daily under a light microscope. If not otherwise stated, all cell lines were kept in 10 cm plastic dishes at 37°C in a humidified atmosphere containing 5% CO_2. They were grown up to 90% confluence and then split onto new dishes. For this purpose cells were first washed with calcium free phosphate buffered saline solution (PBS) and then treated with Trypsin-EDTA solution at 37°C. Once the cells had detached from the culture dish, the Trypsin-reaction was stopped with full medium containing serum and the cells were re-plated in new culture dishes. For culturing of human umbilical vein endothelial cells (HUVEC) the dishes were additionally treated with Collagen-G (0.001% in PBS) for 30 minutes at 37°C.

Substance	Amount
Sodium chloride (NaCl)	8.0 g
Potassium chloride (KCl)	0.2 g
Di-sodium hydrogen phosphate (Na_2HPO_4)	1.44 g
Potassium di-hydrogen phosphate (KH_2PO_4)	0.24 g

Table III-2: Contents of the phosphate buffered saline solution without calcium (PBS-). All the constituents were mixed in 1l of ddH_2O and then the pH value adjusted to 7.4. The solution was then autoclaved sterile and stored at room temperature.

For patch clamp experiments, analysis of gap junctional coupling or immunocytochemistry the cells were seeded on collagen coated cover slips (15 mm diameter) which were placed in 24-well plates normally at a density of 1.5×10^6 cells per well.

Cells which could not be used immediately were regularly frozen for later use. Freezing pauses cells in their metabolic activity. The composition of the freezing medium can be found in Table III-3. DMSO acts in this medium as an antifreeze agent, interfering with the formation of ice crystals as the medium freezes. Therefore cells are protected when they are slowly frozen. When thawing the cells DMSO has to be washed out quickly to avoid damage

to the cells. They were therefore quickly thawed at 37°C in a water bath and then immediately washed in pre-warmed medium once before plating.

HeLa and 3G5 cell line stock tubes were kept in aliquots in liquid nitrogen at -196°C. Pericyte, SMC and endothelial cell primary cultures were used fresh whenever possible and residual material stored for shorter periods of time at -80°C in a freezer or for prolonged storage in liquid nitrogen.

Substance	Percentage
D-MEM	70%
NBCS / FCS	20%
DMSO	10%

Table III-3: Composition of the freezing medium

1.1. HeLa cell culture

HeLa wildtype (ATCC CCC2) and the connexin transfectants HeLa37, HeLa40 and HeLa43 were a kind gift from Professor Dr. Klaus Willecke (University of Bonn). The generation of these cells is described in [156]. The cells were cultivated in Dulbecco's Modified Eagle Medium (D-MEM) supplemented with 10% new-born calf serum (NBCS), 100 U/ml penicillin and 100 µg/ml streptomycin. HeLa cells stably overexpressing connexins were grown in the same medium additionally containing 1 µg/ml puromycin as a selection antibiotic. Cells were trypsinized when they reached confluence and replated in a 1:5 to 1:12 ratio depending on experimental requirements.

1.2. HUVEC isolation and culture

Human umbilical vein endothelial cells (HUVEC) were isolated according to a modified protocol from Jaffe et al. [157] by technical assistants. Umbilical cords were obtained from the department of gynecology and obstetrics of the LMU – University of Munich, Klinikum Grosshadern and Klinikum Innenstadt. They were stored in PBS containing calcium and antibiotics (Amphotericin, Puromycin and Streptomycin) to avoid contamination for a maximum of three days before HUVEC isolation. All buffers and culture media were pre-warmed to 37°C in a water bath prior to usage.

Isolated HUVEC were cultured in endothelial cell growth medium (Promocell) supplemented with growth factors (Table III-4) supplied by the manufacturer. Medium was changed the following day of isolation and cells were kept in culture until they reached confluence. In experiments only passages I and II were used.

Factor	Amount
Basic Fibroblast Growth-Factor, human, recombinant	1.0 ng / ml medium
Endothelial cell growth supplement/Heparin	0.004 ml / ml medium
Epidermal growth-factor, human, recombinant	0.1 ng / ml medium
Hydrocortisone	1.0 µg / ml medium
Phenol red	0.62 ng / ml medium
Fetal calf-serum	0.02 ml / ml medium

Table III-4: Growth factors supplied with the endothelial cell growth media by the manufacturer Promocell. They were stored in aliquots and added prior to use.

1.3. Smooth muscle cells (SMC)

Human umbilical cord smooth muscle cells (SMC) were obtained commercially from Promocell, Heidelberg. They were cultured in high-glucose D-MEM containing 4.5 g/l glucose, supplemented with 20% fetal calf serum (FCS) and 1% Penicillin/Streptomycin.

1.4. Pericytes and 3G5 hybridoma cells

Pericytes and 3G5 cells were cultured in D-MEM containing 1 g/l glucose. The medium was supplemented with 10% FCS and 1% Amphotericin/Penicillin/Streptomycin solution. The non-adherent mouse 3G5 hybridoma cell line (ATCC CRL 1814 [158], American Type Culture Collection, Manassas, VA, USA) was grown in 50 ml flasks.

2. Isolation of pericytes from hamster muscle

2.1. Surgical procedures

Syrian gold hamsters (*mesocricetus auratus*) were euthanized with an overdose of Pentobarbital, shaved and treated with depilatory cream. The animals were then positioned on the stage of a microscope for the further dissection steps.

Figure III-1: The thigh muscle was surgically preparated (left image) and shredded (right image) under a laminar flow hood to maintain aseptic conditions

Following the incision, the thigh muscles (mainly the M. gracilis, the adductors and the M. quadriceps femoris) were dissected and taken out. They were then put into a glass petri dish and minced into small pieces under sterile conditions. The resulting now accessible muscle "glop" was then enzymatically digested with Collagenase A and Trypsin in PBS at 37°C for two hours under constant rotation. The resulting mixture was subsequently washed at 1200 rpm for 5 min at room temperature and the supernatant discarded. The resulting pellet was washed once more in 5 ml D-MEM containing 10% FCS. Cells and debris were resuspended in 10 ml D-MEM with 10% FCS.

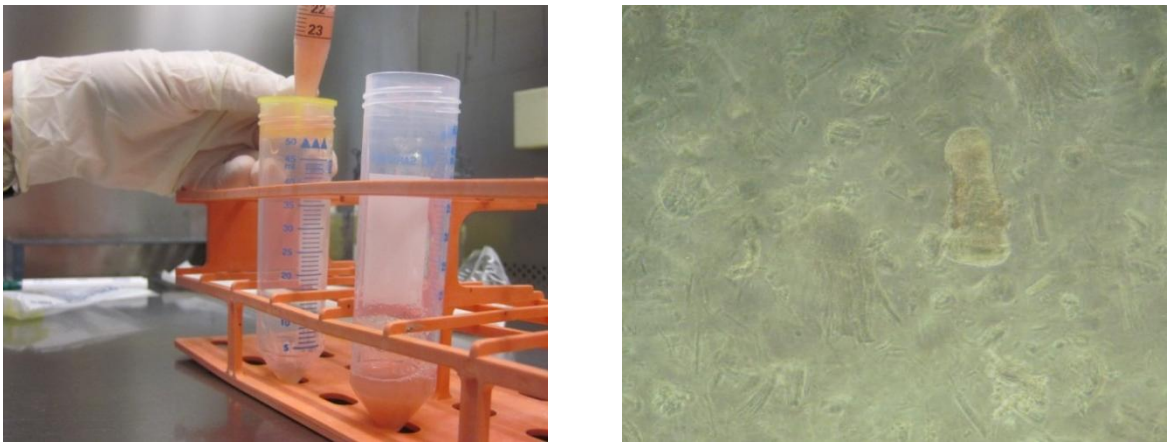

Figure III-2: The minced and digested muscle was passed through a 100 µm mesh (left image). The isolated cells and debris could then be visualized directly following the isolation under a cell culture microscope (right image).

To remove large muscle particles the mixture was then passed through a 100µm mesh and incubated overnight in a 10cm dish (including detached cells and small capillary fragments). The resulting fragments were further digested with Trypsin daily for three more days. For this purpose the supernatant was taken off leaving only attached cells on the plate. It was then centrifuged at 1200 rpm for 5 minutes and the pellet resuspended in 1 ml Trypsin ($5\frac{mg}{ml}$) and 5 ml D-MEM + 1% FCS. This was then kept in a rotating flask for one hour at 37°C. After this incubation it was centrifuged again, washed and resuspended in D-MEM with 10% FCS. The digested cell mixture was then added back to original culture dish.

For further growth and expansion of pericytes in cell culture they were further grown for 8 to 14 days with culture medium replaced every 3 days. With this method between 6 and 20 culture dishes per animal could be obtained for further purification with magnetic beads.

2.2. **Purification of pericytes using the 3G5 antibody**

2.2.1. Background

For the purification of pericytes from cultures of adherent cells, magnetic cell sorting (MACS, Miltenyi Biotec) with 3G5-coated beads was used. 3G5 is a monoclonal antibody of the IgM type (kappa light chain), that was originally produced in mouse by immunizing animals with fetal rat brain. The antibody specifically reacts with an acetylated ganglioside that can be found in a variety of cell types, including pancreatic islets, neurons and human T lymphocytes [158]. In the vasculature the antibody has been used to identify pericytes [159].

2.2.2. Magnetic bead cell separation

To produce this antibody *in vitro*, hybridoma cells were grown in 50 ml flasks as described previously. Antibody containing supernatant was harvested 18 to 24 days after splitting and used immediately or frozen at -20°C for later use. Microbeads coated with rat anti mouse-IgM were mixed with 5 ml of 3G5 antibody containing supernatant for 30 minutes at 4°C. Those beads were then loaded onto a medium sized positive selection (type MS) column and placed in a MiniMACS separator as shown in Figure III-3. To purify pericytes from adherent cell cultures the cells were washed with PBS-, detached by treatment with accutase and loaded onto the separation columns. Subsequently the columns were washed three times with phosphate buffer at pH 6.5 (20 mM HEPES, 100 mM NaCl). For elution of 3G5 positive cells the columns were taken out of the magnetic field and perfused with 2 ml of full medium. The purified population of cells was then plated in 35 mm culture dishes and further cultivated until they were used in experiments. Only cells in passages 1 and 2 were used for experiments, higher passages were not investigated.

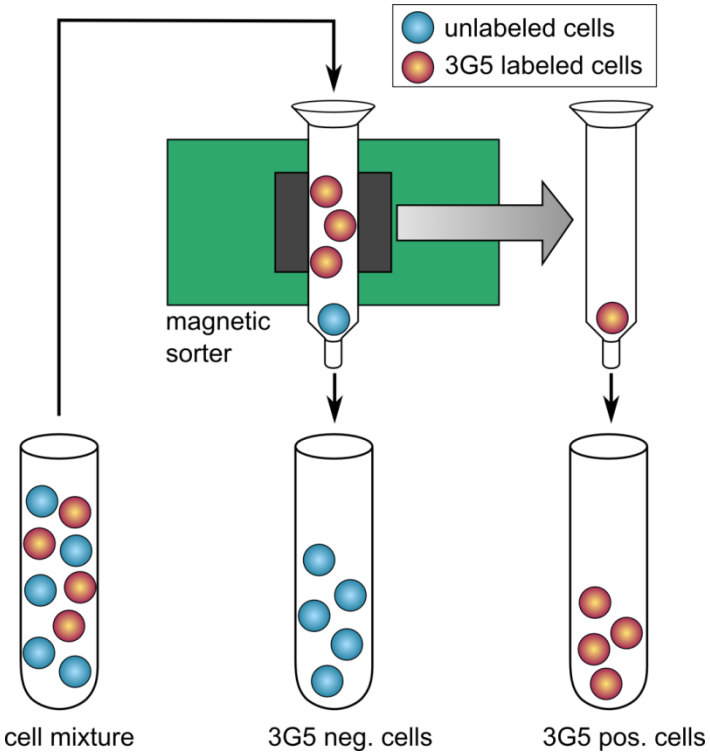

Figure III-3: Schematic representation of the Miltenyi MACS positive magnetic cell separation procedure (modified after: [160]). Cells were labeled with magnetic-bead coupled antibodies against the 3G5 epitope and then passed through a sorting column exposed to a strong magnetic field. This way 3G5 positive cells are held back in the column and can in the final step be eluted separately.

3. Cell transfection with synthetic miRNA and plasmids

3.1. miRNA transfections

RNA interference was performed using synthetic double stranded miRIDIAN microRNA mimic oligonucleotides purchased from Dharmacon (Thermo Scientific). Additionally a non-silencing, pre-validated control from C. elegans was utilized. These mimics were delivered lyophilized and upon arrival dissolved in siRNA resuspension buffer (Qiagen). The stock solution (20 µM) was stored in 40 µl aliquots at -20°C. miRNA transfections were performed with HeLa cells seeded in 6-well plates for co-culture experiments or in 12-well plates for morphology and cell cycle analysis.

Name	Sequence	Species
miR124 mimic	5′ UUA AGG CAC GCG GUG AAU GCC A 3′	H. sapiens
miR15b mimic	5′ UAG CAG CAC AUC AUG GUU UAC A 3′	H. sapiens
miRNA neg. control	5′ UCA CAA CCU CCU AGA AAG AGU AGA 3′	C. elegans

Table III-5: Sequences and source organisms of the synthetic miRNA analoga used in the miRNA transfection and co-culture experiments.

Culture plate format	Volume of culture medium [µl]	Volume of 20 µM siRNA stock solution [µl]	Volume of HiPerFect Reagent [µl]	Final miRNA concentration [nM]
12-well	1100	6	6	100
6-well	2300	12	12	100

Table III-6: Amounts of reagents for cell transfections with miRNA. The transfection protocol was designed according to recommendations given by Qiagen in the HiPerFect user manual

HeLa cells were seeded the day before the experiment to obtain a density of around 70 to 80% confluence on the day of transfection. For transfections miRNA was diluted in culture medium without serum and antibiotics to a final concentration of 100 nM (Table III-6) and HiPerFect transfection reagent (Qiagen) was added. The samples were then incubated for 5-10 minutes at room temperature to allow the formation of the transfection complexes. Finally the miRNA transfection solution was added drop-wise onto the cells directly in the culture plates. No further medium change was performed during the experiments unless otherwise indicated.

3.2. Growth and purification of plasmids

Plasmids for transfection were grown in chemically competent XL-1 blue coli (Stratagene) in standard Lysogeny Broth (LB) medium. The ingredients listed in Table III-7 were dissolved in 1 l of ddH_2O and then autoclaved. To ensure specific growth of transformed bacteria 100 mg/ml Ampicillin was added to the medium just before use.

Plasmids were purified in small quantities (up to 20 µg DNA) with the QIAprep Spin Miniprep Kit (Qiagen). Large scale plasmid purifications (up to 500 µg DNA) were

performed with the Maxi Plasmid Kit (Qiagen) or with the NucleoBond Xtra Kit (Macherey-Nagel) according to manufacturer's instructions.

Substance	Amount
Bacto-tryptone	10 g
Yeast extract	5 g
NaCl	10 g

Table III-7: Contents of LB bacterial growth medium.

3.3. Transfection with expression plasmids

For cell transfections with expression plasmids SuperFect transfection reagent (Qiagen) was used according manufacturer's instructions. This reagent chemically is an activated dendrimer that possesses a "defined spherical architecture, with branches radiating from a central core and terminating at charged amino groups"[3]. Complexation with DNA yields a net positive charge that facilitates binding to negatively charged receptors on the cell surface and improved uptake.

Cell transfections with plasmid DNA were carried out in 12-well plates, 6-well plates or in 10cm dishes. Cells were seeded the day before transfection in a density that they would reach 70-80% confluence on the next day. For HeLa cells this equaled to about $1x10^5$ cells per well of a 12-well plate, $2x10^5$ cells per well of a 6-well plate and $2x10^6$ cells in a 10 cm dish.

The amounts of DNA used are given in the respective experimental chapters. If lower amounts of expression plasmids were needed, an empty vector pUC18 was co-transfected to ensure equal amounts of total DNA in all transfections.

On the day of transfection plasmid DNA was diluted in growth medium without serum or antibiotics (SFM) to obtain the final volume given in Table III-8 and SuperFect transfection reagent (Qiagen) was added. To allow the formation of transfection complexes the samples were incubated for 5-10 minutes at room temperature. In the meantime the cells were washed once with PBS-. After the incubation time full medium containing serum and antibiotics was added to the transfection complexes and this mixture was then applied onto the cells. The cells were further cultivated for 2-3 hours under standard cell culture conditions before they were washed and medium replaced with regular full culture medium.

Culture plate format	DNA [µg]	Final volume of DNA in SFM[µl]	Volume of SuperFect Reagent [µl]	Volume of full medium [µl]
12-well	1.5	75	7.5	400
6-well	2.0	100	10.0	600
10 cm	10.0	300	60.0	3000

Table III-8: Pipetting scheme of DNA and SuperFect reagent for transfection of adherent cells with expression plasmids indifferent cell culture systems. Protocol and amounts followed manufacturer's instructions

[3] SuperFect transfection handbook, page 7, Qiagen 12/2002

4. Light microscopy of cells and tissues

4.1. Introduction

Fluorescence microscopy represents a commonly used laboratory technique for visualizing the subcellular location of antigens that have been stained with fluorescent dyes. Depending on the physical characteristics of the dye and the labeled antibody, selective labeling of proteins, lipids and sugars can be performed. In the current study Alexa Fluor dyes (Invitrogen) were used [161]. These dyes exhibit a relatively high brightness and are little prone to photobleaching [162]. For two-color experiments, dyes with different excitation/emission characteristics were chosen. The staining pattern was subsequently visualized on a fluorescence microscope.

4.2. Microscopy setups

Optical microscopy studies were performed on three different microscopes. Cell culture images of live cells were taken on an inverted cell culture microscope Fluovert FU (Leitz) with a handheld digital camera DSC-W100 (Sony). Immunofluorescence stainings of pericytes for Cx43, NG2, αSMA, PDGFR-β and vWF were examined on an Axiovert 200M fluorescence microscope (Zeiss) using a 63x/1.40 oil lens and recorded with the AxioVision package (Zeiss). The fluorophores were excited at 488nm and 543nm wavelength with a HBO100 mercury vapor lamp (Zeiss). Confocal microscopy in tissue sections was done on laser scanning microscope LSM-410 (Zeiss) using a Zeiss 63×/1.2 water or a Zeiss 63×/1.4 oil objective. In fluorescence microscopy negative controls were always analyzed in parallel.

4.3. Antibodies

Antigen	Species	Dilution	Manufacturer
NG2	rabbit	1:50	Santa Cruz, Heidelberg
NG2	mouse	1:50	Abcam, Cambridge, UK
α-smooth muscle actin (αSMA)	mouse	1:100	Sigma, Taufkirchen
von Willebrand Factor (vWF)	rabbit	1:100	Sigma, Taufkirchen
Platelet derived growth factor receptor beta (PDGFR-β)	rabbit	1:100	Santa Cruz, Heidelberg
K_V 1.5	rabbit	1:50	Sigma, Taufkirchen
Connexin 43	rabbit	1:100	Sigma, Taufkirchen

Table III-9: Overview over the primary antibodies used for immunostainings.

Antigen	Species	Label	Dilution	Manufacturer
Anti-rabbit	goat	Alexa Fluor 546	1:200	Invitrogen, Karlsruhe
Anti-mouse	goat	Alexa Fluor 488	1:200	Invitrogen, Karlsruhe

Table III-10: Fluorescently labeled secondary antibodies used for immunostaining and flow cytometry.

4.4. Staining of cells from cell culture

Immunostaining of adherent cells cultivated in cell culture was performed using Lab-Tek chamber slides (Nunc / Thermo Scientific). To facilitate pericyte growth these slides were coated with collagen G (Biochrom) prior to seeding as described before. The cells were subsequently incubated at standard growth conditions overnight and then fixed and stained with specific antibodies.

4.4.1. Staining procedures

As a first step slides carrying pericytes or other cells of interest were washed in PBS+ three times after removing the culture medium. They were then fixed in 3.7% Formaldehyde for 10 minutes at room temperature and, if necessary, permeabilized with 0.3% Triton-X100 for 1 minute immediately after fixation. After this step the slides were washed again three times with PBS+. To avoid unspecific binding of the antibodies the samples were then blocked for 20 minutes in 1% bovine serum albumin, fraction V, fatty acid free (Sigma-Aldrich) at room temperature. This PBS/BSA solution was also used to dilute primary and secondary antibodies. Incubation with primary antibody was subsequently performed overnight at 4°C. Unbound antibody was then removed by washing with PBS+ and the slides incubated with the appropriate secondary antibody for 30 minutes at room temperature in the dark. For microscopy and storage the samples were covered with a cover glass in Immu-mount mounting medium (Shandon / Thermo Scientific).

4.5. Staining of muscle sections

4.5.1. Sample preparation and staining protocol for thigh muscle

Samples of hamster thigh muscle were embedded in paraffin and subsequently sectioned into 5µm slices. For immunostaining the respective slides were rinsed under running cold tap water and deparaffinated and rehydrated using a standard xylene-ethanol protocol given in Table III-11.

Reagent	Time
Xylene	2 x 3 minutes
Xylene 1:1 with 100% ethanol	3 minutes
100% ethanol	2 x 3 minutes
95% ethanol	3 minutes
70% ethanol	3 minutes
50% ethanol	3 minutes

Table III-11: Outline of the Xylene-ethanol procedure that is necessary to deparaffinize tissue samples embedded in paraffin prior to staining.

Substance	Amount
Trypsin	50 mg
dd H_2O	10 ml
Mix to dissolve, store at -20°C	

Table III-12: Preparation of the 0.5% Trysin buffer that was used for the enzymatic antigen retrieval in tissues before staining with antibodies

Deparaffinated slides were kept constantly in tap water step to avoid drying. Slides were then treated with 0.5% trypsin buffer (Table III-12) for 30 minutes at 37°C for antigen retrieval. Tissue samples were permeabilized with 0.3% Triton-X solution for 30 minutes and washed three times with PBS+. Blocking of unspecific antibody binding was performed using 1% BSA in PBS+. Primary antibodies were diluted in 1% BSA containing PBS+ and incubated at 4°C overnight. Dilutions of individual antibodies are given in Table III-9. On the next day the slides were washed three times and then incubated with the appropriate fluorescent labeled secondary antibody for 1h at room-temperature at a 1:200 dilution.

4.5.2. Sample preparation and staining protocol for cremaster muscle

Sections from hamster cremaster muscle were prepared similarly to thigh muscle sections. They were embedded in paraffin and sectioned 16µm slices to allow the observation of longitudinal vessels. Deparaffinization and rehydration was performed as described in Table III-11 and for blocking endogenous peroxidase a 0.5% H_2O_2 in 100% methanol solution was added for 10 minutes. Epitope unmasking was performed by treating with 10% Pronase E (Merck) in Tris buffer (50 mM Tris-HCl, 5 mM EDTA at pH 7.5) for 10 minutes. The samples were then blocked with PBS+ containing 1% BSA and 0.025% Tween. Primary Antibody binding was performed in 1% BSA containing PBS+ at 4°C overnight. Antibody dilutions were the same as in hamster thigh muscle sections. For a better display of the vessels TRITC-conjugated Lectin from Bandeiraea simplicifolia (Sigma) was added together with the fluorescent labeled secondary antibody (1:200) for 1 hour.

4.6. **Direct staining of cell membranes with PKH-26**

In some experiments in this thesis co-culture experiments were performed that required the separate analysis of the two cell populations. For this purpose a fluorescent labeling of one cell population with the integral membrane dye PKH-26 (Sigma, Taufkirchen) was used. PKH-26 offers sufficient brightness as well as stability and the staining can be performed very quickly using a custom adapted protocol for adherent cells, which allows the staining directly in 10 cm culture dishes.

Before the staining procedure the adherent cells in a 10 cm dish were washed thoroughly three times with PBS- and then pre-covered with 500 µl of manufacturer supplied Diluent C. For preparation of the staining solution 3 µl of PKH-26 were diluted in 500 µl of diluent C, mixed well by gently shaking and then added on the culture plate. The cells were then incubated for 4 – 5 minutes at 37°C in the dark. Afterwards the staining solution was aspirated and the reaction stopped by the addition of 1 ml of FCS. After removal of the FCS the plate was washed three more times with PBS- to remove residues of unbound and unstopped PKH-26 and then used directly in the experiment.

5. Western Blotting

Western blotting is a standard laboratory procedure used to transfer proteins that have previously been separated by one-dimensional gel electrophoresis onto a carrier membrane for further detection. It has originally been described by George Stark at Stanford University in 1979 [163] and was later modified to use nitrocellulose membranes by.

5.1. Sample preparation

Adherent cells were washed with PBS solution without calcium (PBS-) and detached from culture dishes by trypsin-EDTA (1 ml / 10cm dish) at 37°C. The cells were pelleted by centrifugation at 6708g for 5 minutes in a cooled centrifuge at 4°C and washed with PBS-. Cell lysis was performed using RIPA buffer on ice for 15 minutes. A new stock solution of RIPA buffer was prepared prior to each experiment with fresh addition of protease and phosphatase inhibitors. Sodium orthovanadate (Na_3VO_4) stock solution (200mM) was activated prior to its first usage by repeated boiling and subsequent adjustment of the pH value to 10.0 until the solution remained colorless and the pH was stable at 10.0. The lysed cells were then centrifuged again for 10 minutes at 9700g at 4°C to pellet cell debris and insoluble lysis products. Lysates were either used immediately or stored at -20°C for later analysis.

The total protein content of the sample was quantified with a bicinchoninic acid (BCA) assay (Pierce) according to manufacturer's instructions. Bivalent cuprous ions react with proteins to monovalent copper and this copper can be quantitatively measured by complexation with bicinchoninic acid through formation of a purple colored solution. Sequential dilutions of 2 mg/ml BSA solution served as an internal calibration curve in each assay. Measurement was performed in duplicate using 96-well plates (Corning) and a Tecan photometer at 550 nm.

Substance	Amount
Tris-HCl (pH 7.5)	20 mM
NaCl	150 mM
EDTA	1 mM
EGTA	1 mM
NP-40	1%
sodium deoxycholate	1%
sodium pyrophosphate	2.5 mM
β-glycerophosphate	1 mM
Na_3VO_4	1 mM
Leupeptin	1 µg/ml

Table III-13: Composition of RIPA cell lysis buffer

Proteins have to be denatured for the antibodies to recognize their specific epitopes. This was accomplished by use of sodium dodecyl sulfate (SDS) and boiling at 95 – 100°C for 5 minutes. With this procedure the secondary and tertiary structures of the proteins are destroyed and the epitopes become unmasked for recognition.

Samples were therefore diluted in 4x SDS sample buffer (Table III-14), based upon the original Laemmli buffer recipe given in [164]. All proteins become negatively charged upon attachment of SDS with the size of the charge linearly dependent on the length of the protein.

Therefore proteins can be separated depending on their molecular weight in the SDS polyacrylamide gel electrophoresis (SDS-PAGE). β-Mercaptoethanol was added to reduce disulfide bonds within the proteins to ensure a linear configuration.

Substance	Amount
Tris (pH 6.8)	250 nM
SDS	8 %
Glycerol	40 %
Bromophenol blue	0.008 %
β-Mercaptoethanol	20 %

Table III-14: Composition of 4x concentrated SDS sample buffer

5.2. **Discontinuous SDS polyacrylamide gel-electrophoresis**

The gels used in electrophoresis are hydrophilic, three-dimensional networks of hydrocarbon chains. In this project gels containing 12 % acrylamide suitable for separation of proteins in the range of 10 – 70 kDa have been used. All gels consisted of two parts: A strongly buffered and stable resolving gel and a weakly buffered and loose stacking gel poured on top. This "two-gel" approach leads to a better resolution by creating a voltage discontinuity and therefore concentrating the sample at the gel boundary. Since the stacking gel has very large pores and a low ionic strength all proteins migrate comparatively fast through this gel to the border with the resolving gel. They then concentrate at this thin junction and migrate together into the resolving where they are finally separated into clean bands.

After mixing Acrylamide, Tris and SDS according to Table III-15 and Table III-16 the addition of APS and TEMED initiated gel formation. A comb was inserted and removed again when the gels were polymerized.

Substance	Amount
Acryamide/bis-acrylamide 30%/0.8%	40%
Tris pH 8.8	375 mM
SDS	0.1%
APS	0.05%
TEMED	0.05%

Table III-15: Constituents of a 12% resolving gel

Substance	Amount
Acryamide/bis-acrylamide 30%/0.8%	13%
Tris pH 8.8	125 mM
SDS	0.1%
APS	0.05%
TEMED	0.1%

Table III-16: Composition of a 4% stacking gel

After polymerization the gel apparatus was placed in the running chamber and the buffer reservoirs filled with electrophoresis running buffer (Table III-17). 30 µg of protein was loaded onto the gel for each sample and the colored molecular weight ladder "PageRuler"

(Fermentas) served as a size standard. The gels were run at a current of 20 – 35 mA until bromophenol blue reached the lower end of the gel.

Substance	Amount
Tris	124 mM
Glycine	960 mM
SDS	0.5%

Table III-17: Compostion of the electrophoresis running buffer used for running SDS polyacrylamide gels

5.3. **Semi-dry blotting**

A semi-dry electro-blotting technique was used to transfer the separated proteins onto the nitrocellulose membrane. To this end the gel was carefully removed from the glass plates and put onto the nitrocellulose membrane and a stack of blotting paper soaked in transfer buffer as shown in Figure III-4. Since treatment with SDS masks all the positive charges and gives every protein a net negative charge, they migrate towards the anode onto the blotting membrane. Current was limited to a maximum calculated by the following formula: $current\ [mA] = area\ [cm^2] * 0.8$. Depending on the molecular weight of the protein of interest blotting time varied between one and two hours.

Substance	Amount
Tris	50 mM
NaCl	150 mM
Tween 20	0.1%

Table III-18: Composition of western blot transfer buffer

Figure III-4: Schematic drawing of the layers used for semi-dry blotting of proteins. The acrylamide gel is placed on top of the transfer membrane between two stacks of buffer soaked Whatman paper.

5.4. **Detection**

To avoid unspecific binding the membrane was incubated in 1x blocking solution (Roche) for one hour under constant agitation. Primary antibodies were diluted in Tris buffer containing 0.1 % Tween (TBS-T, Table III-20) and 0.5x blocking solution. Incubations were performed for 2h at 37°C. Subsequently the membrane was washed three times for five minutes in TBS-T buffer. The membrane was then incubated for one hour with horse radish peroxidase (HRP) conjugated secondary antibody at room temperature. Antibody binding was visualized using

the enhanced chemiluminescence kit (Applichem) on a Hamamatsu gel recording system and Wasabi imaging software.

Antigen	Species	Dilution	Manufacturer
Connexin 37	Rabbit	1:600	Alpha diagnostics, San Antonio, USA
Connexin 40	Rabbit	1:600	Alpha diagnostics, San Antonio, USA
Connexin 43	Rabbit	1:1000	Sigma
K_v 1.5	Rabbit	1:100	Sigma
GAPDH	Mouse	1:1000	Chemicon, Hampshire, UK
Anti-rabbit HRP conjugate	Goat	1:5000	Calbiochem
Anti-mouse HRP conjugate	Goat	1:5000	Calbiochem

Table III-19: Overview of the antibodies used for western blotting

Substance	Amount
Tris-HCl (pH 7.4)	50 mM
NaCl	150 mM
Tween-20	0.3 %

Table III-20: Composition of Tris-buffered saline containing Tween (TBS-T). After dissolution of the components the pH was adjusted to 7.6 with HCl.

5.5. **Membrane stripping and re-probing**

To ensure equal loading the membrane was stripped and re-probed with anti-GAPDH antibody. To this end the membrane was incubated for one hour at room temperature in the stripping solution shown in Table III-21.

Substance	Amount
Glycine	0.2 M
NaCl	0.5 M

Table III-21: Composition of the stripping buffer for Western Blotting

6. Flow Cytometry

6.1. Principle and parameters

Flow cytometry, sometimes better known under the generic name “FACS” is a routine laboratory method for the live analysis of single cells in the range of 400 nm to 40 µm. It allows for the rapid multi-parameter analysis of thousands of events per second [165]. The instrument used for the experiments in this thesis was a Becton Dickinson FACSort flow cytometer. All further description and technical data refer to this instrument.

Functionally cells that are to be analyzed pushed from the sample tube through an injection tube. Sheath fluid then draws the cells along through the flow chamber and positions them in the middle of the laser beam by means of hydrodynamic focusing.

Two light scattering parameters are measured directly without further light filtering. Forward scatter (FSC) is a morphological parameter that is dependent on the relative size of the cell, while side scatter (SSC) is measured perpendicular to the laser beam and depends on the relative granularity / inhomogeneity of the analyzed cell. Three additional fluorescence channels can be used to investigate surface markers or after permeabilization intracellular protein levels, cell viability, apoptosis, membrane potential or calcium levels.

For this purpose optical filters are positioned in the light path to separate the signals emitted from the different fluorochromes. These fluorochromes absorb the laser light from the argon laser at 488 nm and emit at a specific longer wavelength. The signal is quantified with photomultipliers and further analyzed using CellQuest software.

6.2. Staining for surface antigens

Adherent cells were initially washed with PBS- and then detached with accutase at 37°C until the cells were in a single cell suspension. They were then re-suspended in growth medium and washed once in PBS containing 1% bovine serum albumin. Fixation was performed using a 3.7% formaldehyde solution. All centrifugation steps in this protocol were carried out at 352g for 3 minutes at room temperature.

The staining protocol was based on a standard flow-cytometry protocol and adapted for staining of NG2. To this end the cell pellet was centrifuged and the supernatant decanted. In the residual volume of approximately 100 µl the cells were incubated with 4 µl of anti-NG2 antibody (Abcam) for 45 minutes at room temperature followed by washing twice in a PBS/BSA solution. 4 µl of an Alexa-Fluor 488 conjugated goat anti mouse secondary antibody (Table III-10) was then added and incubated for additional 30 minutes at room temperature. After one more washing step 5000 cells were analyzed on the flow cytometer.

6.3. **Sorting of fluorescently labeled cells for miRNA analysis in co-cultures**

In a part of the study co-culture experiments were necessary to analyze the potential direct transfer of miRNA from one cell to an adjacent cell via gap junctions. Therefore a method was needed to analyze the cells separately after the co-culture to avoid the inclusion of donor cells in the measurements. For this purpose the FACSort flow is equipped with a mechanical sorting unit that can operate in three different modes of purity. All experiments were performed with the purity set to "exclusion". The sort rate was manually adjusted with the feed pressure to be around 300 events/second.

The co-culture protocol itself is described in detail in chapter III10. Briefly, at the start of the co-culture experiment the miRNA acceptor cells were labeled with the red fluorescent dye PKH-26 as described on page 29 and plated with miRNA transfected donor cells in 6-well plates. After 2 days of co-culture they were harvested, pelleted in a 50 ml centrifuge tube at 1500rpm for 7 minutes, resuspended in PBS- and then directly subjected to flow-assisted cell sorting. Gating was set on cells with positive fluorescence for PKH-26 in the FL-2 channel of the flow cytometer. 10.000 events were stored on the computer and an average of around 70.000 acceptor cells identified, isolated and collected. Re-analysis for PKH-26 positive cells from the sorted population indicated a purity of the isolated cells in excess of 98% as shown in Figure III-5.

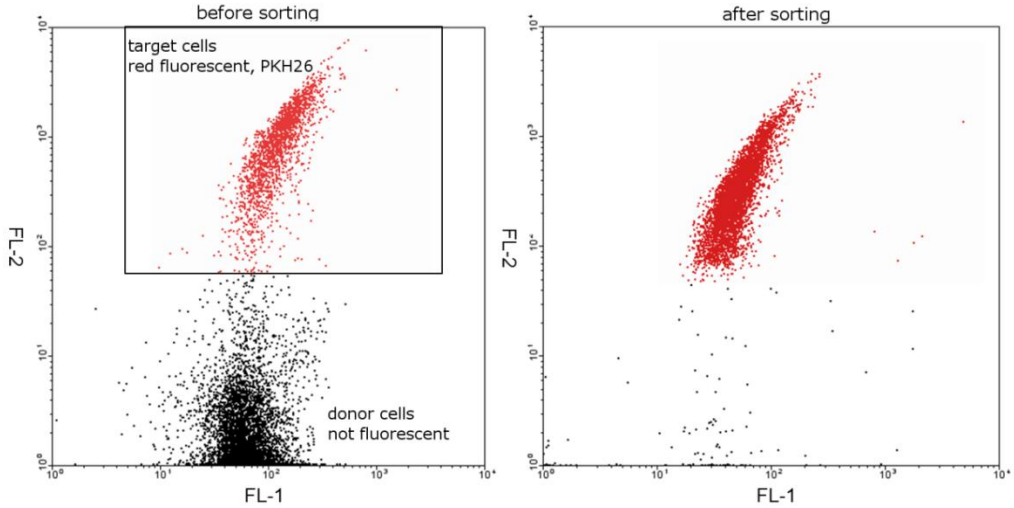

Figure III-5: Flow cytometry dot plots of the green (FL-1) and the red (FL-2) fluorescence channel. Before cell sorting (left) donor and acceptor cells form two clearly distinguishable populations. In a second measurement after cell sorting only the upper, PKH-26 labeled target cell population can be seen (right).

Sorted cells were collected in 50 ml tubes coated with BSA by short rinsing with 0.1% BSA solution prior to use. Following the sort cells were pelleted in a table top centrifuge at 1200rpm for 7 minutes and lysed immediately in 150 µl of passive lysis buffer for luciferase measurements as described in chapter 11.

6.4. Cell cycle measurements

6.4.1. Background and methodology

Cell cycle describes the series of events in the life cycle of a eukaryotic cell. Depending on the cellular growth state the cell cycle can be divided into different phases leading to division and proliferation of the cell [166]. Measurement of the current cell cycle phase of a cell is based on quantifying the cellular DNA content. This is accomplished by staining nucleic acids with propidium iodide (PI) followed by flow cytometry. PI is a DNA binding dye which shows a greatly increased fluorescence upon binding to double stranded nucleic acids. Therefore there is a linear correlation between cellular DNA content and emitted fluorescence.

Cells whose cell cycle is currently in the G0 or G1 phase possess a diploid set of chromosomes and therefore emit a certain amount of fluorescence. To be able to enter mitosis the whole cellular genome has to be duplicated in the S phase. This leads to an increase in fluorescence in flow cytometry. At the beginning of the G2 phase the cell has accumulated a double, tetraploid set of chromosomes and PI fluorescence is therefore doubled compared to resting cells in G0/G1 phase.

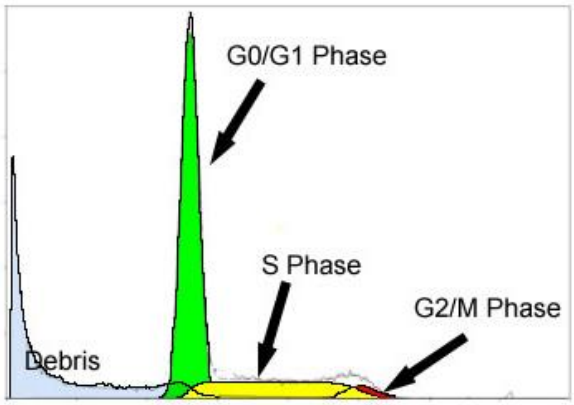

Figure III-6: Histogram of a flow cytometric DNA content measurement. Staining intensity with propidium iodide is directly prportional to the cellular DNA content and can therefore be used as a marker for the cell cycle stage distribution in the cell culture. image source: [4]

A common source of error in this method is caused by two or more cells sticking together in so called doublets or triplets. Two cells containing only a single set of chromosomes show up in the flow cytometer with a fluorescence signal equal to a single cell in G2 phase. To be able to detect and exclude this error it is possible to further analyze the electrical pulse generated in the photomultiplier tube. Signal area correlates with DNA content and signal width with the size of the cell or cell aggregate respectively. Therefore stepwise increases in signal width signify an aggregate of multiple cells and can be excluded from further analysis.

[4] http://www.phnxflow.com/MultiCycle.stand.alone.html, retrieved on 19.04.2012

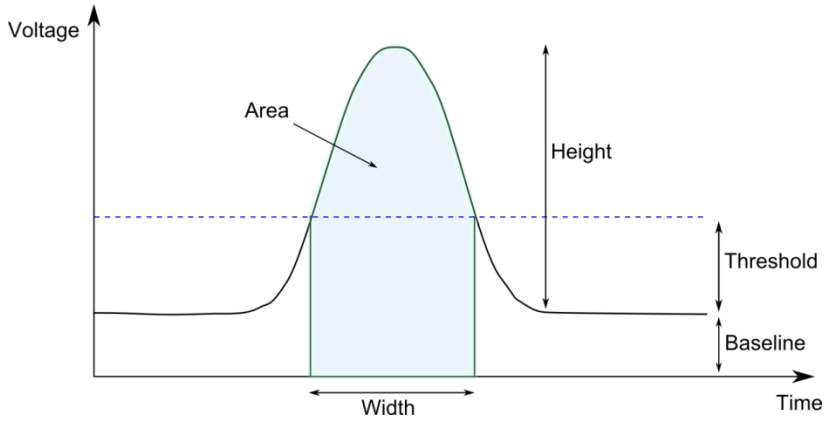

Figure III-7: Parameters measured on the PMT pulse in a flow cytometer

6.4.2. Experimental procedures

For cell cycle measurements cells were washed with PBS - and detached from the culture plate with trypsin until the cells were in a single cell solution. Detachment was stopped using full medium and the cells pelleted by centrifugation at 1200 rpm for 5 minutes. Subsequently, the supernatant was removed by aspiration and the pellet resuspended in 200 µl PBS -. For fixation and permeabilization the cells were then transferred into 5 ml FACS tubes containing 4 ml of ice-cold 70 % ethanol and incubated over-night at 4°C to help resolving sub-G1 peaks.

On the next day all the cells were pelleted at 1500 rpm for 3 minutes and resuspended in 300 µl of PI mastermix. Following 30 minutes incubation at 37°C, DNA content could be quantified directly in the flow-cytometer. FSC and SSC were used to distinguish cells from debris and a second gate was set onto single cells as described above. Percentages of cells in each phase were calculated by defining regions in a FL2 histogram.

Substance	Stock solution	PI master mix
Propidium Iodide	1 mg/ml	40 µl
RNase A	100 µg/ml	10 µl
PBS-	1x	950 µl

Table III-22: Preparation of PI staining buffer for cell cycle analysis. Propidium Iodide is a fluorescent DNA binding dye, RNAse A was added to degrade any leftover RNA to exclude co-quantification of RNA.

7. Patch clamp analysis

Patch clamp analysis was kindly performed in the lab of Prof. Dr. Wolfram Nagel, Physiology, LMU Munich.

7.1. Introduction

Patch clamp analysis is a technique to study the properties of membrane channels in cells. It was developed by Erwin Neher and Bert Sakmann and quickly became an indispensable tool. Both scientists received the Nobel Prize in Physiology in 1991. Patch clamping can be used in a variety of ways depending on the scientific approach. In whole cell patch clamping, multiple membrane channels are measured simultaneously over the membrane of the whole cell (Figure III-8).

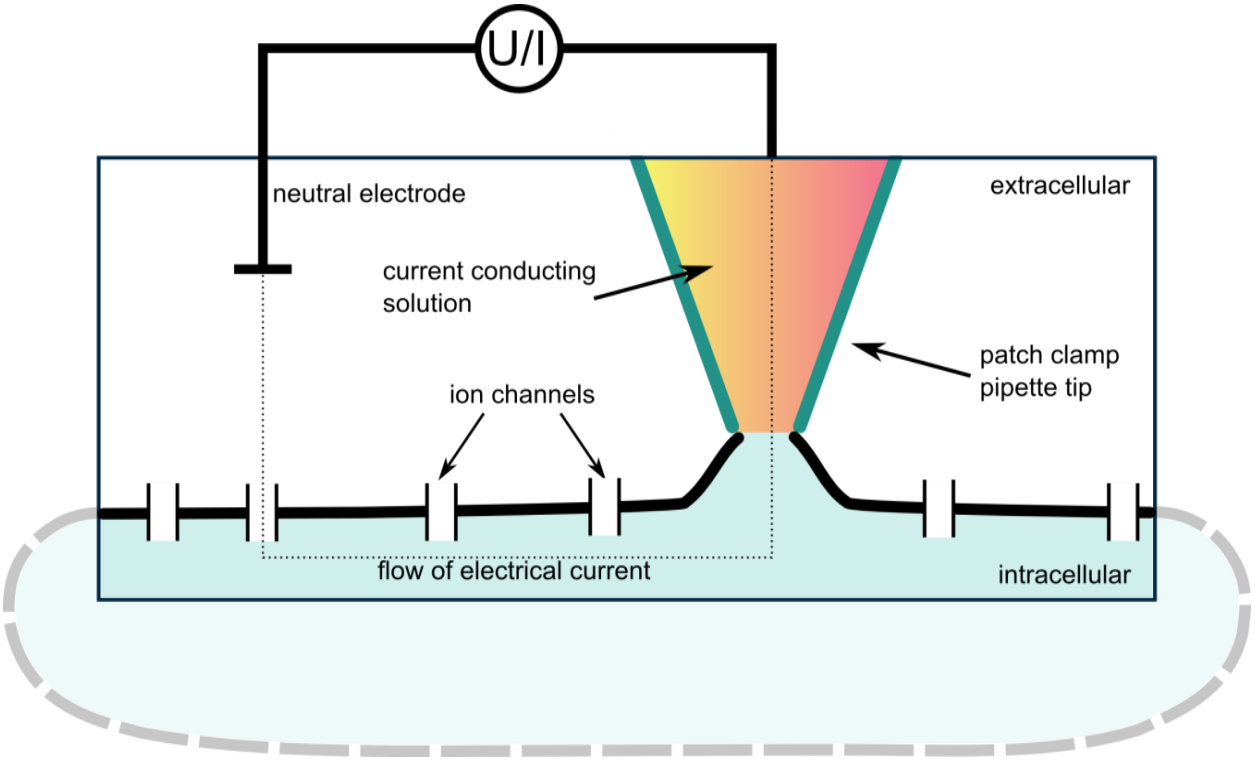

Figure III-8: Principle of patch clamping in whole cell mode. The pipette tip is lowered to the cell surface until it has contact with the membrane. The cell membrane within the area covered by the electrode is then broken by gentle suction and the electrical connection formed.

7.2. Experimental procedures

Patch clamping was used to analyze the membrane channel composition of hamster skeletal muscle pericytes. The dependency of the current on an applied voltage or changing ion concentrations as well as changes of the current induced by pharmacological treatment of the cells allowed drawing conclusions on the underlying channel ion specificity and type.

Primary pericytes were used 2 to 4 days after final selection and cells were seeded on the glass bottom of a custom made chamber. The setup was mounted on the stage of a Zeiss Axiovert MXX inverted microscope. Movement of micropipettes was performed using a piezo driven 3D micromanipulator. Micropipettes were prepared from borosilicate fiber glass tubing on a Sutter P77 puller and subsequently fire polished. Electrodes were filled with current conducting solution (Table III-23) and input resistance was in the range of 2 to 4 MΩ. Whole cell recordings were made with an Axopatch 200A patch clamp amplifier and its output was digitized with a Digidata 1200B AD-interface under control of the PC software PClamp 9.0. I/V relations were plotted using Clampfit and exported to Origin for further evaluation. By definition currents are measured from inside to outside, therefore "outward currents" are positive currents. Both, a flow of positively charged ions from the inside to the outside or equally of negative ions from the outside to the inside is termed an outward current.

Amount	Substance
120 mM	K-gluconate
5 mM	EGTA
2 mM	$MgCl_2$
10 mM	HEPES (pH 7.2)
4 mM	Na-ATP

Table III-23: Cellular pipette solution used for whole cell patch clamping

Experimentally a glass micropipette with an open tip was lowered onto the cell membrane under continuous control of resistance and capacitance, while a second, neutral electrode was placed in the culture bath. An increase of resistance indicated contact to the membrane. By suction a so called "gigaseal" was formed. In the next step the integrity of the cell membrane was broken by repeatedly applying low pressure through gentle suction and the electrode had a direct connection to the intracellular space. Establishment of the patch was indicated by a drop in resistance to values around 100 MΩ and an increase of capacitance to the value of the whole cell. Voltage and current across a biological membrane is primarily determined by the composition of the ion-channels set in the membrane. Either voltage or current can be kept unchanged while the respective other parameter is measured.

Measurements of the resting potential were conducted without sending current through the cell after adjusting the current flow to zero. Stimulation experiments always started with cells clamped at the resting potential and voltages were altered stepwise in 10 mV increments. Measurements were taken in the -120 mV to +70 mV range for a time of 100 to 200 ms. I/V diagrams always depict steady state currents.

Ion channel inhibitors and varying concentrations of potassium were used to further investigate the electrophysiological characteristics of the cellular ion channels. To apply the pharmacological agents the experimental bath (volume ~ 0.5 ml) was continuously superfused at a rate of 2 ml/min. In some experiments the chloride ions in PBS were substituted by gluconate on an equimolar basis. Three different substances were used to pharmacologically modulate potassium channel activity in the isolated cells: Flufenamic acid (FFA), 4-aminopyridine (4-AP) and tetraethylammonium (TEA). Respective chemical properties and structures are shown in Table III-24 and Figure III-9.

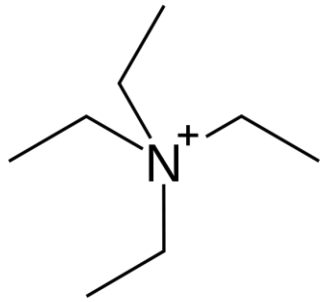

Tetraethylammonium (TEA)

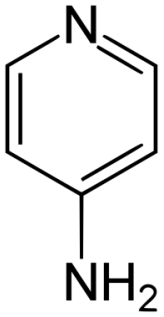

4-Aminopyridine (4-AP)

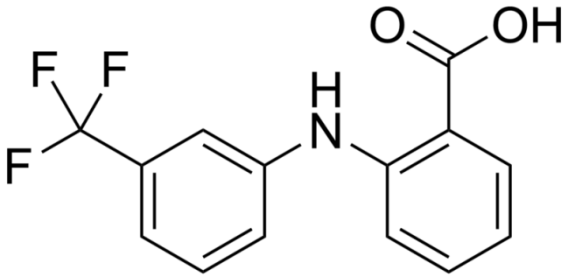

Flufenamic acid (FFA)

Figure III-9: Chemical structures of the potassium channel modulating agents. Source of all images: [5]

Substance	Action	Target	Conc. range	IC50
4-AP	Inhibitor	Voltage dependent K^+ channels	0.1 – 5 mM	288 µM in Hek293[6] 537 µM in CHO[7] 290 µM in MEL [167]
TEA	Inhibitor	Unsel. K^+ channels	10 mM	330 µM in MEL [167]
FFA	Activator Inhibitor	K^+ channels Ca^{++} activated Cl^- channels	10 – 300 µM	No data available 7 µM in adipocytes [168] 28 µM in oocytes [169]

Table III-24: Substances used to pharmacologically modulate K^+ channels (All supplied by Sigma).

[5] Wikipedia, all images are in the public domain
[6] Chantest cell line data sheet, available online: http://www.chantest.com/media/cms/pdf/spec_CT6138.pdf
[7] Chantest cell line data sheet, available online: http://www.chantest.com/media/cms/pdf/spec_CT6137.pdf

8. Quantification of gap junctional communication

8.1. Dye injection assay

Gap junctions represent channels between the cytoplasm of two adjacent cells. They allow for the free diffusion of small molecules up to around 1 kD size [41-45]. Therefore gap junctional coupling can be analyzed *in vitro* by injection of small molecular fluorescent dyes and subsequent monitoring of the spreading of the fluorescence signal to neighboring cells. For the current study the dye Alexa Fluor 488 was used at 3.5 mM concentration adapted from a protocol from Kameritsch et al [170].

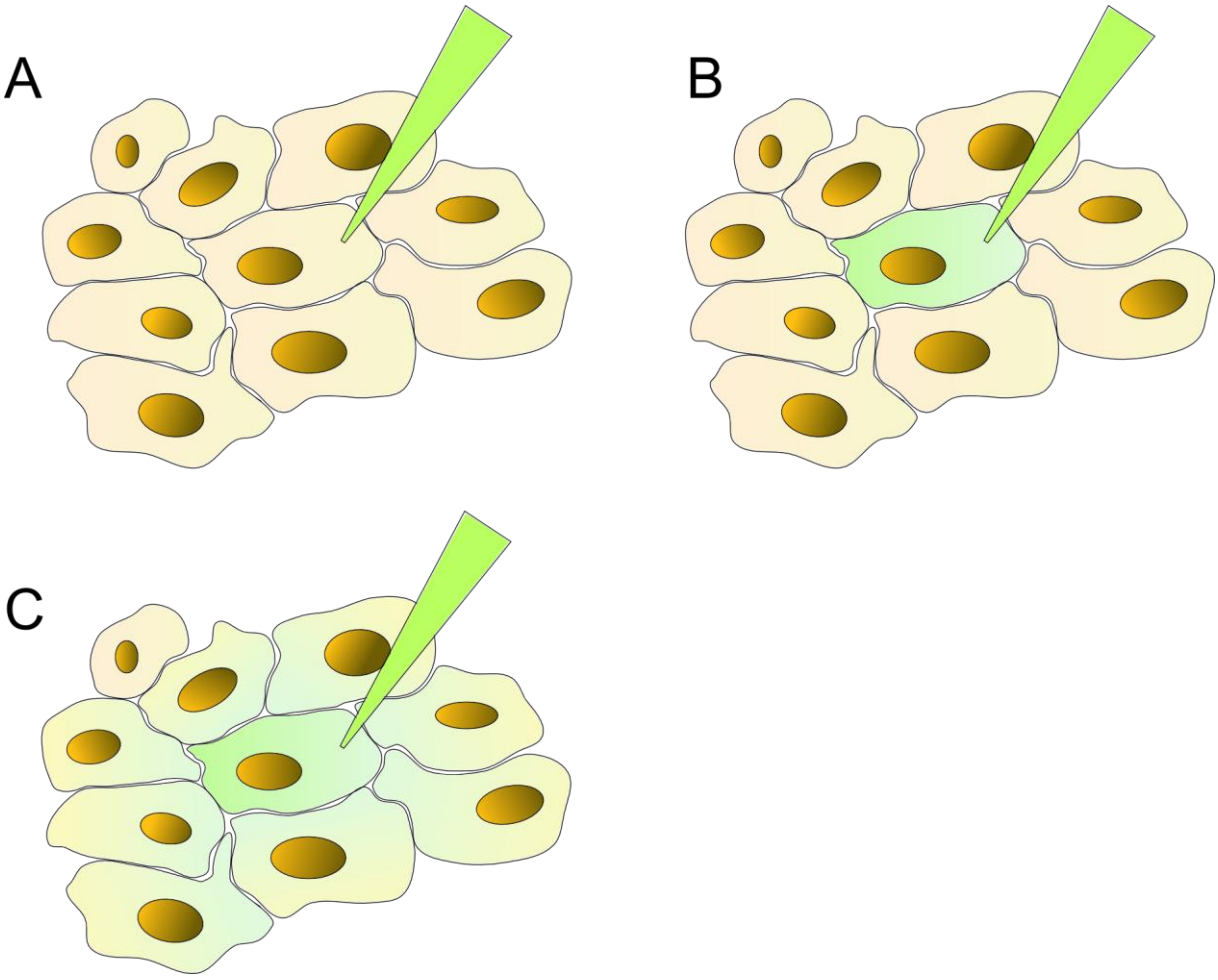

Figure III-10: Principle of a dye injection assay to analyze gap junctional coupling. **(A)** before start of the experiment, **(B)** injected cell is stained with Alexa 488, **(C)** spreading of the dye to adjacent cells

To analyze cell to cell communication co-cultures of HUVECs and pericytes were plated on collagen coated glass cover slides. To be able to definitely distinguish the two co-cultured cell populations HUVEC were labeled with the red lipophilic membrane dye PKH-26. Prior to the measurement the cells were incubated for 10 minutes in HEPES buffer containing N^{ω}-nitro-L-arginine (LNA, 30µM) to inhibit the endogenous NO-formation and superoxide dismutase (SOD, 50 – 500 U/ml) to eliminate superoxide anions. This treatment was used to achieve controlled starting conditions since both, NO and superoxide anions have been shown before to affect gap junctional communication [170-172].

Substance	Amount
NaCl	125 mM
KCl	3 mM
NaH_2PO_4	1.25 mM
$CaCl_2$	2.5 mM
MgCl	1.5 mM
Glucose	10 mM
HEPES, pH 7.4	10 mM

Table III-25: Contents of HEPES buffered saline solution

All injections were performed using the Femtojet injection system from Eppendorf in a custom made chamber on a heated microscope stage. Alexa Fluor 488 was injected using a dye filled micropipette at a tip pressure of 80 mmHg with injection duration of 0.5 s. Subsequently the fluorescence signals were recorded for 10 minutes after injection with a CCD camera (Till Vision, Gräfelfing). The absolute number of fluorescent cells after injection was taken as a quantitative measure for gap junctional coupling.

8.2. "Parachute" dye transfer assay

As a second means of quantifying gap junctional coupling between HUVEC and pericytes a so called parachute assay for flow cytometry was used. In this assay, as shown in Figure III-11, 100% confluent donor cells were pre-labeled in green with a 500 nM Calcein-AM solution for 30 minutes at 37°C. After very thorough washing, which is crucial to avoid background staining by remaining Calcein-AM, the cells were placed back in culture medium and "parachuted" with red fluorescent PKH-26 labeled acceptor cells. At certain time points cells were then trypsinized into a single cell solution and analyzed on a BD FACScan flow cytometer for red and green fluorescence. The FACScan flow cytometer is identical to the FACSort in the optical path, filter characteristics and detectors with the only exception being the absence of the sorting unit. Red acceptor cells can only acquire green fluorescence if they are coupled to donor cells via open gap junctions and take up the dye this way. Therefore the percentage of double positive cells and the mean green fluorescence of PKH-26 positive cells allow the quantitative analysis of gap junctional communication.

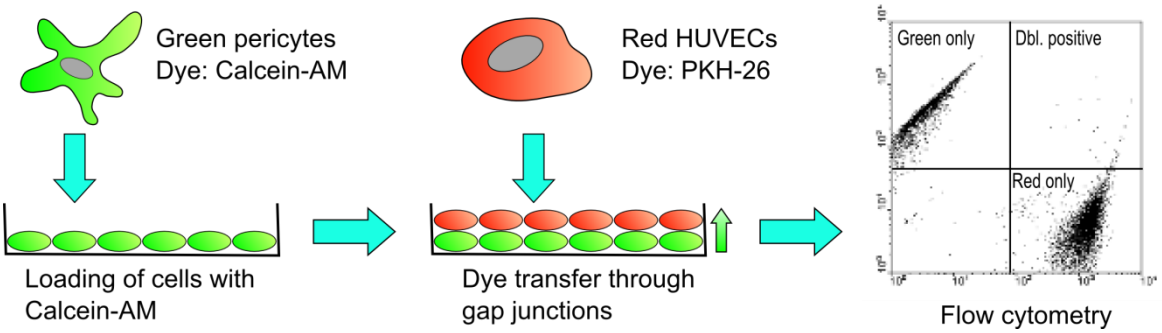

Figure III-11: Principle of the parachute dye transfer assay. HUVEC were fluorescently labelled with the dye Calcein-AM, which is intracellularly hydrolysed and therefore trapped intracellularly (left). Pericytes that were labeled with the red fluorescent membrane dye PKH-26 were then added (middle) and the percentage of double positive cells evaluated in flow cytometry (right).

9. Optical membrane potential measurements

9.1. Background

Optical membrane potential measurements were performed as a functional assay for the conduction of a hyperpolarization from pericytes to endothelial cells. Functionally the fluorescent dye $DiBAC_4(3)$ (Bis[1,3-dibutylbarbituric acid]trimethine oxonol). $DiBAC_4(3)$ is a membrane potential sensitive indicator, that enters depolarized cells and binds to intracellular proteins and membranes. Upon binding fluorescence is enhanced and a red-shift can be observed. Depolarization of the cellular membrane increases the influx of $DiBAC_4(3)$ and therefore leads to a stronger fluorescence signal. Since $DiBAC_4(3)$ is negatively charged it is not taken up by mitochondria and therefore not susceptible to mitochondrial interference. It has excitation optimum around 480 nm and emits preferentially at 505 nm. The method applied in this thesis has been described before [173, 174] and is now performed with minor modifications.

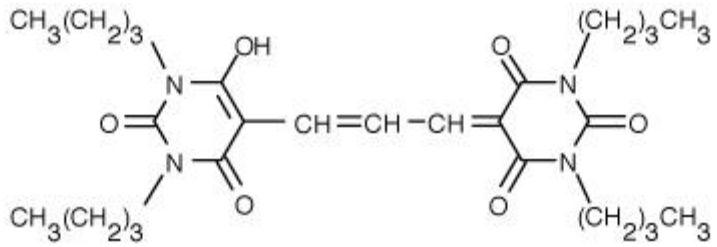

Figure III-12: Chemical structure of $DiBAC_4(3)$ (Image source: [8])

9.2. Experimental procedures

Optical membrane potential measurements were performed on a computer-controlled microscope setup (Till Photonics). Excitation was provided by a monochromator from a Xenon lamp at 480 nm wavelength and emission was detected at 505 nm with a cooled CCD camera. The setup was mounted on an inverted microscope Axiovert S100 (Zeiss).

For each experiment co-cultures containing PKH-26 labeled HUVEC and unlabeled pericytes were incubated for 20 minutes with HEPES containing SOD/LNA and 4µM $DiBAC_4(3)$. 10 seconds after starting the measurement 300 µM flufenamic acid was added to calculate the magnitude of the effect. Under these conditions reduced fluorescence indicated a depolarization of the cell membrane.

[8] Sigma-Aldrich website, retrieved: 19.09.2011

10. miRNA co-culture assay

10.1.1. Overview over the experimental model

For the quantification of miRNA transfer HeLa cells served as a model system that allowed a comparison of the presence and absence of gap junctional coupling between cells. Wildtype HeLa cells do not express connexins and therefore are communication deficient, whereas stable transfectants with connexin 43 regain this feature. This way a system comprising donor cells transfected with miR124 and acceptor cells containing a miR124 specific detection system could be established under coupled and under control conditions (Figure III-14). The miR124 sensitive detection system was constructed by inserting a miR124 specific recognition site in the 3' UTR of an established luciferase expression vector. The amount of luciferase protein synthesized and consequently also the amount of light generated therefore is inversely proportional to the amount of miR124 present in the acceptor cell (Figure III-13).

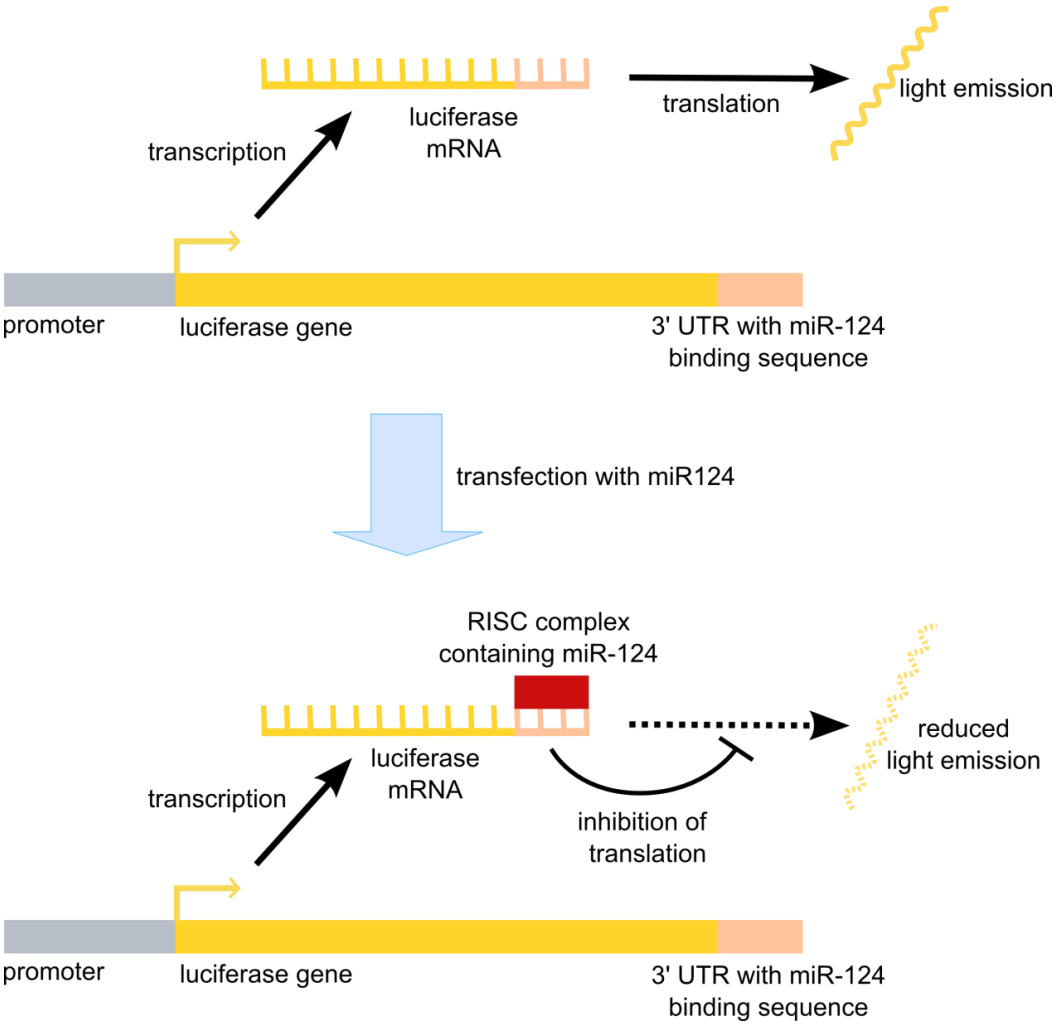

Figure III-13: Assay principle of the luciferase system to quantify the amount of miR124 activity *in vitro*. Under control conditions luciferase mRNA is transcribed from the vector construct in transfected acceptor cells and then translated unhindered into luciferase protein. The activity of this enzyme can be quantified by measuring the amount of emmited light (top panel). If miR124 is present it can recognize a specific binding site in the 3' UTR of the luciferase mRNA and through this induce translational silencing leading to reduced light emmission (bottom panel).

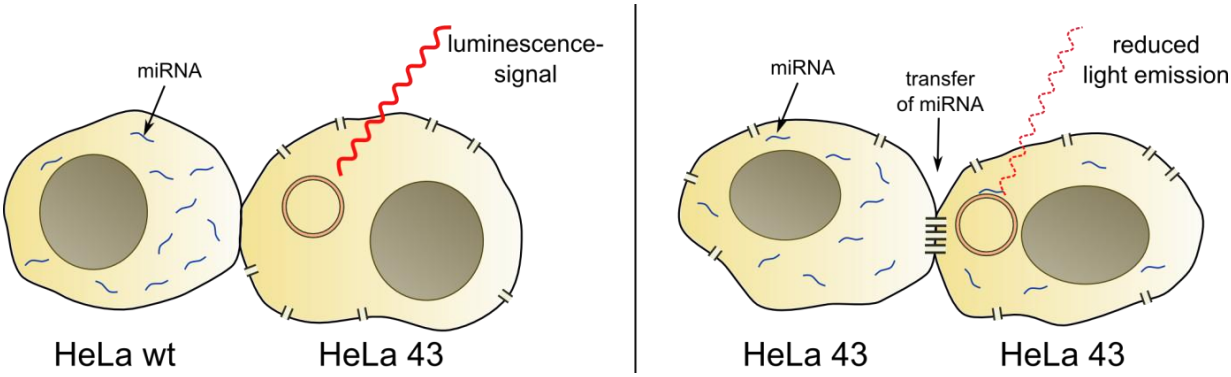

Figure III-14: Experimental design of the co-culture experiments. Donor cells containing miR124 are co-cultured with acceptor cells that have been transfected with a miR124 sensitive luciferase reporter construct. If no gap jucntional transfer of the miRNA is possible a strong luminescence signal can be detected in the luminometer (left panel). If in contrast miR124 is transferred from donor to acceptor cells via gap junctions the signal intensity is attenuated (right panel).

10.1.2. Detector vector constructs

The miRNA detection constructs were generated using the commercially available vector pIS2 that was obtained from the Addgene plasmid repository (#12177). It was originally derived from pRL-SV40 by adding additional cloning sites. As shown in Figure III-15 the plasmid contains a Renilla luciferase reporter driven by the SV40 early enhancer/promoter. To render the luciferase expression sensitive to miRNA, a dimeric, fully synthetic miRNA recognition site was inserted via *Sac*I and *Xba*I restriction digestion followed by T4 ligation at the site indicated in Figure III-15.

```
     CTG GCA TTC ACC GCG TGC CTT ATG GCA TTC ACC GCG TGC CTT AT
TCGA GAC CGT AAG TGG CGC ACG GAA TAC CGT AAG TGG CGC ACG GAA TA GATC
```

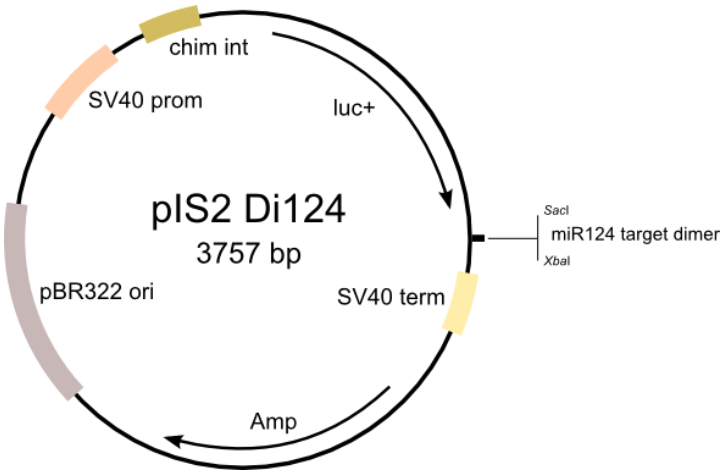

Figure III-15: Structural elements of the pIS2 vector with the sequence of the synthetic miR124 recognition dimer inserted between the *Sac*I and *Xba*I restriction sites in the 3' UTR of the luciferase gene (luc+).

To normalize for cell number variations and inconstant transfection efficiencies a second luciferase plasmid, pGL3 control that drives the constitutive expression of firefly luciferase under an SV40 promoter was always co-transfected.

10.1.3. Experimental procedures for co-cultures with miR124 with FACS sorting

HeLa wildtype and HeLa43 cells were split into 6-well plates on the day before transfection. On the next day donor cells were transfected with 100 nM synthetic miR124 mimic (Dharmacon) according to the amounts given in Table III-26. In parallel the acceptor cells were stained fluorescently with PKH-26. The cells were subsequently left in the incubator for two hours and then very thoroughly washed with PBS. All cells were detached from their culture dishes by treatment with accutase and washed by centrifuging at 1500 rpm for 7 minutes in a table-top centrifuge. After resuspension in full medium the cell number was determined in a Neubauer counting chamber. Co-cultures were mixed in a 3:1 to a 5:1 donor to acceptor cell ratio and plated at 70 – 80 % confluency into 6-well plates. On the next day the whole co-culture was transfected with the detection plasmids as shown in Table III-27. Details on the transfection protocol are given in chapter III3. 48 hours after putting the cells in co-culture, they were detached with accutase as a single cell solution and subjected to flow cytometric cell sorting as described in chapter 6.3. Following this procedure purified acceptor cells were obtained strongly diluted in FACS sheath fluid and therefore pelleted at 1700rmp for 7 minutes in a table-top centrifuge. The cells were lysed directly in passive lysis buffer (Promega) and luciferase activity measurements taken immediately in a luminometer (Berthold Instruments).

Substance	Amount
Serum free medium	88 µl
Synthetic miRNA (20µM stock)	12 µl
HiPerFect reagent	12 µl

Table III-26: Amounts of the reagents for a 100nM transfection with miRNA in one 6-well

Substance	Amount
pGL3 control plasmid	7.5 ng
pIS2 Di-124	3 ng
pUC18	1 µg

Table III-27: Amounts of the detection plasmids used to transfect a 6-well for the co-culture experiment

10.1.4. Experiments without cell sorting including mutated detection plasmids

Further experiments were performed to experimentally verify the transfer of miRNA through gap junctions in a modified system with additional controls. As a second miRNA, miR15b was chosen. miR15b potentially plays an important role in vascular biology through the regulation of VEGF expression [175, 176].

The co-culture protocol was furthermore modified to be performed without the flow cytometric sorting step. As a supplementary control, three bases in the seed recognition sequence were mutated, similar to the methodology used in [177] in order to inhibit the miRNA binding. The sequences of the wild-type and respective modified binding dimers are

given in Table III-29. Cell numbers were strictly standardized in all experiments using an automated cell counter (Beckman Coulter Z2).

On the day before transfection 10^6 cells were plated in a 10 cm dish to serve as acceptor cells and 200,000 cells per 6-well were seeded as donor cells. On the following day, acceptor cells were transfected directly in the 10 cm culture dishes with the miR15b detection plasmids pIS2 in the amounts given in Table III-28. Transfections with the mutated miR124 detection plasmid were performed according to Table III-27 in 10 cm culture dishes and scaled up by the factor 8, compensating for the difference in culture dish area. Simultaneously donor cells were transfected with either 100 nM synthetic miRNA mimic or miRNA negative control (Dharmacon) in the 6-well plates (amounts are given in Table III-26). All cultures were incubated for 1 h with the transfection solution and then washed thoroughly three times with PBS-. To allow for the uptake of residual transfection solution into the cells, cell cultures were left in the incubator for two to three additional hours. Cells were then detached with accutase and counted in an automated cell counter (Beckman-Coulter Z2). 125.000 cells were put in co-culture in 24-well plates in a 5:1 ratio for 48 hours. Following this incubation cells were washed in PBS- and lysed directly in the culture plate by addition of 1x passive lysis buffer (PLB, Promega). All experiments were performed in triplicates and means calculated for further evaluation.

Substance	Amount
pGL3 control plasmid	200 ng
pIS2-miR15b	1 µg
pUC18	5 µg

Table III-28: Amounts of the detection plasmids used in the miR15b experiments for transfection in 10 cm culture dishes.

miR124 target dimer with seed recognition sequence mutations
CTG GCA TTC ACC GCG Tcg gTT ATG GCA TTC ACC GCG Tcg gTT AT TCGA GAC CGT AAG TGG CGC Agc cAA TAC CGT AAG TGG CGC Agc cAA TA GATC
Native miR15b target dimer
CTT GTA AAC CAT GAT GTG CTG CTA TTG TAA ACC ATG ATG TGC TGC TAT TCGA GAA CAT TTG GTA CTA CAC GAC GAT AAC ATT TGG TAC TAC ACG ACG ATA GATC
miR15b target dimer with seed recognition sequence mutations
CTT GTA AAC CAT GAT GTG aTc CcA TTG TAA ACC ATG ATG TGa TcC cAT TCGA GAA CAT TTG GTA CTA CAC tAg GgT AAC ATT TGG TAC TAC Act AgG gTA GATC

Table III-29: Sequences for the miR15b vector inserts and the 3-5 mutated miR124 dimer. In the top panel the native miR15b target dimer sequence is shown, in the lower two panels the three mutations in the seed recognition sequence are given in lower case for the miR15b and miR124 target dimers

11. Luciferase gene expression assay

11.1. Background

Luciferase reporter gene activity was quantified with a Dual-Luciferase Assay kit (Promega). In this system two individual reporter luciferase proteins are expressed and they can be quantified in subsequent reactions. This allows for the use of an internal control that provides a baseline for the normalization of experimental data for factors such as transfection efficiency, cell number, growth characteristics and cell lysis efficiency.

In the assay used in this thesis firefly (*Photinus pyralis*) and Renilla (*Renilla reniformis*) luciferases coded on two different plasmids were used. These two enzymes have distinct evolutionary backgrounds and therefore developed different substrate and co-factor requirements. *In vitro* they can be measured sequentially from a single tube by quenching firefly luciferase luminescence before adding the specific Renilla luciferase substrates.

11.2. Experimental procedures

Passive lysis using the supplied passive lysis buffer (PLB) was either performed directly in the plates for transfected cells or within the 50 ml collection tubes obtained in FACS sorting. The manufacturer's protocol was modified to use only half the amount of reagents.

For this purpose a 5x stock solution of PLB was diluted with distilled water by adding 1 volume of PLB to 4 volumes of water. For each well 500 µl of 1x PLB was prepared. Cells were then washed once in PBS- and 500 µl of 1x PLB was added. The plate was then placed on an orbital shaker for 15 minutes at room temperature to allow for complete cell lysis. Meanwhile the luciferase assay substrate LAR II was thawed from -80°C stocks and 50 µl of Stop&Glo solution prepared from the manufacturer provided 50x stock solution by diluting with the supplied Stop&Glo buffer.

50 µl of LAR II was pre-dispensed into luminometer tubes and 10 µl of cell lysate added by pipetting directly into the liquid. Firefly luminescence was then quantified in a Berthold LB9507 tube luminometer with a 10s measurement time. Subsequently 50 µl of 1x Stop&Glo solution was added and Renilla luminescence quantified for another 10 s. Finally Renilla readings were normalized to firefly luminescence.

12. Statistical analysis

Data were collected and organized in Microsoft Excel spreadsheets. Summary files containing means of all experimental data were assembled to facilitate graphing and statistical evaluation of the data. For statistical computing the corresponding data was imported and analyzed using the statistics package SPSS 20 (IBM). In all experiments error probabilities (p-values) smaller than 0.05 were considered significant. Graphs were created either in Excel 2010 (Microsoft), Sigmaplot 8.0 (Systat Software) or Origin (Microcal). The tests used and the resulting p-values are additionally mentioned in the respective figure legends.

Differences between the distributions in the experiments on the spreading of a calcium wave from HUVEC to pericytes (chapter IV4.3) were analyzed with the nonparametric Kruskal-Wallis test for independent samples. A previous Kolmogorov-Smirnov test did not yield normal distribution of the data.

The differences between the treatment groups for cell cycle analysis (chapter IV5.2) were examined using a Wilcoxon matched-pair signed ranks test since for small sample sizes it is not possible to test adequately for normal distribution.

Data on the time course of the transfer of the small molecular weight dye calcein (chapter IV5.3) were analyzed with the SPSS module for univariate general linear model analysis. This statistical tool allows performing the analysis of variance (ANOVA) for experiments with two or more factors. This way the differences over the time course and the differences between the different groups could be considered.

The data on miRNA transfer through gap junctions experiments using miR124 and cell sorting was evaluated a Wilcoxon matched-pair signed-rank test, following normalization of the data to the not co-cultured control (chapter IV5.5.1). In these experiments due to the low sample number normal distribution could not be assumed.

In the miR15b experiments (chapter IV5.5.2) a paired samples Wilcoxon signed ranks test was used since the underlying data were shown not to be normally distributed according to the Kolmogorov-Smirnov test.

IV Results

1. Isolation of cells showing a pericyte-like phenotype

1.1. Growth characteristics and cell morphology

Isolated and purified cells showed a characteristic pericyte-like morphology, consistent with previous reports on pericytes. The direct comparison with human umbilical vein endothelial cells (HUVEC) and smooth muscle cells (SMC) showed distinct morphological differences and clearly delineated those cell populations. As depicted in Figure IV-1 they had an irregular shape with long processes protruding from large and flat cell bodies. Their size was approximately 150 x 100 µm, although long extensions from the cell body could extend even further.

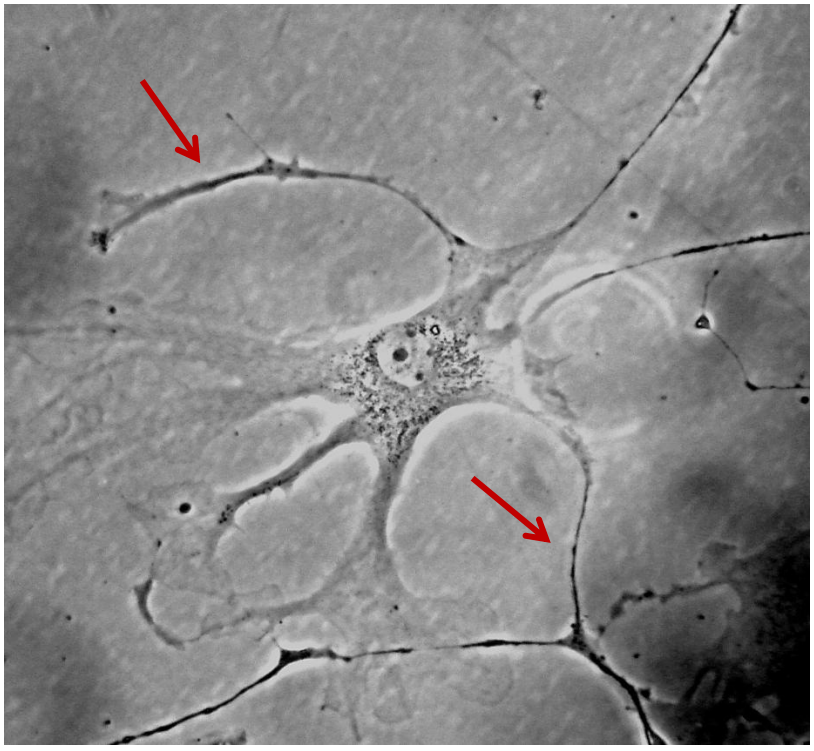

Figure IV-1: Morphology of a hamster skeletal muscle pericyte at day 15 in cell culture showing the typical flat cell soma and long extending protrusions (arrows).

1.2. Pericyte medium selectively supports pericyte growth

To analyze the selecting effect of pericyte culture medium, primary pericyte cultures, HUVEC and porcine arterial endothelial cells (PAEC) were grown in pericyte medium for two weeks. Images were recorded on days 0, 7 and 14 to analyze changes in cell morphology. As is shown below this medium favors the selective growth of pericytes over endothelial cells. Interestingly, HUVEC and PAEC cultures also seem to contain a small amount of pericytes that survive in these cultures, when the endothelial cells have already died.

Primary hamster culture in pericyte medium

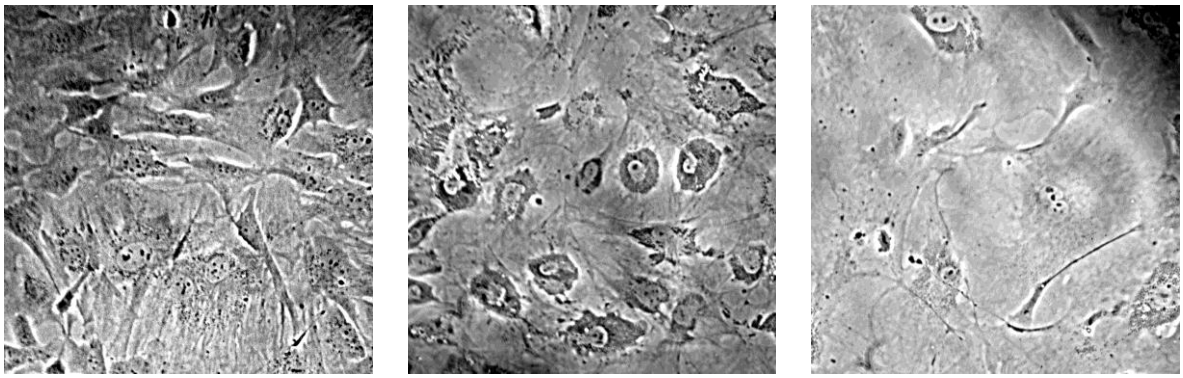

day 0 day 7 day 14

HUVEC in pericyte medium

day 0 day 7 day 14

PAEC in pericyte medium

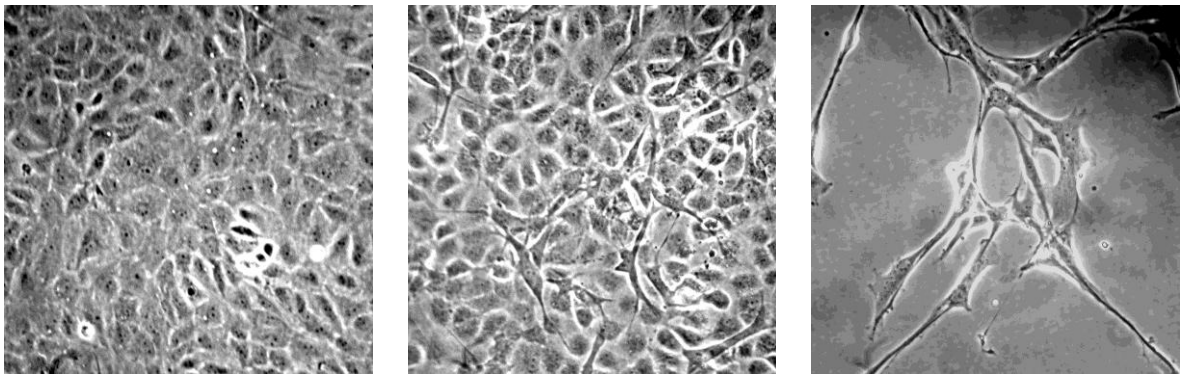

day 0 day 7 day 14

Figure IV-2: Representative images of a primary hamster pericyte (top), HUVEC (middle) and PAEC (bottom) culture at days 0, 7 and 14 grown in pericyte medium. Pericyte medium selectively promotes the growth of pericytes over endothelial cells in mixed cultures on days 7 and 14.

1.3. **Expression of pericyte markers**

The isolated and bead-isolated cells were analyzed for the expression of typical pericyte markers after 16 – 30 days in culture in passage one or two. For this purpose three different methods were used to demonstrate the expression of previously published pericyte markers in the isolated cells. In this respect western blotting served as a sensitive way to detect marker-proteins in whole cell lysates, while immunofluorescence staining yielded data on the (sub-) cellular localization and flow-cytometry allowed the co-analysis of multiple markers on the single cell level. Since there seems to be no single and universally accepted pericyte marker, a panel of markers was selected to characterize the cells.

1.3.1. Qualitative analysis: Western Blotting

Detection of the marker antigens in cell lysates of HUVEC, SMC and PC was performed using western blot analysis. Data from a representative experiment are shown. HUVEC and SMC served as controls for the most probable cellular contamination in the culture. While pericytes stained positive for αSMA, NG2 and PDGFR-β, they were negative for vWF (Figure IV-3). vWF is an essential endothelial protein and accordingly was found to be present in HUVEC. SMC and pericyte cultures were negative for vWF (n=3 independent cell cultures, the unspecific dot in the SMC lane was present only in the blot shown and is of unknown origin). Data from a representative experiment is shown (Figure IV-3).

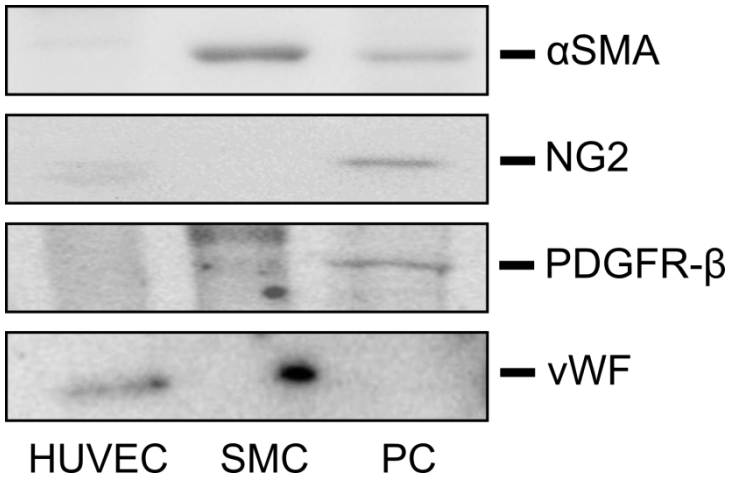

Figure IV-3: Western Blot analysis for the expression of pericyte markers. The isolated pericytes express the typical pericyte marker proteins PDGFR-β, NG2 and αSMA. HUVEC and SMC were used as controls. Images depict typical results as observed in 3 independent cell cultures.

1.3.2. Analysis of pericytic markers in immunofluorescence staining

To further characterize the pericytic phenotype of single cells in culture, immuno-cytochemical double-staining with specific antibodies was performed. NG2, αSMA and PDGFR-β have been described in detail in the previous chapter. In our cultures about 80-90% of the cells stained double positive for NG2 and αSMA or double positive for αSMA and PDGFR-β (Figure IV-4; n=4 independent cell cultures each). In contrast, no staining was detectable with the endothelial cell marker von Willebrand factor (vWF) while HUVEC as endothelial controls stained positive for vWF.

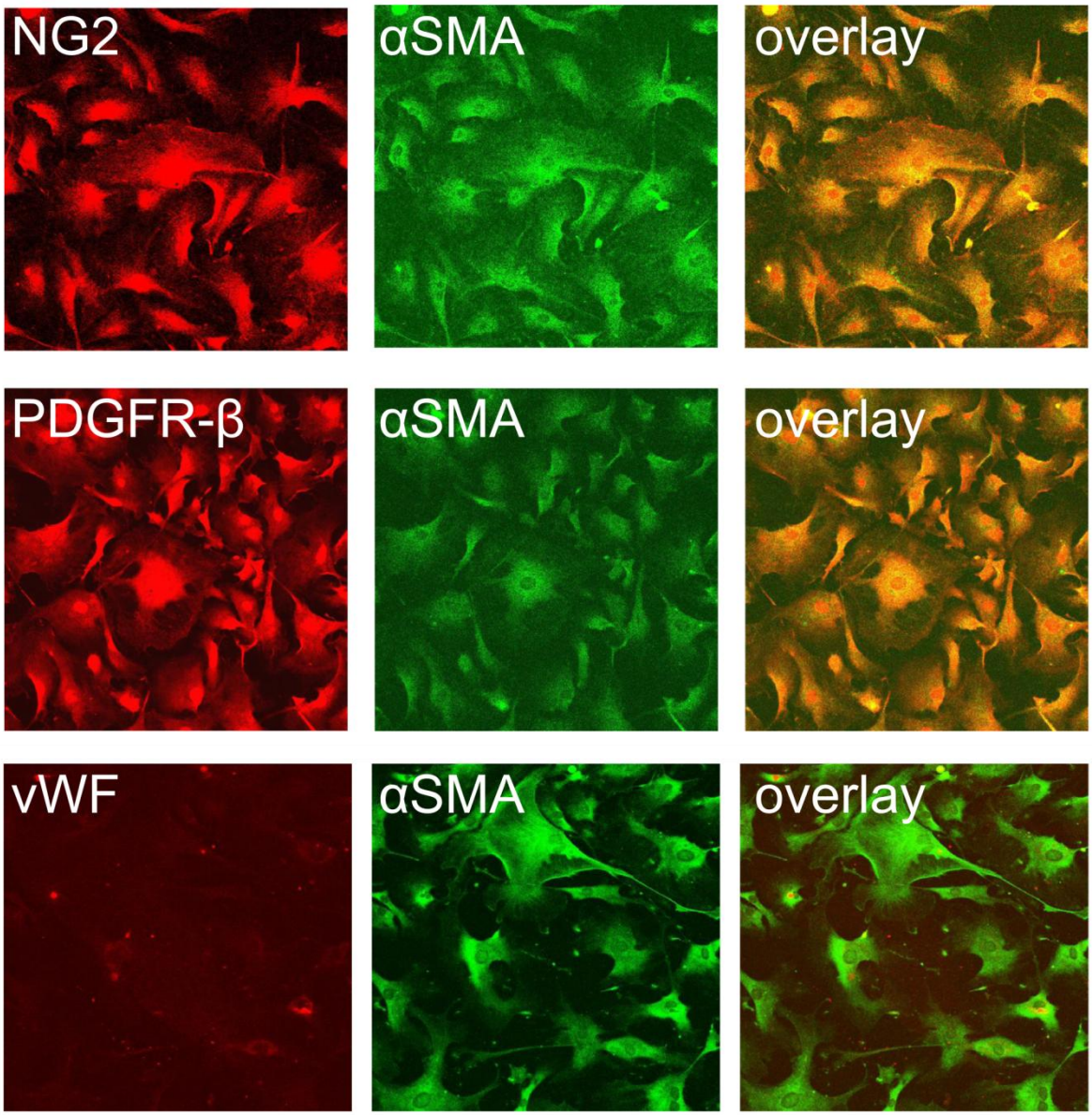

Figure IV-4: Representative images showing positive staining of pericytes in culture for the established pericyte markers NG2 and PDGFR-β (Top and middle panels, n=4, representative images shown). On the lower panel pericytes show no staining for the endothelial marker vWF (n=4, representative image shown).

1.3.3. Quantitative analysis: Flow cytometry

To obtain a more precise quantitative estimate of the pericyte content in the purified and selectively grown cultures, five cultures were additionally analyzed for NG2 expression in flow cytometry. In accordance with estimates from immunocytochemistry, this analysis indicated a mean percentage of NG2 positive cells of 81% ± 4.7% (mean ± SD).

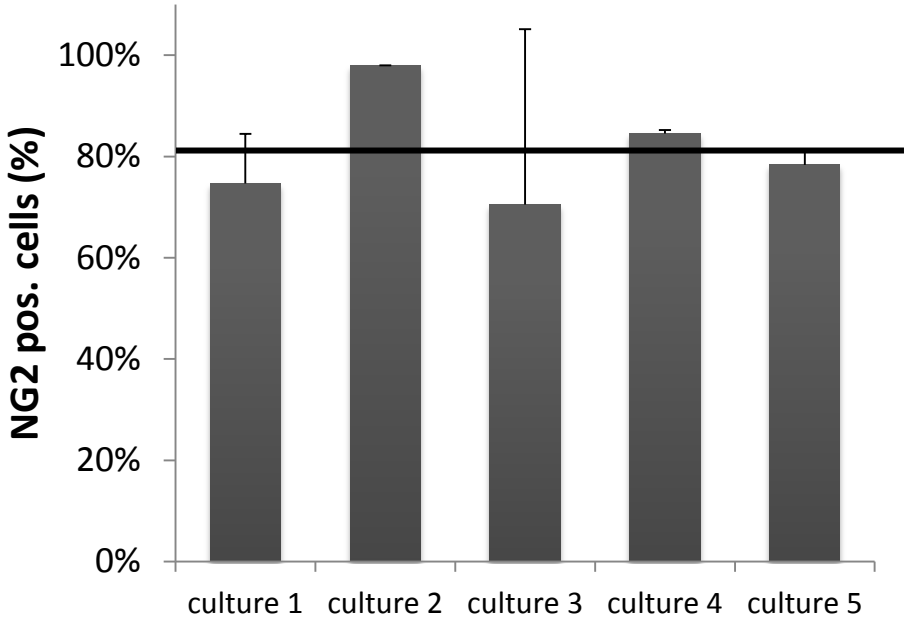

Figure IV-5: Quantitative analysis of NG2 expression in five individual pericyte cell preparations using flow cytometry. On average 81 % of the cells in the total population were positive for NG2 (horizontal line). Cultures 1 to 4 were stained with a rabbit antibody (Santa Cruz), while culture 5 was stained with a mouse antibody (Abcam), n = 3-6 measurements per cell isolation, means ± SD.

1.4. **Detection of pericytes in muscle sections**

1.4.1. Methodology

In the next step sections from hamster cremaster were analyzed with regard to pericyte markers. Pericytes have been described to be found in close vicinity of small vessels and are expected to stain positive for the markers that have been found in western blotting and flow cytometry. For this purpose cross and longitudinal sections of thigh and cremaster muscle were subjected to immunohistochemistry. A staining for lectin was used to identify the endothelium of microvessels.

1.4.2. αSMA positive cells are found in the immediate vicinity of skeletal muscle microvessels

Since hamster pericytes were positive for the expression of αSMA in western blotting and immunostainings, αSMA was chosen as a marker protein to analyze the *in vivo* presence and distribution pattern of pericytes in hamster cremaster muscle. Paraffin sections were stained with a mouse antibody against αSMA and microvessels visualized by co-staining with fluorescently labeled lectin. Vascular smooth muscle cells also stained positive for αSMA in tissue sections but could be distinguished by their characteristic shape and the lack of further marker expression ($K_V1.5$).

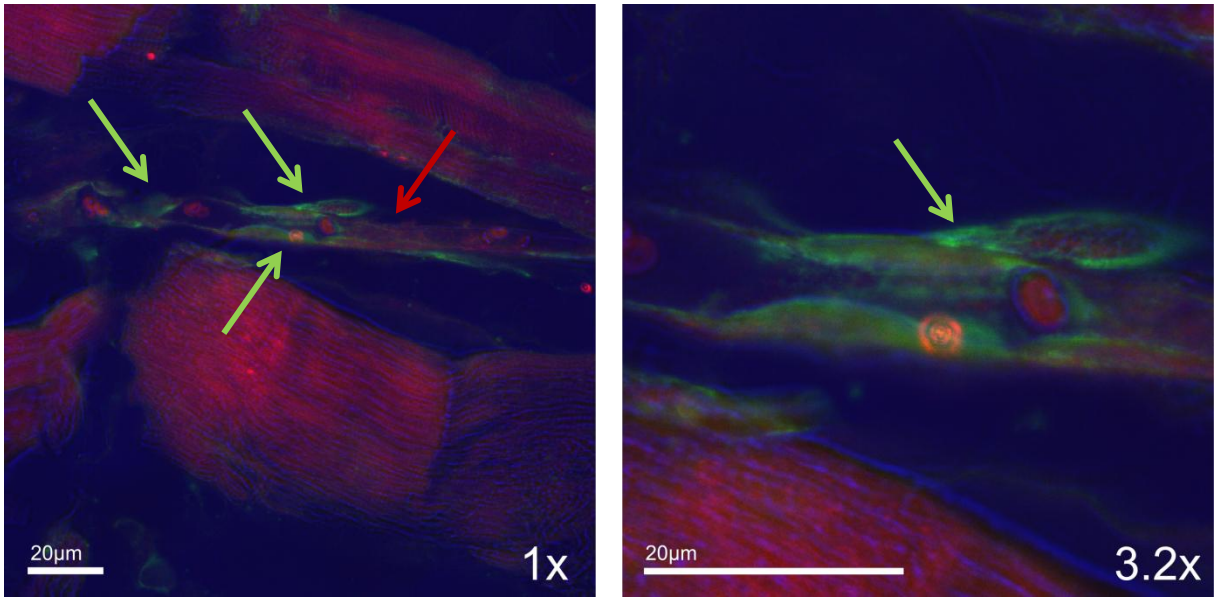

Figure IV-6: Staining of αSMA positive cells (green staining and arrows) in 16µm paraffin sections of hamster cremaster muscle, vessel staining was performed with lectin (red fluorescence and arrow). Red staining within the vessel is likely caused by erythrocyte autofluorescence. Representative confocal images were taken with a 63x objective, zoom 1x (left), zoom 3.2x (right); Scale bars: 20 µm

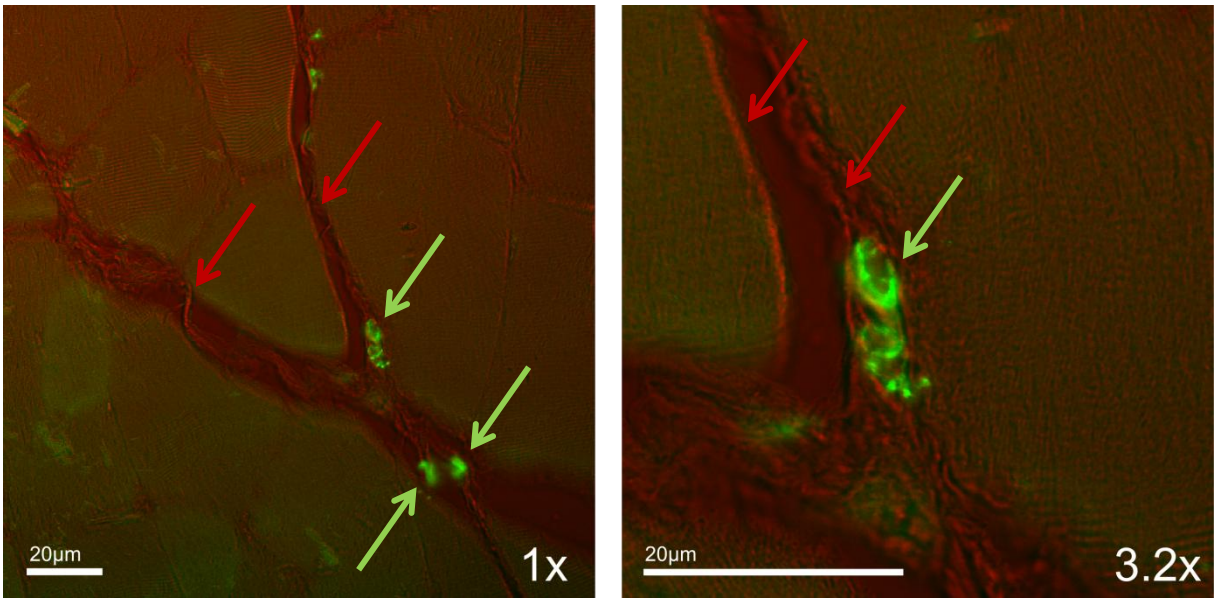

Figure IV-7: Staining of NG2 positive cells (green staining and arrows) in 5µm paraffin sections of hamster cremaster muscle. Vessels were stained with lectin (red fluorescence and arrows); Representative confocal images were taken with a 63x objective, zoom 1x (left), zoom 3.2x (right); Scale bars: 20 µm

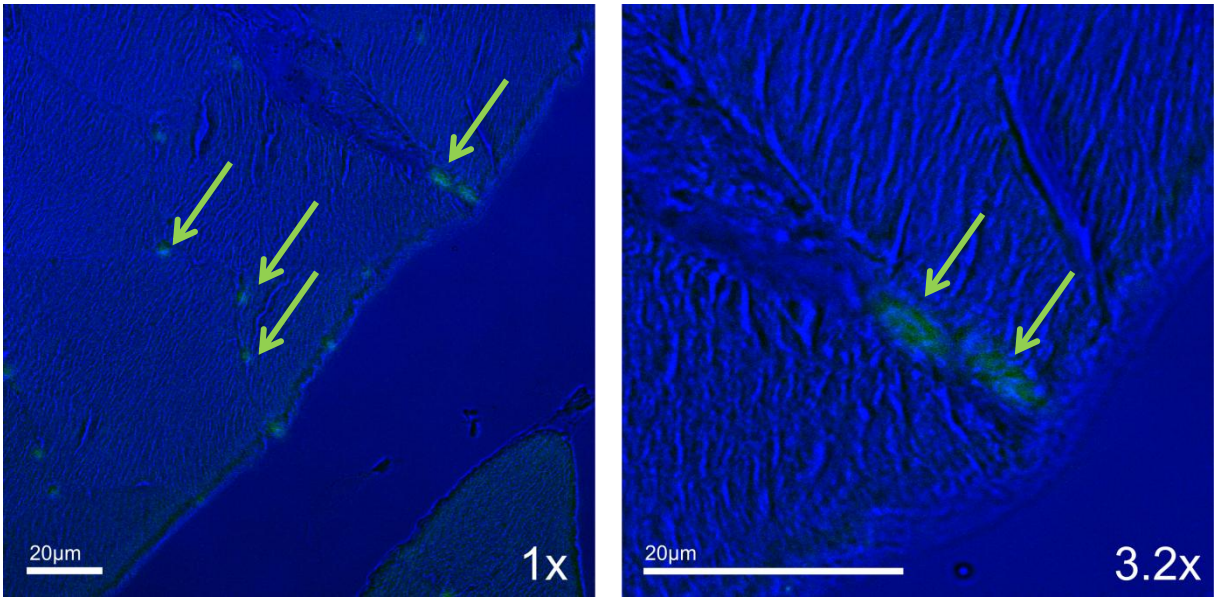

Figure IV-8: Staining of 3G5 positive cells (green fluorescence and arrows) in 5 µm hamster cremaster muscle paraffin sections; Confocal images taken with 63x objective, zoom 1x (left), zoom 3.2x (right); Scale bars: 20 µm

1.4.3. Sympathetic nerve cords along microvessels are also stained with 3G5

Staining of isolated hamster microvessels for 3G5 positive cells also cells yielded a string like fluorescence pattern that was most likely not caused by pericytes. Since neurons have also been described to be recognized by the 3G5 antibody this pattern is presumably caused by sympathetic innervation of the vessel ([178, 179], Figure IV-9).

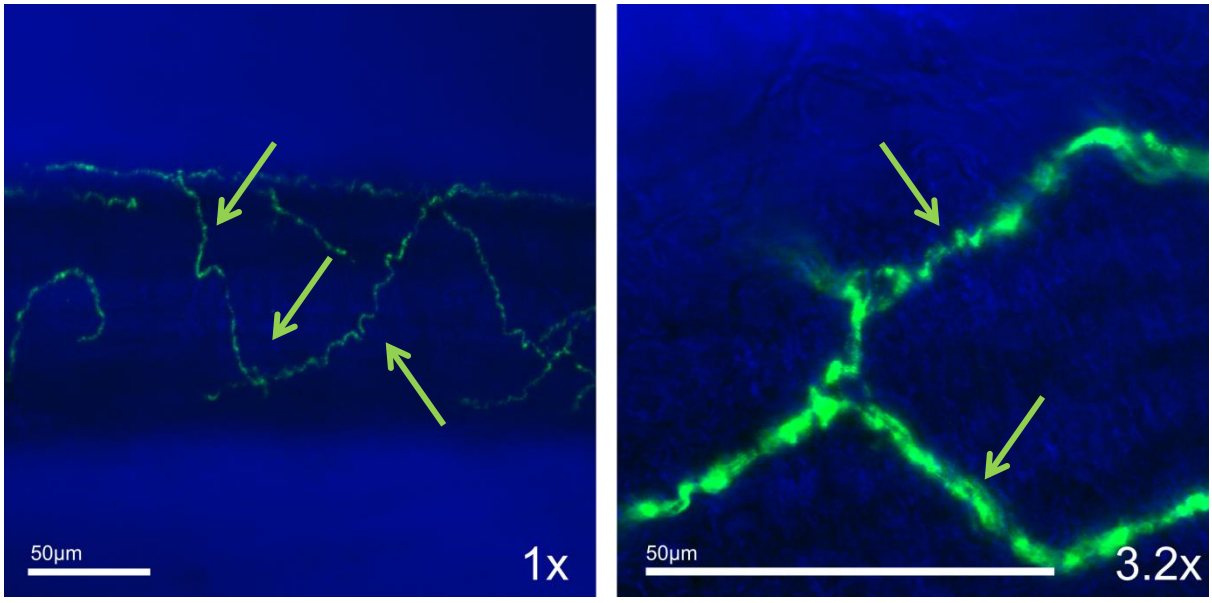

Figure IV-9: Staining of hamster microvessels against the 3G5 antigen shows a specific linear fluorescence on the outside of the vessel most likely resulting from neuronal cells from the sympathetic nervous system (green arrows). Confocal images at two independent sites and with different magnifications are shown.40x objective, zoom 1x (left), zoom 3.2x (right); Scale bars: 50 µm

2. Pericytes can generate electrical signals using K_V1.5 potassium channels

Pericytes of capillaries are situated at the interface between the endothelial layer and the tissue cells. There they could act as signal generators and mediators for an electrical signal that is conducted along the vessel wall (endothelium). An essential prerequisite to generate a hyperpolarization is the presence of functional potassium channels [48]. For this reason patch-clamp experiments were performed to elucidate the presence of potassium channels in pericyte membranes.

2.1. Electrophysiology points towards K_V1.5 membrane potassium channels

2.1.1. About 30 percent of pericyte cultures show voltage dependent channel activity

More than 200 cells in 60 cultures were subjected to patch clamp analysis. 44 cultures (73.3%) exhibited a complete lack of channel activity (whole cell conductance < 0.1 pS/pF), independent of culture age and duration of incubation. Input resistance of these cells was high and could not be altered by depolarizing voltage application, I/V relationships were completely linear. Furthermore application of FFA did not alter the activities. In contrast, despite no apparent differences in the isolation protocol, 16 cultures with a total of 48 cells showed a voltage-dependent channel activity of variable degree in the depolarizing range. In these cultures essentially all cells exhibited the activity.

Resting membrane potential measurements indicated differences between cells with channel activity and cells that did not exhibit channel activity. While in cells without channels resting potential was in the range between -20 to +10 mV, in cells with channels it showed values in the -20 to -60 mV range. Membrane capacitance was determined in whole cell mode to be between 30 and 600 pF. Voltage perturbation towards depolarization resulted in a rapid activation of the channels within 25 ms for up to 200 ms (Figure IV-10).

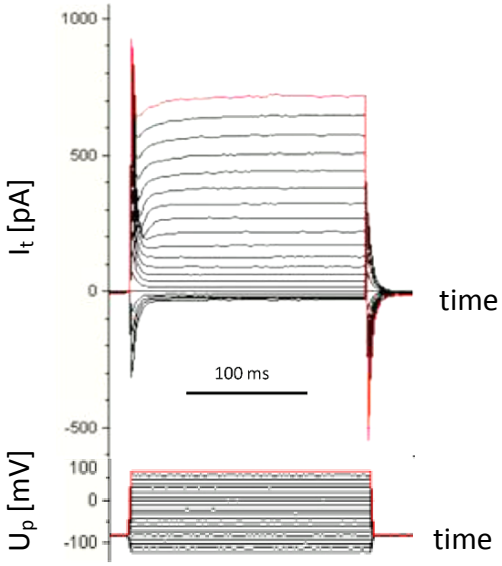

Figure IV-10: Cells from pericyte cultures show a voltage dependent channel activity in whole cells patch

2.1.2. The voltage dependent activity is likely mediated by voltage gated potassium channels

In order to clarify the ion specificity of these channels the extracellular potassium concentration in the bath was increased 10-fold from 3 mM to 30 mM. This intervention induced only a small shift in the current/voltage (I/V) relationship (data not shown). In order to analyze the effect more sensitively the antiphlogistic drug flufenamic acid (FFA) was used in addition. In pericyte cultures FFA strongly increased the voltage-dependent current in the presence of 3 mM potassium (open vs. filled circles in Figure IV-11). Furthermore under these conditions an increase of the extracellular potassium concentration to 30 mM led to a change in the reversal potential of the voltage / current (I/V) relationship by 51 mV, which is close to a Nernstian response (filled squares vs. open circles in Figure IV-11). The experiment was conducted three times in cultures that exhibited a particularly high channel activity yielding similar results.

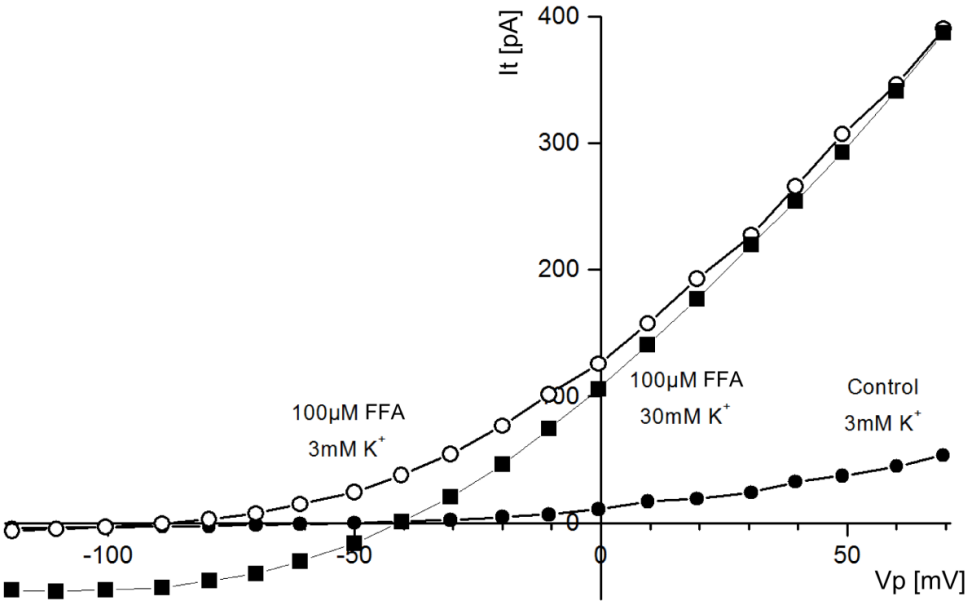

Figure IV-11: Electrophysiologic properties of potassium channel activity under treatment with FFA and elevated K^+ concentrations from a typical experiment

2.1.3. TEA and 4-AP modulate membrane channel activity

To investigate the channel properties in more detail additional channel modulating substances were used. In the current study two different blockers of potassium channels were chosen to characterize the nature of the involved channels in more detail: tetraethylammonium (TEA) and 4-aminopyridine (4-AP). TEA at 10 mM was ineffective. In contrast application of 4-AP reduced the slope of the I/V in the depolarizing range dose dependently and reversibly. At 10 mM 4-AP, the I/V relationship was virtually linear over the entire analyzed range. The resting membrane potential decreased to about -20 mV. In pericytes from hamster skeletal muscle the half-maximal effective concentration for channel inhibition by 4-AP was 1.25 mM (Figure IV-12B) determined at 0 mV.

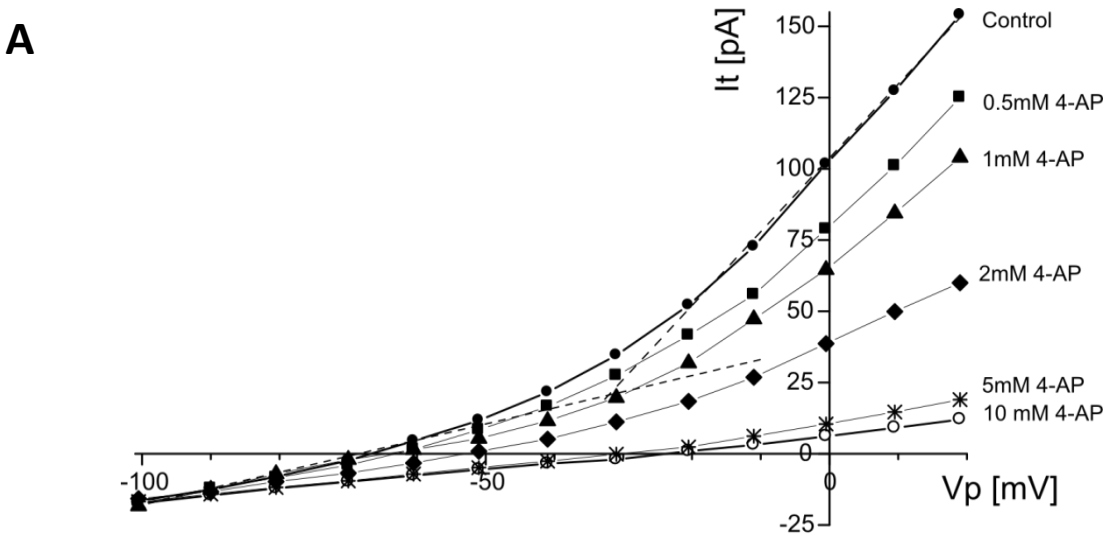

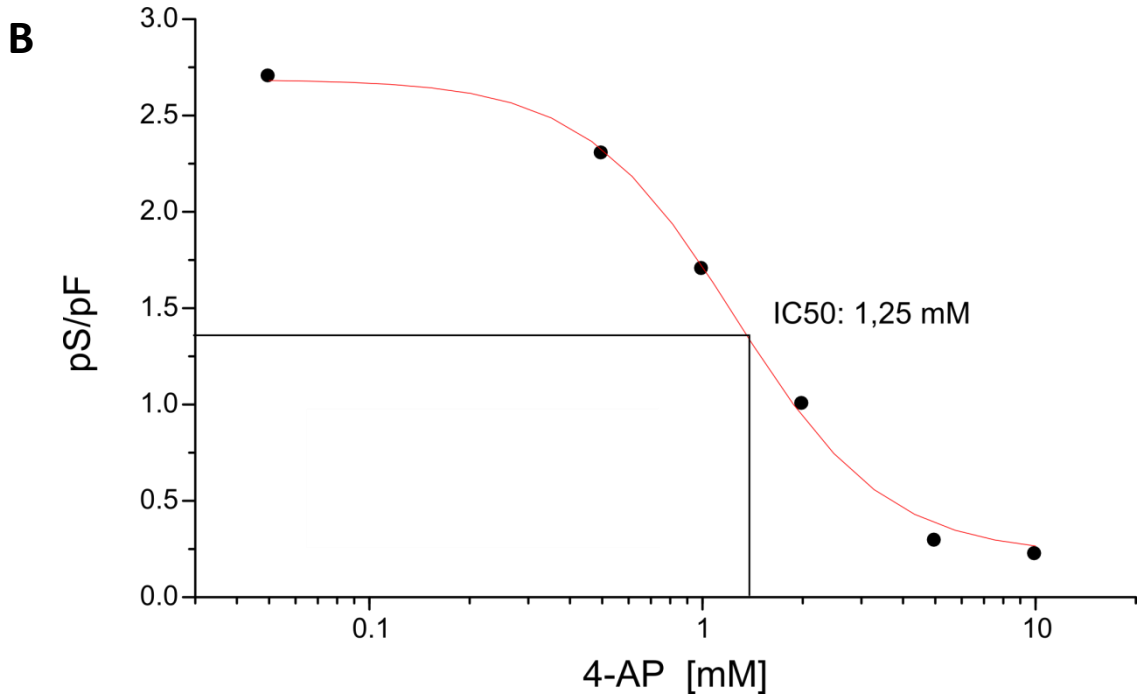

Figure IV-12: **(A)** Dose-dependent inhibition of the patch-current by 4-AP in pericytes, **(B)** dose-response relationship of the experiment shown in A for the slope at a potential of 0 mV

2.1.4. Analysis of further channel involvement

Control experiments were conducted to exclude any influence of calcium or other types of potassium channels on the results shown above. For this purpose channel blockers and specific stimuli were used. Glibenclamide (n=5, data not shown), an inhibitor of ATP-sensitive potassium channels showed no effect, either spontaneously or in the presence of FFA. Similarly exposure of the cultures to the muscle metabolites lactate (n=4, 10 mM), ATP (n=3, 1 mM) and adenosine (n=2, 500 µM) had no effect within 15 minutes (data not shown).

Chloride channels are sensitive to inhibition with flufenamic acid and should therefore have been blocked in most of the experimental setups shown mentioned before. To increase the reliability of these findings additional experiments were performed in which the bath chloride was replaced with gluconate. As shown in Figure IV-13 there was no effect on baseline conductance or I/V relationship excluding Cl^- channel effects in the cultured pericytes.

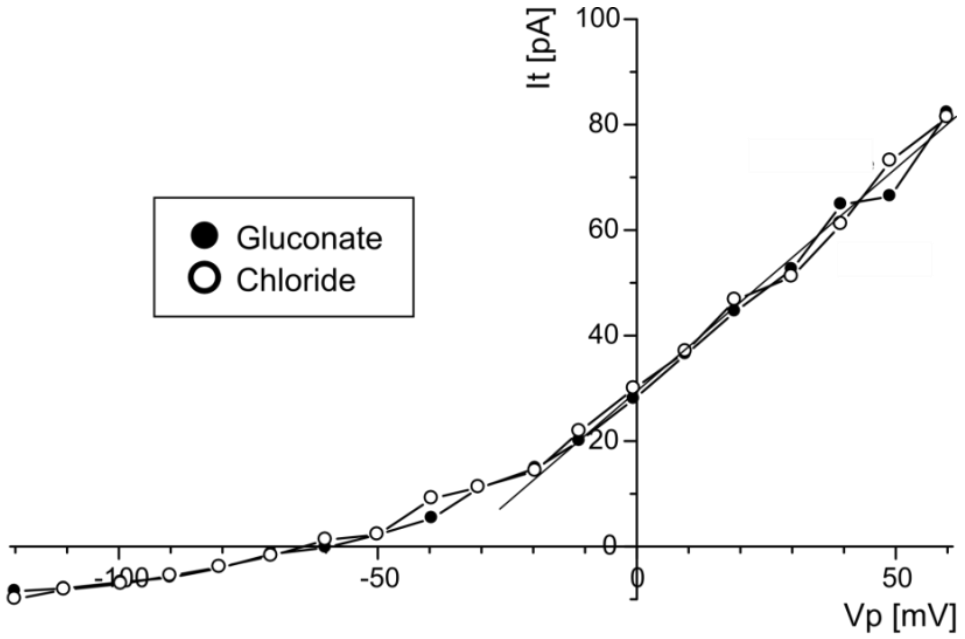

Figure IV-13: The replacement of chloride with gluconate in the culture medium induced no change in the I/V relationship

2.2. Western Blot shows the presence of K_V1.5 channels

Since the electrophysiological properties and inhibition characteristics clearly pointed towards K_V1.5 channels in the membrane the expression of these channels was analyzed in western blotting. In these experiments HUVEC and HeLa cells served as positive controls. Although the polyclonal antibody used in this experiment was only tested by the manufacturer for specific reactivity in rat and mouse cells, a clear band at the right height could also be detected in hamster skeletal muscle pericytes as shown in Figure IV-14.

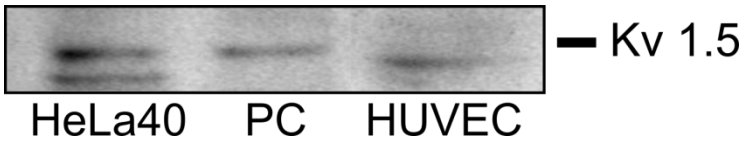

Figure IV-14: Western blotting with a polyclonal rabbit antibody (Sigma) demonstrates the expression of the K_V1.5 channel protein in cultured pericytes. HeLa cells and HUVEC served as positive controls.

3. K_V1.5 positive cells are present in tissue sections

To confirm the presence of K_V1.5 expressing pericytes *in vivo*, tissue sections were stained for the expression of K_V1.5 in NG2 positive cells. As shown by confocal microscopy in Figure IV-15, single cells in close vicinity to small vessels stained double positive with both markers. The expression of K_V1.5 therefore does not seem to be restricted to cells under cell culture conditions, but also occurs *in vivo*.

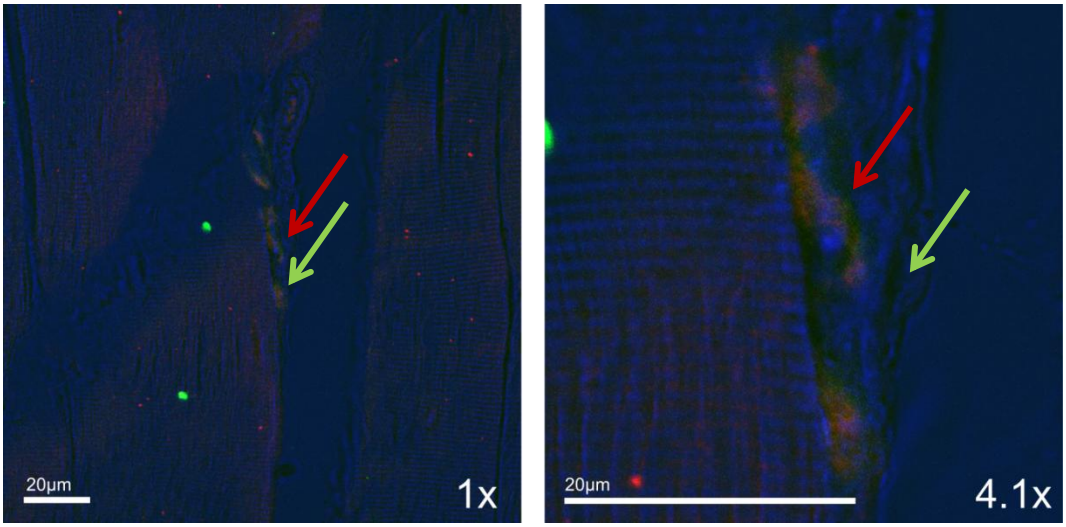

Figure IV-15: Immuno-staining of a microvessel in 5 µm hamster cremaster paraffin sections with antibodies against NG2 (red fluorescence and arrows) and K_V1.5 (green fluorescence and arrows); The two antigens co-localise in the same cell in the vessel wall. 63x objective, zoom 1x (left) and 4.1x (right); Scale bars: 20 µm

Interestingly the distribution of K_V1.5 positive cells was not uniform in the microcirculatory system. Instead cells expressing this marker were found predominantly at sites of vascular branching as shown in Figure IV-16.

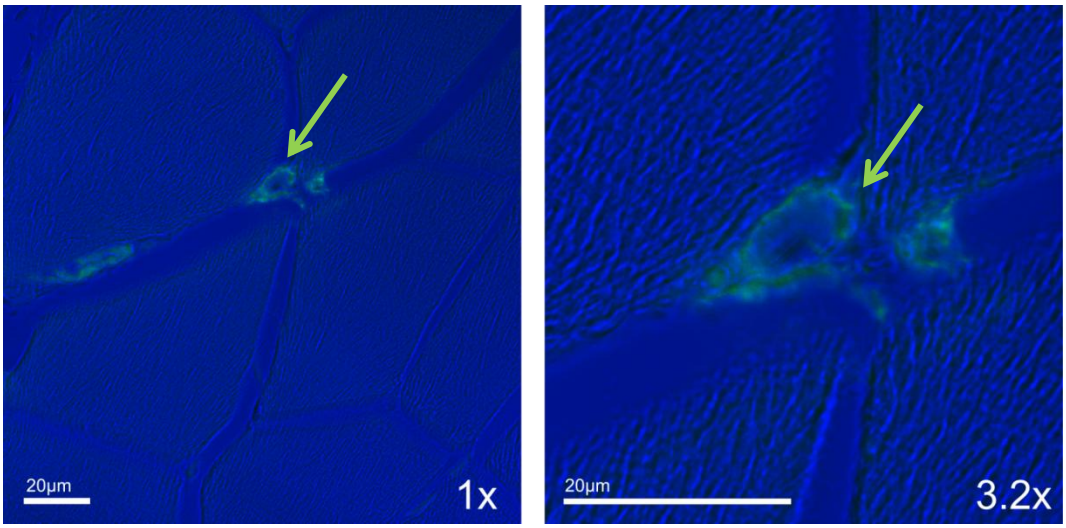

Figure IV-16: Staining of a vascular branching in hamster cremaster muscle for reactivity with an antibody against K_V1.5 (green fluorescence and arrows); 63x, zoom 1 (left) and 3.2 (right). Scale bars: 20 µm

4. Pericytes communicate with adjacent endothelial cells via gap junctions

4.1. Pericytes express the gap junction protein Cx43

In order to find out whether the cultured pericytes are able to form functional gap junctions the expression of connexin (Cx) proteins as a prerequisite for gap junctional communication was investigated. Cell lysates of primary pericyte cultures were tested for the expression of the vascular connexins Cx37, Cx40 and Cx43 at the protein level by western blotting. Stably transfected HeLa cells served as positive controls and connexin deficient HeLa wildtype cells (HeLa wt) as negative controls in these experiments. While no expression of either Cx37 or Cx40 was detectable in pericytes (PC), they showed expression of Cx43 (Figure IV-17).

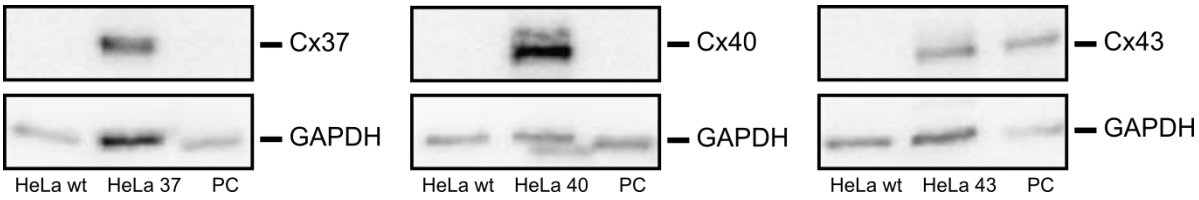

Figure IV-17: Western Blot analysis for the expression of Cx37, Cx40 and Cx43 in pericytes. Stably transfected HeLa cells expressing Cx37, Cx40 or Cx43 served as positive controls and HeLa wt cells as negative controls. Pericytes express specifically Cx43, but not Cx37 and Cx40.

Immunofluorescence stainings of Cx43 in primary pericyte cultures with a connexin 43 selective antibody showed the typical dotted staining pattern for Cx43 in the membrane mainly at contact sites with adjacent cells (Figure IV-18, [180]).

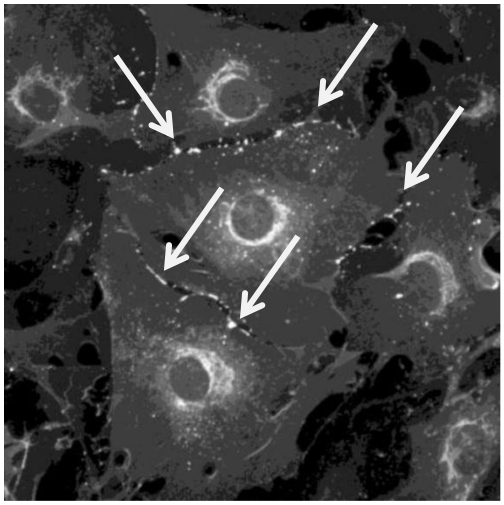

Figure IV-18: Immunofluorescence staining for Cx43 expression in pericyte cultures. Cx43 is mainly localised at the membrane especially at cell-cell contacts (arrows).

4.2. **Pericytes form functional gap junctions with endothelial cells**

To analyze for functional gap junction coupling between pericytes and endothelial cells, co-culture experiments with pericytes and HUVEC were performed. For this purpose n=40 pericytes in five co-cultures were observed over a time of 5-10 minutes. In Figure IV-19 on the left image, a pericyte injected with the gap junction permeable fluorescent dye Alexa Fluor488 can be seen surrounded by endothelial cells at the beginning of the experiment. Five minutes later the spread of the fluorescent dye to those neighboring cells can be observed as an increase in fluorescence in HUVEC.

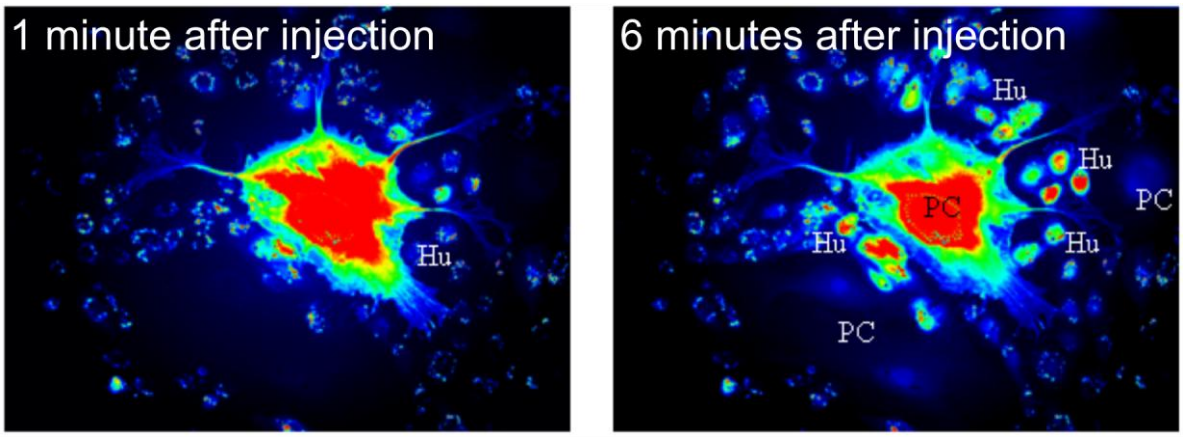

Figure IV-19: The small molecular fluorescent dye Alexa Fluor 488 spreads from an injected pericyte (PC) to neighboring HUVEC (Hu) through gap junctions within 6 minutes after injection. Color intensities indicate strength of the fluorescent signal. While 1 minute after injection only a weak signal can be seen in HUVEC, after 5 minutes the signal strength strongly increases. Representative images from n=40 PC in 5 cultures shown.

4.3. **A hyperpolarization can be conducted from pericytes to endothelial cells**

Functional gap junctions could mediate a conducted dilation from pericytes to endothelial cells. To address this question the microscopy setup was modified to use membrane potential measurements as a functional read-out. Remarkably flufenamic acid (FFA) at a concentration of 300 µM was able to induce a hyperpolarization only in part of the pericytes, but had no such effect in HUVEC. Therefore HUVEC were pre-labeled with the red fluorescent dye PKH-26 to allow for easy identification and put in co-culture with pericytes. Under these conditions HUVEC directly in the vicinity of PC reacting to FFA (n=7) also showed a hyperpolarization of their membrane potential, but more remote cells did not (n=4 PC cultures and n=4 HUVEC donors). Of note long incubation times (more than 30 minutes) abolished the effect, but also inhibited the gap junctional transfer of Alexa 488. This suggests a slowly developing, $DiBAC_4(3)$ mediated inhibition of gap junctional communication.

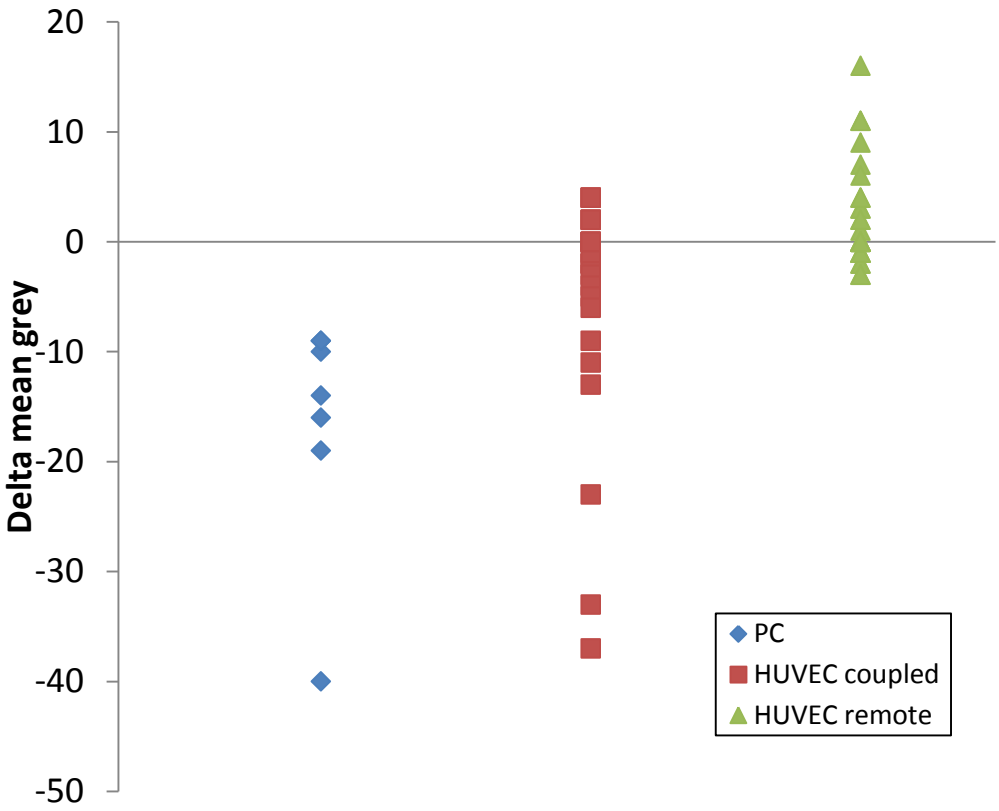

Figure IV-20: A flufenamic acid induced hyperpolarisation can spread to HUVEC that are coupled via gap junction channels but not to remote cells. HUVEC that had been directly coupled to pericytes showed a similar decrease in their delta mean grey value (red squares v s. blue diamonds) whereas remote HUVEC did not exhibit this effect (green triangles). The distributions of the three groups were significantly different ($p<0.001$. Kruskal-Wallis test for independent samples).

5. Gap junctions as a potential communication pathway between pericytes and endothelial cells

In order to investigate further possibilities of signal transduction at the gap junctional interface, experiments were conducted in which HeLa cells transfected with miRNA were co-cultured with miRNA-detector HeLa cells in the presence and absence of connexin expression, which is a prerequisite for gap junction formation. For this purpose a literature search on miRNA was performed in PubMed to select a well characterized miRNA with an experimentally validated target sequence that is not expressed in HeLa cells. The neuronal miRNA miR124 satisfied these criteria adequately [142] and was therefore selected for the subsequent experiments. Furthermore it is known to be an inducer of neuronal differentiation in N2A cells and to act by de-repressing a neuron specific gene set on the transcriptional level [181]. HeLa cells were used because of their absence of connexin expression in the wildtype.

5.1. miR124 induces a neuron-like phenotype in HeLa cells

Direct transfection of HeLa cells with miR124 led 2-3 days post transfection to distinct morphological changes in the HeLa phenotype. The cells acquired a more elongated shape with large protrusions that often extended towards other cells. These morphological changes suggest cell differentiation and the induction of a neuron-like phenotype in these cells.

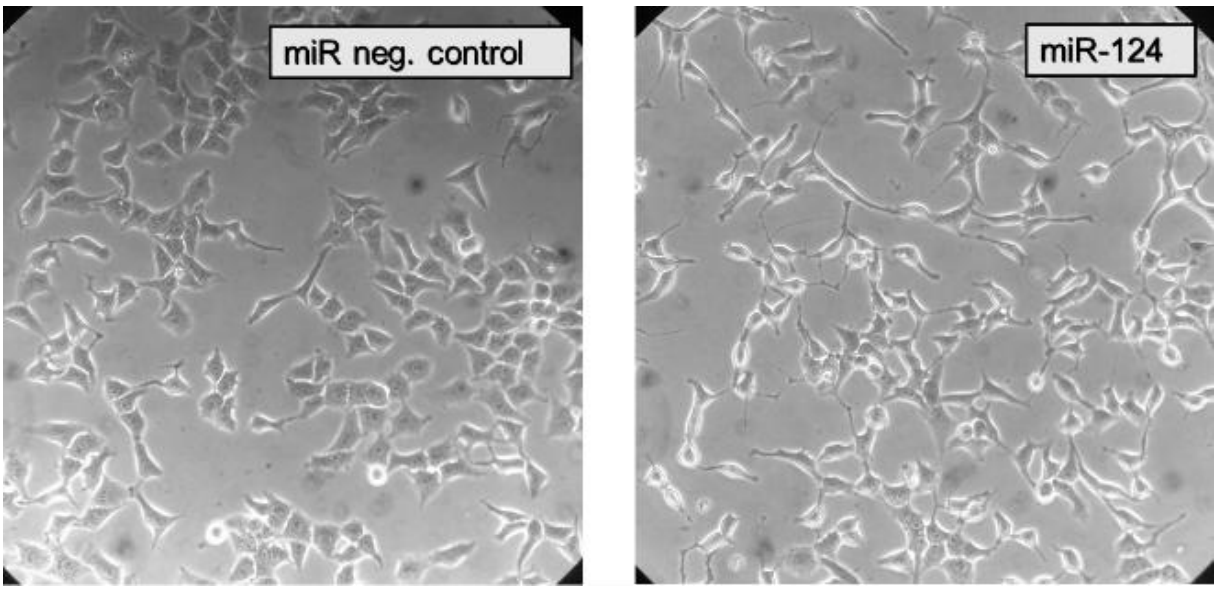

Figure IV-21: A neuron-like phenotype is observable in HeLa cells 2-3 days post transfection with 100 nM miR124; representative images of three independent experiments shown on the same scale

5.2. **miR124 leads to a cell cycle arrest in HeLa cells**

Flow cytometric analysis of cell cycle phases of mir124 transfected HeLa cells 2 days post transfection indicated a cell cycle arrest in the G0/G1 phase. While in untransfected and negative control transfected cells 64% and 66% were in the G0/G1 phase at the time of analysis, miR124 transfected cultures contained 82% cells in G0/G1 phase (Figure IV-22). In these experiments care was taken for the cultures not to reach confluence until they were harvested.

Due to the limited sample size (n=4 experiments) it was not possible to check adequately for normal distribution of the data. Therefore a conservative approach was chosen and a non-parametric statistical test performed. The paired Wilcoxon Signed Ranks test on the percentage of cells currently in G0/G1 phase between the groups was not significant for all comparisons, probably also due to the small size of the groups (p=0.465 between untreated and neg. control transfected cells and p=0.063 for the comparison of miR124 transfected cells with either of the two other groups).

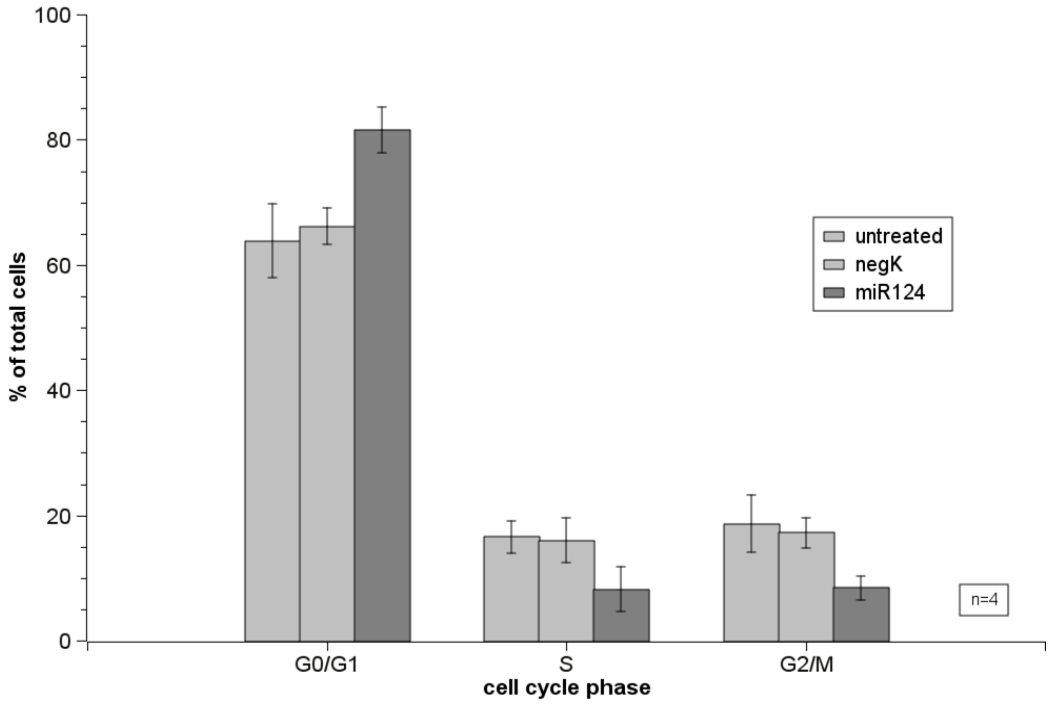

Figure IV-22: Distribution of cell cycle phases in untreated, neg.control transfected and miR124 transfected HeLa cells. Transfection with synthetic miR-124a induced a strong increase of the percentage of cells in the G0/G1 phase, indicating a cell cycle arrest in G0/G1 phase (means ±SD, n=4).

5.3. **Dye coupling through gap junctions is preserved after transfection with miR124**

Since it could not be excluded that the transfection with miR124 had an influence on gap junctional coupling a parachute dye transfer assay was performed with the miRNA transfected cells. For this purpose HeLa wt, as well as HeLa43 cells were transfected with miRNA and two days later dye transfer was quantified using flow cytometry. As shown in Figure IV-23 no significant inhibition or induction of gap junctional communication could be observed.

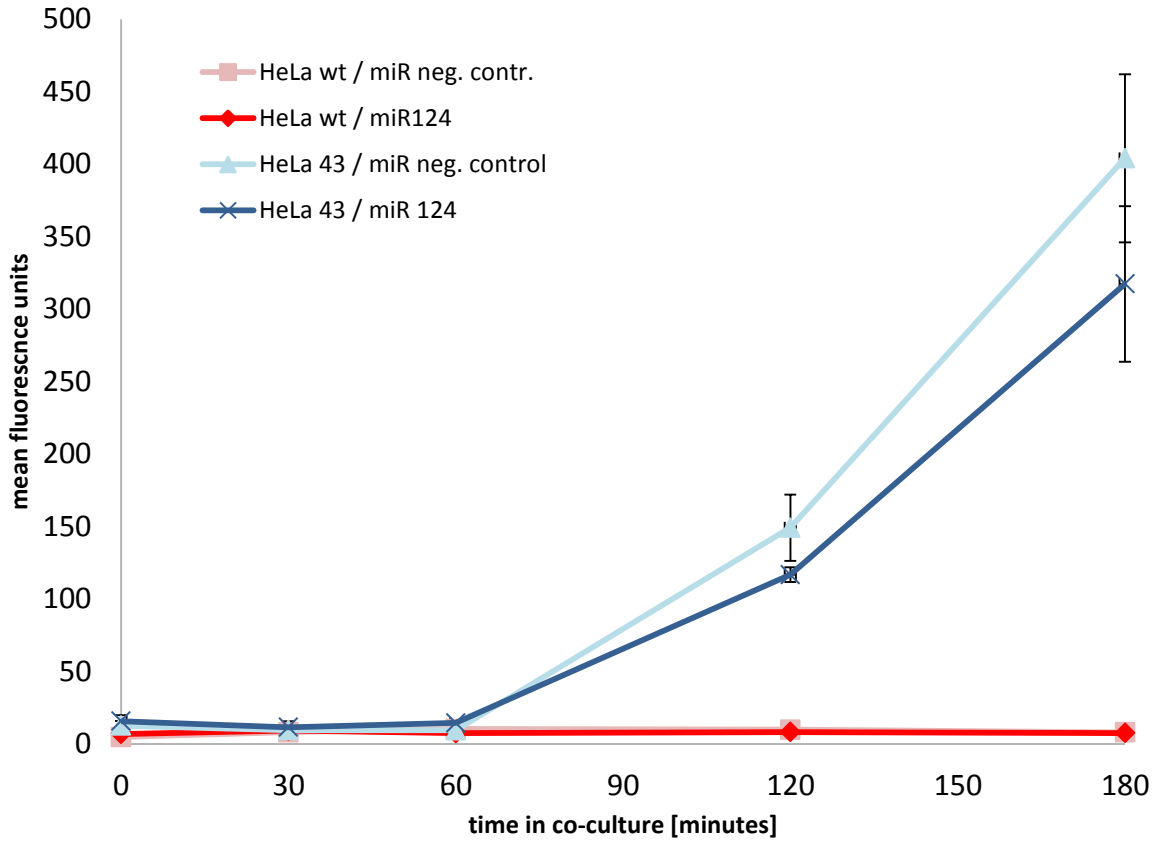

Figure IV-23: Graphical representation of dye coupling over time in a parachute assay (n=3, means +/- SEM); Statistically significant differences exist within the time course of the fluorescence intensity in HeLa43 cells ($p<0.001$), but not for the time course in HeLa wt cells ($p=0.757$). Transfection with miR124 is no significant factor for either HeLa43 cells ($p=0.204$) or HeLa wt cells ($p=0.838$). HeLa43 and HeLa wt are significantly different in the progression of the fluorescence intensity over time ($p<0.001$). (univariate general linear model analysis)

5.4. **miR124 decreases the luciferase activity in directly transfected HeLa43**

The efficiency of miR124 induced reporter gene silencing in the luciferase reporter system was quantified in HeLa43 cells. To this end HeLa43 were co-transfected with the reporter plasmids and miR124 or miRNA control. On the next day luminescence was quantified. In these experiments, transfection with miR124 resulted in a 85% decrease in reporter gene expression levels compared to control transfected cells (Figure IV-24) after two days. This indicates that the system sensitively and specifically quantifies intracellular miR124 concentrations.

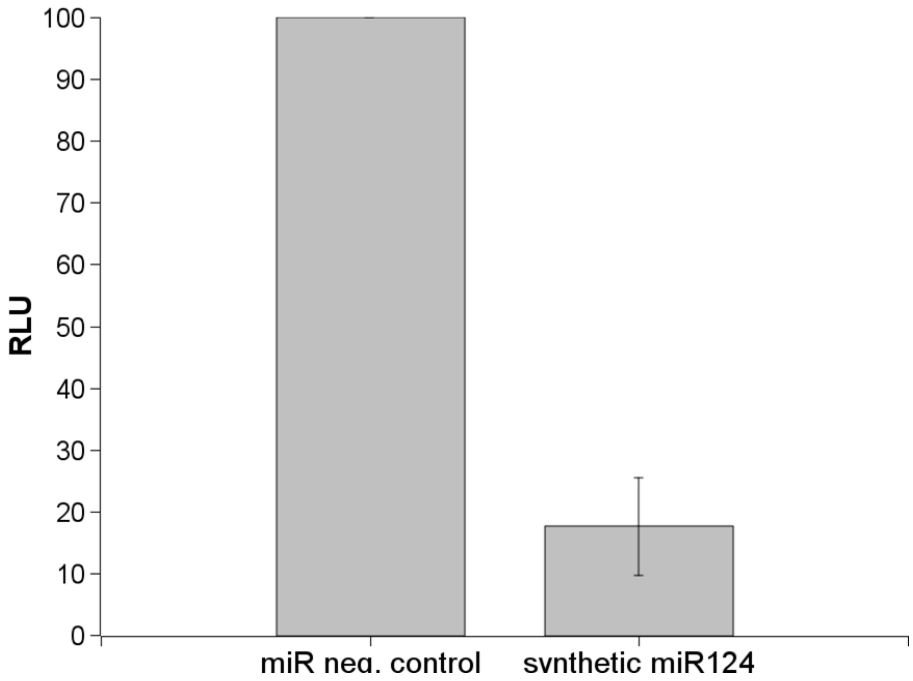

Figure IV-24: Luciferase activity measured in HeLa43 cells co-transfected with miR124 and the luciferase reporter plasmid showing a strong downregulation compared to cells transfected with a non-silencing negative control miRNA and the luciferase reporter (n=3, means ±SEM).

5.5. **Analysis of gap junctional miRNA transfer in co-cultures of Cx43 transfected HeLa cells**

5.5.1. Co-cultures with transfer of miR124

Since the transfection of miRNA and reporter plasmid in one cell population resulted in a strong response in the next step we attempted to measure a potential miRNA transfer through gap junction channels in Cx43 expressing HeLa cells. For this purpose reporter gene transfected Hela43 cells were co-cultured with "donor" HeLa cells transfected with miR124. These "donor" cells were either connexin deficient (HeLa wt, Figure IV-25 A) or expressed connexin 43 (Figure IV-25 B). HeLa cells that were solely transfected with the luciferase reporter plasmids served as a control (Figure IV-25 A).

While co-culture with HeLa wt cells did not have a significant effect on luciferase expression levels in the acceptor cells, co-culture with miR124 transfected HeLa 43 significantly diminished luciferase expression and therefore light emission (p=0.043, Wilcoxon matched-pair signed-rank, Figure IV-25B).

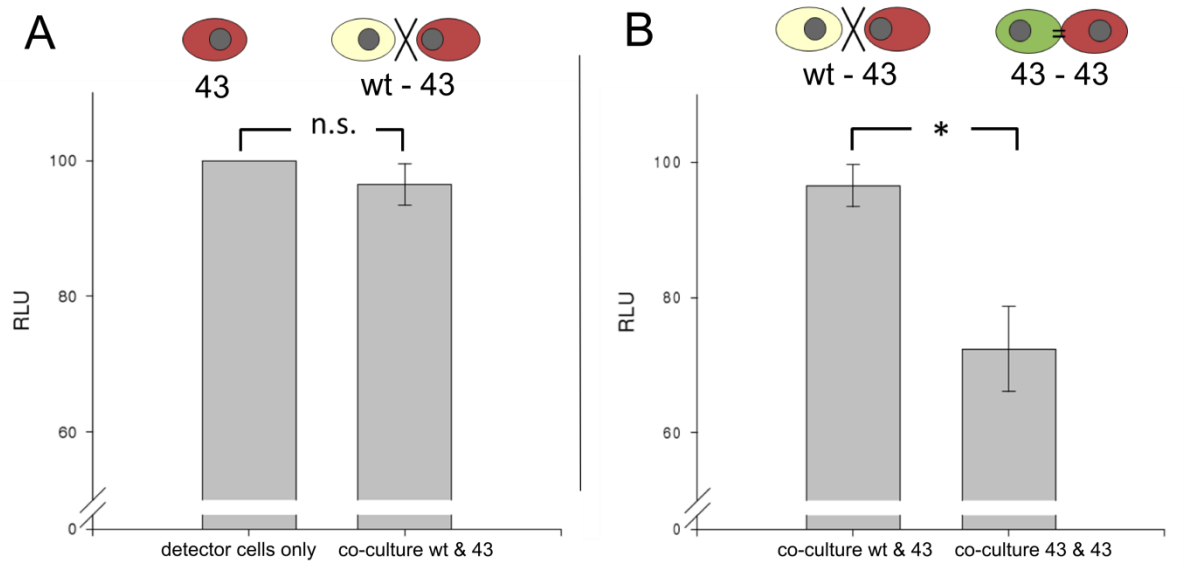

Figure IV-25: Co-culture with miR124 transfected cells diminished luciferase activity generated by detector cells only, if donor, as well as detector cells express functional Cx43 and the cells therefore can couple via gap junctions (n=5, means +/- SEM normalized to wt-controls, * denotes p<0.05, Wilcoxon match-pair signed-rank). RLU represents *relative luminescence units* showing Renilla luciferase measurements normalized to Firefly luciferase measurements from the same sample.

After these experiments showed promising results for the potential intercellular transfer of miRNA between cells, further experiments were designed to characterize the observed effect in more detail. These experiments were conducted without the sorting step that had been used before and also included a control detection plasmid that was mutated in the miRNA recognition site.

In this set of experiments directly miR124 transfected detector cells showed a strong decrease in normalized luminescence activity confirming correct operation of the detection system (bar 6 in Figure IV-26A). This miR124 induced decrease was completely abolished in the mutated detector system (bar 6 in Figure IV-26B).

In contrast to previous results under co-culture conditions no attenuation of the luciferase signal could be observed in detector cells that had been in co-culture with miR124 transfected donor cells for two days (Figure IV-26A). Remarkably, despite constant cell number and culture circumstances, detector cells with the wildtype detection construct that were not in co-culture with miRNA transfected donor cells showed a much higher RLU value compared to the co-cultured HeLa detector cells (bar 5 in comparison to bars 1 through 4 in Figure IV-26A). Experiments with detector cells that had been transfected with the mutated detection plasmid also did not show any attenuation of the luciferase signal following co-culture with miR124 transfected donor cells (bars 1 through 5 in Figure IV-26B). In these cells the above described increase in detector cells without co-culture was not detectable (bar 5 in Figure IV-26B). Since only three experiments were performed no statistical evaluation is shown.

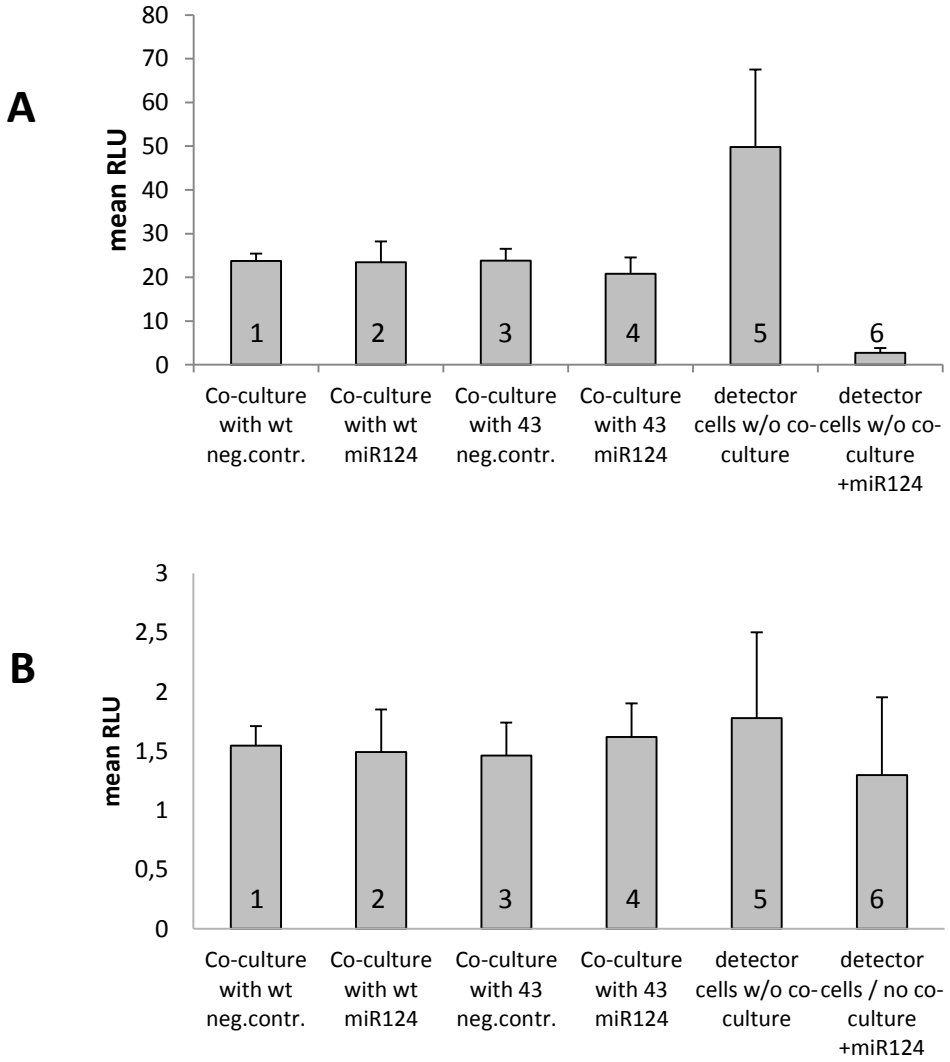

Figure IV-26: Relative luminescence values for 2d co-cultured HeLa cells in the modified experimental setup without cell sorting (n=3, means +/- SEM). (A) shows experiments with the wildtype miR124 target luciferase construct, (B) shows results for the 3-5 mutated miR124 target luciferase plasmid. Lower mean RLU values in the experiments with the mutated plasmid are mainly caused by noticeably lower raw Renilla luciferase activity values. The reason for these altered raw expression levels is yet unknown and might lie in the plasmid as well as in the transfection procedure. RLU represents *relative luminescence units* showing Renilla luciferase measurements normalized to Firefly luciferase measurements from the same sample.

5.5.2. Co-culture experiments using miR15b

In view of these divergent results the system was further adapted to use the second miRNA miR15b and its respective detection system ("miR15b wild-type plasmid"). In these experiments as well a mutated miR15b detection plasmid was used that had base exchanges in the positions 3 to 5 of the seed recognition sequence of the miRNA ("mutated plasmid", for details see the "Materials and methods" section). To enable statistical analysis experiments were repeated seven times.

Figure IV-27A shows the results from the wildtype plasmid, Figure IV-27B from the mutated plasmid. While direct transfection with miR15b resulted in a significant downregulation of luciferase activity in the wildtype transfected cells (p=0.018, Figure IV-27A, bar 6), luciferase activity in cells transfected with the mutated plasmid remained unchanged (p=0.128, Figure B, bar 6), confirming the correct operation of the detection plasmids.

Co-culture of miR15b donor cells with detector cells containing the miR15b sensitive plasmid showed no significant attenuation of luciferase activity in connexin 43 expressing cells compared to donor cells transfected with a negative control plasmid (p=0.051, bars 3 and 4 in Figure IV-27A). Moreover, there were no statistically significant differences between either co-culture experiment and the not co-cultured control detector cells (bars 1 through 4 compared individually to bar 5 in Figure IV-27A, for p-values see Table IV-1).

Using the mutated detection system luciferase measurements in co-culture experiments with connexin deficient donor cells were generally higher than in co-cultures with Cx43 expressing HeLa cells (bars 1 and 2 compared to bars 3 and 4 in Figure IV-27B, not statistically evaluated) and compared to not co-cultured detector cells (p=0.028 and p=0.018 for the comparisons of bars 1-5 and bars 2-5 in Figure IV-27B). Also in this system there was no statistically significant difference between co-cultures with miR15b and negative control miRNA transfected Cx43 donor cells (p=1.000, bars 3 and 4 in Figure IV-27B).

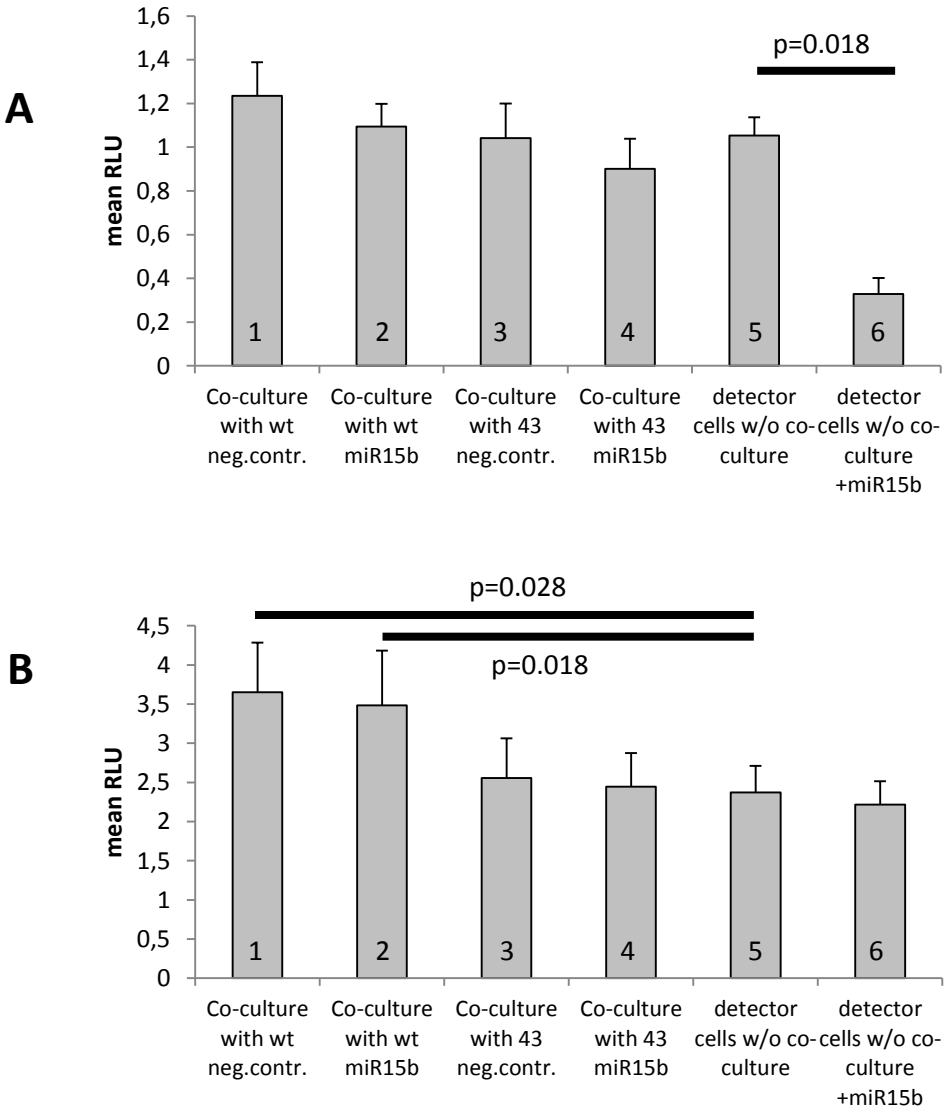

Figure IV-27: HeLa43 co-culture experiments with miR15b for the intercellular transfer of miRNA. **(A)** experiments with the wildtype miR15b detection plasmid (n=7-13, means ± SEM) and **(B)** with the plasmid with the mutated miR15b recognition sequence (n=7, means ± SEM). p-values smaller than 0.05 from the analyzed comparisons given in the next table are marked with bars. RLU represents *relative luminescence units* showing Renilla luciferase measurements normalized to Firefly luciferase measurements from the same sample.

Groups compared	p-value wt-plasmid	p-value mutated plasmid
1 – 2	0.173	0.499
3 – 4	0.051	1.000
5 – 6	0.018	0.128
1 – 5	0.221	0.028
2 – 5	0.507	0.018
3 – 5	0.515	1.000
4 – 5	0.260	0.866

Table IV-1: Statistical comparison of the subgroups from the miR15b transfer experiments. The numbers in the first column refer to the respective bars in the previous figure. p-values were calculated with a paired samples Wilcoxon signed ranks test and the results are shown separately for

the wildtype plasmid (left column) and the mutated plasmid (right column). Significant values are marked in red.

V Discussion

1. Establishment and validation of an isolation protocol for hamster skeletal muscle pericytes

Although pericytes have been first described nearly 140 years ago they still remain not fully understood and especially studies on pericytes in peripheral organs such as skeletal muscle are scarce. Most studies on pericytes were performed in neuronal tissue, especially in pericytes from bovine retina [182, 183] and brain [184], whereas there are only few or single reports from lung [185], skin [186, 187], heart [188] and pancreas [189].

It is therefore difficult to say, whether "peripheral" pericytes have the same properties as those of neuronal organs. Moreover there are obvious differences within one organ with respect to the type of vessel they are associated with, i.e. veins and arteries [190-192]. Furthermore changes can occur: for example the expression of the NG2 epitope becomes up-regulated along venules during microvascular remodeling [193] and pericytes contribute to the vascular adaption processes during hyperoxia in the retina [194]. This suggests that pericytes represent a very plastic cell type. Indeed, pericytes have been shown to have the inherent potential to differentiate into other terminally differentiated cell types depending on the stimulus. In this respect they might be similar to embryonic mesoangioblasts in their ability to differentiate to SMC [67, 69, 195, 196], skeletal muscle cells [67] osteoblasts and adipocytes [197], chondrocytes, phagocytes [198] and fibroblasts [69, 196, 199].

The identification of pericytes and their further differentiation relies heavily on the detection of certain surface markers. For example, a recent publication analyzed pericytes from skeletal muscle biopsies for their myogenic potential studying the markers alkaline phosphatase, NG2, PDGFR-β and αSMA [67]. In agreement with our study, the authors found that the expression of specific markers was not generally found in all pericytes but only in subsets of the whole population. The markers also are not restricted to pericytes. While alkaline phosphatase is also expressed in endothelial cells of heart and skeletal muscle, NG2 represents a marker for pericytes/smooth muscle cells in the developing vasculature [200]. Further, not purely pericyte specific markers have been proposed recently, such as the ATP-sensitive potassium-channel $K_{ir}6.1$ (also known as Kcnj8) and sulfonylurea receptor 2, (SUR2, also known as Abcc9), as well as delta homologue 1 (DLK1). Interestingly $K_{ir}6.1$ could only be detected in brain pericytes of mouse embryos, but was undetectable in pericytes in skin and heart [63]. Using a negative approach, previous studies have attempted to identify pericytes by the absence of typical characteristics of neighboring cell types such as the endothelial cell marker CD31, diI-acetylated low-density lipoprotein uptake, cytokeratin 5, 6, and 18, and the S100 protein [187].

All current data in the literature indicate that, due to this high structural and functional heterogeneity [78], there is no single and exclusive pericyte marker available that will work equally well in all tissues. Therefore in the current study a stepwise isolation and characterization protocol was used that involved immunomagnetic isolation of skeletal muscle pericytes via the 3G5 epitope and further cultivation of the cells in a selective medium to enrich pericytes and reduce potential contamination with other cell types.

The surface antigen 3G5 represents a well-established marker of vascular pericytes [159, 186, 201], that has previously also been identified in the foci of calcification in complicated atherosclerotic plaques [202], suggesting a role in vascular pathology. Furthermore a small

population of bone-marrow derived mesenchymal stem cells is also known to stain positively for 3G5 [203]. The 3G5 ganglioside antigen has also been well characterized in microvascular pericytes [158] although cellular expression levels of 3G5 have been reported to vary in cell culture [158, 204]. One of the reasons for this observation might not be heterogeneity of the population itself but rather varying expression levels during the cell cycle [205]. This preselection on 3G5 has the inherent risk that subsets of pericytes may have been not analyzed or that bone marrow derived cells may have been included.

A further step to select pericytes was the use of a pericyte specific medium. This medium was created to inhibit the growth of potentially contaminating endothelial and smooth muscle cells and did not contain the growth factors needed by these cell types. In the same manner the plastic culture dishes were not coated with collagen or fibronectin since pericytes have been described before not to be dependent on exogenous substrates for adhesion and be able to synthesize their own matrix [206-208].

The discriminating effect of the medium could be clearly shown in HUVEC and PAEC cultured in pericyte medium (Figure IV-2). While 3G5 purified pericyte cultures kept growing, endothelial cells gradually died over time leaving a few cells that resembled pericytes. Of note an enrichment of cell types occurred in long term passaged PAEC cultures that expressed pericyte markers and exhibited a cell morphology resembling pericytes. The reason for this phenomenon might be that single6 contaminating pericytes had overgrown the PAEC over time (see also: [159]).

Despite advances in the molecular characterization of pericytes, because of their strong heterogeneity, morphological criteria and growth patterns are still considered a relevant part of the definition of a pericyte. One of the features commonly ascribed to pericytes is nodule formation in confluent cultures [68, 209]. These pellets are embedded into a self-synthesized extracellular matrix with prominent amounts of sulfated proteoglycans and type II collagen [197]. Furthermore they have been described to be “large and well spread with irregular edges and prominent stress fibers.” [187].

As shown in Figure IV-1 the morphology of the isolated cells on day 15 was in accordance with these criteria. Furthermore the cells in the culture dish showed distinct variations in phenotype and were varying in size and in the length of their protrusions. This could be an indication of the cells originating from different vascular backgrounds, e.g. venous and arterial, although under prolonged culture conditions the *in vivo* marker pattern is impossible to trace [190, 210]. For example no expression of NG2 has been reported *in vivo* in venous pericytes [190], but it became expressed during induction of vascular remodeling [193]. For these reasons the heterogeneity allows no inferences on the primary vascular region from which the pericytes were obtained.

On the protein level the cultured cells were positive in western blotting for alpha-smooth muscle actin, NG2 and PDGFR-β. If there was a potential contamination with endothelial cells it was low enough not to give a signal for vWF in the blots.

Considering that there is a wide range of pericytic phenotypes and markers, global analytical methods such as western blotting or rtPCR can only yield information on their average distribution in a cell population. Subsets of cells or typical combinations of markers can only be detected by additional methods such as immunostaining and imaging of cells. For this reason also immunostainings were performed to analyze marker expression on the single cell level.

Four different marker proteins were chosen that have been described in pericytes before. α-smooth muscle actin (αSMA) represents as a marker protein that stains positively in smooth muscle cells from the wall of blood vessels, the gut wall and the myometrium. It has been described to occur also in microfilamentous bundles in pericytes [211]. Receptors for platelet derived growth-factor β (PDGFR-β) have been described to transduce proliferation and migration signals in pericytes which are needed in wound healing and angiogenesis but can also be found in tumor vasculature [115, 212-216]. They seem to fulfill a vital function since mice lacking the respective ligand PDGF-B suffer from pericyte loss and develop microaneurysms [217]. NG2 is a proteoglycan that is expressed in the walls of neovascular structures. According to Ozerdem et al. [74] "NG2 is expressed in the embryonic heart by cardiomyocytes, in developing macrovasculature by smooth muscle cells, and in nascent microvessels by vascular pericytes" and can therefore be regarded as a valid pericyte marker. As a control marker to identify any potential contamination with endothelial cells, the endothelial glycoprotein *von Willebrand Factor* (vWF) was used.

In the immunostainings a majority of the cells stained positive for at least one of the markers NG2, PDGFR-β and αSMA (Figure IV-4) while they were negative for the endothelial marker vWF. A small proportion of the cells did not stain for any of the markers used here. These cells might either represent pericytes that are de-differentiating or trans-differentiating into another cell type or the marker expression could be cell-cycle dependent as has been hypothesized before [205]. Of course it cannot be completely excluded that those cells are from a different origin and only resemble pericytes in some but not all respects, such as myofibroblasts [186, 218]. Still those cells have been sorted for the 3G5 antigen and they were able to grow in selective pericyte medium on untreated plastic dishes [67]. Also not all markers were always present in the same cell indicating heterogeneity among the isolated skeletal muscle pericytes. One of the reasons for this observation might lie in the isolation method. It did not favor the isolation of pericytes from one specific localization in the vascular bed, therefore pericytes that *in vivo* fulfill different functions and are adapted to different metabolic and environmental needs may have been co-purified and cultured. However there is no evidence for this pattern to be a cell culture artifact, since all the markers that were found in cells during cell culture were also found in tissue sections. Furthermore in the *in vivo* immunohistochemistry studies there were distinct differences in the expression pattern of the markers depending on the localization of the cell with respect to the vascular region. This was especially the case with the potassium channel $K_V1.5$ being expressed predominantly by cells localized at sites of vascular branching. Furthermore the selection of investigated markers represents only a small fraction of the cellular proteins having been described as relatively characteristic for pericytes. Therefore more differences are very likely to exist.

2. Pericytes as signal generator and mediator cells

Skeletal muscle pericytes are located at the crossroads between the effector cells controlling vascular tone (smooth muscle cells), the electrical signal conductors (endothelial cells) and the energy consumers (skeletal muscle cells). They could therefore be involved in generating and transducing signals from the tissue to control conducted dilation as mentioned in the introduction. Acting as activity-sensors they may well relay signals derived from working skeletal muscle into an endothelial hyperpolarization that is needed for upstream signal propagation needed to coordinate local and upstream vessel dilations. Due to their long processes they are able cover a large area, thereby locally integrating signals from cells located both up- and down-stream of the pericytes.

Even under inhibition of NO- and prostacyclin-synthesis some endothelium dependent, agonist-induced vasodilatations remain preserved to a variable extent [219-223]. Therefore, an endothelium-derived, vasodilating factor apparently plays an important role in the regulation of vascular tone. Since this mechanism involves endothelial cells and is dependent on hyperpolarization it has been termed an endothelium derived hyperpolarizing factor (EDHF) dependent dilation. Although it was first described by Bolton in 1984 underlying the action of carbachol on smooth muscle and endothelial cells in guinea pig mesenteric arteries [224], until today no unique factor responsible for all known EDHF-dependent dilations could be identified. The current concept therefore is more of an endothelium dependent dilation that involves smooth muscle cell hyperpolarization than a single factor.

Two non-exclusive concepts are therefore considered to be involved: On the one hand EDHF as a collective term for several soluble factors that diffuse from endothelial cells to smooth muscle cells and induce a local hyperpolarization, and on the other hand EDHF representing not a factor but direct electrical coupling between endothelial and smooth muscle cells via gap junctions. The factors that have been shown to induce EDHF dependent dilations are summarized in Table V-1. Interestingly, the primary mediators of EDHF effects seem to be heterogeneous between different sections of the vascular bed, between different organs and even between male and female subjects with estrogen representing one factor in the latter [225-228]. It has therefore been even proposed to dismiss the term EDHF completely and refer to the individual mechanisms in a specific vascular bed directly [229]. Furthermore, perturbations of the EDHF system are speculated to be involved in cardiovascular disease and dysregulation of blood [230, 231].

Molecule	Source	Target
	Chemical EDHF activity	
PGI_2 / Prostacyclin	COX 1 and 2	Prostacyclin receptor
EETs	EDHF synthase/cytochrome P450 epoxygenase	SK_{Ca} and IK_{Ca}
H_2O_2	Catalase	SK_{Ca} and IK_{Ca}
K^+		SK_{Ca} and IK_{Ca}
	Electrical EDHF propagation	
Gap junctions		TRPV4 and SK_{Ca}

Table V-1: Some of the suggested components in the EDHF mediated response (modified from [232])

The generation of a membrane hyperpolarization in endothelial cells is generally regarded as the initial step in an EDHF mediated response. The signal elicited e.g. by binding of muscarinic receptor agonists, such as Ach, methacoline and muscarine to specific receptors on

endothelial cells induces an increase in the intracellular calcium concentration via second messengers such as IP_3. This in turn activates calcium dependent potassium channels (K_{Ca}) [233-235], that mediate an efflux of K^+ ions out of the cell, consequently hyperpolarizing the membrane. This effect seems to be mainly mediated by intermediate (IK_{Ca}, $K_{Ca}3.1$) and small conductance (SK_{Ca}, $K_{Ca}2.3$) potassium channels [236-240].

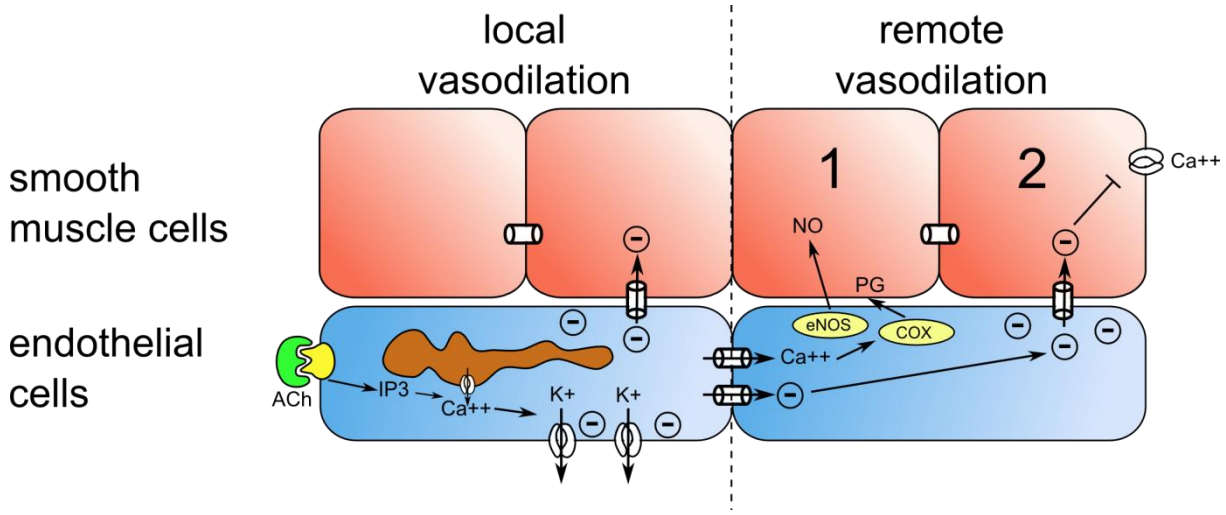

Figure V-1: Schematic representation of the classical model for conducted dilation. Acetylcholine (ACh) binds to muscarinic receptors on the surface of the endothelial cell (EC) leading to a release of calcium from intracellular stores mediated by the second messenger IP_3. This rise in intracellular Ca^{++} in turn activates IK_{Ca} and SK_{Ca} potassium channels leading to a hyperpolarization depicted by the symbol Θ across the EC membrane. Since smooth muscle cells (SMC) in the underlying Tunica media are coupled to adjacent EC via gap junctions, the electrical signal spreads locally and the hyperpolarization of the SMC results in a hyperpolarization of local SMC. In the SMC membrane hyperpolarization decreases the opening probability of voltage gated Ca^{++} channels which causes SMC relaxation and consequently a vasodilation. Additionally the increase in intracellular calcium also induces the activation of the enzymes 'endothelial NO synthase' (eNOS) and cyclooxigenase (COX) in EC (in the picture only shown in the cell on the right). Their enzymatic products nitric oxide (NO) and prostaglandins (PG) diffuse to adjacent SMC (NO into the cell, PG to membrane receptors) and by this also contribute to the vasodilation. EC are not only coupled to SMC but also to other EC in the Tunica intima. Therefore the ACh signal can also be passed on to other EC upstream via two distinct mechanisms through gap junctions. (1) chemically through the diffusion of the intracellular calcium wave (a process that is slower and limited in range) and (2) as an electric signal by conduction of the membrane depolarization (representing an EDHF conducted mechanism). In the coupled EC the mechanisms described above result in a remote vasodilation (Image based on: [241])

For skeletal muscle pericytes to contribute to this regulatory system they need to fulfill a number of prerequisites. First they need to have adequate receptors to sense the metabolic state of the surrounding microenvironment. This has been shown in pericytes from neuronal tissues for a wide range of receptors, e.g. purinergic receptors [242] and ATP sensitive membrane channels [96], as well as demonstrating that pericytes are pH sensitive [92]. Although most of these studies were performed in brain pericytes, it seemed very likely to find a similar pattern of receptors also in skeletal muscle pericytes. Interestingly, in this study no effect could be induced by treating the cells with lactate, ATP and adenosine while measuring transmembrane voltage and current in patch-clamp. Therefore these stimuli are unlikely to lead to a membrane hyperpolarization in skeletal muscle pericytes. Further possibilities such as decreases in pH value, hypoxia, inorganic phosphate and carbon dioxide

have not yet been analyzed. Additionally a combination of the aforementioned stimuli might lower the concentration threshold for each individual stimulus to induce an effect.

In the next step any activation event has to result in the generation of a hyperpolarizing signal at the pericyte membrane that can, as a third step, be transferred through gap junction channels to coupled endothelial cells. Therefore the electrical signal generation potential as well as the gap junctional coupling of skeletal muscle pericytes was analyzed. To this end electrophysiological studies were performed to investigate the expression of ion channels in the membrane of skeletal muscle pericytes by whole cell patch clamp. In these tests voltage stimulation of the cell membrane resulted in a rapid activation of membrane channels within 25 ms (Figure IV-10) with no inactivation during voltage perturbation. This represents a clear characteristic of voltage gated channels. However, only about a third of the analyzed cell cultures exhibited a voltage-dependent channel activity. So it seems that signal generation most likely is a function that is not a function of all pericytes. As was laid out before, pericytes are not a homogenous population of cells but rather form a phenotypic continuum that serves a broad range of functions with electric signal generation being only one of them. So the ability to generate this signal might be restricted to a subset of pericytes that, depending on variations in culture and isolation conditions was in some cases enriched in cell culture and in some cases not present at all. Interestingly, channel activity was more pronounced in smaller cells that were not so flat.

To investigate the ion specificity of the channel, the extracellular potassium concentration in the bath was increased 10-fold from 3 mM to 30 mM. Under these conditions a diminished K^+ efflux against the increased extracellular K^+ concentration could be measured, suggesting the presence of potassium channels. Treatment with flufenamic acid (FFA) which, among other effects described in more detail below, has been shown to activate K_V channels led to a change in the reversal potential of the voltage / current (I/V) relationship by 51 mV, close to a Nernstian response. The magnitude of the effect was therefore close to the change predicted for a selectively potassium-permeable channel.

To examine the channel properties in more detail additional potassium channel modulating substances were used. In the current study two different blockers of potassium channels were chosen: tetraethylammonium (TEA) and 4-aminopyridine (4-AP). While TEA can block all types of potassium channels depending on the concentration used, it is most effective on K_{Ca} channels [243]. For K_V channels a minimum blocking concentration of >5 mM has been reported [244-247]. In the pericyte experiments TEA at 10 mM was still ineffective, further suggesting K_V channel activity, since K_{Ca} channels should be blocked at this concentration completely.

4-AP is one of the three isomeric amines of pyridine. Despite its pharmacological uses in the treatment of multiple sclerosis [248], it is a relatively selective blocker of the K_V1 family of voltage activated potassium channels. It has been reported to block at concentrations around 200 µM to 500 µM [167, 249], without significant effect on the sodium and calcium conductances. Application of 4-AP reduced the slope of the I/V in the depolarizing range dose dependently and reversibly. At 10 mM 4-AP, the I/V relationship was virtually linear over the entire analyzed range. This finding further supports the assumption of K_V channel activity in the pericyte membrane.

To exclude the involvement of further ion channel types on the electrophysiological response, glibenclamide, an inhibitor of ATP-sensitive potassium channels was used. Under the experimental conditions used here it showed no effect, either spontaneously or in the presence

of FFA. Any influence of Cl^- channel effects in the cultured pericytes was investigated by replacing the bath chloride with gluconate. This intervention had no effect either on the baseline conductance or the I/V relationship. Furthermore FFA is a known inhibitor of Cl-channels and therefore they were most likely blocked in the previous experiments. From these data the involvement of Cl^- channels in the transmembrane electrical currents is highly unlikely.

FFA was found to stimulate channel activity. FFA is a member of the pharmacological family of fenamates. Clinically it is used as a non-steroidal anti-inflammatory drug to alleviate inflammation and pain [250] through dose dependent inhibition of TNFα- and LPS-induced NF-κB activation and COX-2 expression [9]. Additionally it has multiple effects on ion channel activities. It has been shown before to inhibit gap junctional communication [251], calcium activated chloride channels [169], voltage-gated sodium channels [252], TRPM2 channels [253] and non-selectively cation channels [254]. Furthermore it has the potential to activate potassium channels [255, 256], as well as TRPC6 [257] and TRPA1 [258] channels. So far we were not able to identify a natural, endogenous stimulator of the channels in addition to FFA. As already mentioned above, exposure of the cultures to the muscle metabolites lactate, ATP and adenosine had no effect on the I/V relationship within 15 minutes observation time.

In summary the electrophysiological studies pointed towards a potassium channel from the K_V1 family. Especially the potassium channel $K_V1.5$ is known to be widely expressed in the microvascular system, the endothelium and some smooth muscle cells (SMC), although this seems to be rather rare [259, 260]. It belongs to the delayed rectifier class and to the Shaker potassium channel subfamily. Upon stimulation it is able to generate a membrane hyperpolarization by allowing the efflux of intracellular K^+ ions as could be shown experimentally with FFA.

To test the presence $K_V1.5$ channels cell lysates were subjected to western blotting and immunocytochemical stainings with specific antibodies. These studies confirmed $K_V1.5$ on the protein, as well as on the cellular level. Furthermore it was also confirmed in stainings of tissue sections from hamster cremaster muscle. Although SMCs also stain positively for αSMA the observed staining pattern strongly suggests that most of the stained cells in the vicinity of skeletal muscle microvessels actually are pericytes. As shown in Figure IV-6 cells that exhibit the typical pericyte shape and distribution can be found in the direct vicinity of microvessels. These results were confirmed using NG2 (Figure IV-7) and 3G5 (Figure IV-8) antibodies to stain further pericytic markers in hamster muscle thin sections. Similar to the αSMA stainings, single cells exhibited a positive staining also for these markers indicating the presence of pericytes around skeletal-muscle microvessels *in vivo* and making an *in vivo* function of this channel in skeletal muscle pericytes highly likely. Especially the finding that $K_V1.5$ positive pericytes are preferentially located at sites of vascular branching is interesting and could represent an important feature in their putative function as signal generators and mediators.

[9] Source: Calbiochem datasheet, Cat. No. 343075, revised 14-July-03

3. Coupling of skeletal muscle pericytes to endothelial cells as part of signal transduction processes

In the microcirculation but not in large vessels it has already been shown that endothelial cells and smooth muscle cells are coupled via gap junctions. As pointed out before, electrical signal transduction via gap junctions between endothelium and smooth muscle is part of conducted dilation. Gap junctional communication requires very close vicinity of the plasma membranes of the two cells involved. Indeed, cell protrusions from endothelial or, more rarely, vascular smooth muscle cells can be observed in "holes" of the internal elastic lamina separating the respective cell layers. In these myo-endothelial junctions the opposing cells are coupled via gap junctions. This phenomenon has been first described in small arteries from dog heart in 1957 [261].

Gap junctional coupling plays a central role in conducted dilation. This could be shown by inhibiting myo-endothelial gap junctions with blocking antibodies which abolished the EDHF induced vasodilation in rat small mesenteric arteries [262]. Gap junctions therefore are an integral part of the current explanation of the EDHF signaling pathway [55, 263, 264]. Myo-endothelial coupling has furthermore been shown to play an important role in the acetylcholine (ACh) induced and Ca^{++} mediated vasodilation that induces a hyperpolarization in the smooth muscle cells [47, 265, 266].

Here we show that also pericytes and EC can couple via gap junctions. Coupling of pericytes with other cell types has been shown before to exert a regulatory function in the microvascular environment. The coupling between pericytes and polymorpho-nuclear neutrophils (PMN) for example has been attributed to a role in the regulation of vascular permeability by the production of sulfidopeptide leukotrienes [267]. Conducted dilation via the endothelium on the other hand is a very rapid process, occurring virtually instantly after the initial local stimulation, suggesting a mechanism involving electrical coupling via gap junctions rather than diffusion of mediators [268]. Therefore, if pericytes are local signal generators in the process of conducted dilation, their direct coupling via gap junctions to the endothelium would be essential. Gap junctional coupling has been described before between pericytes and capillary endothelium in the embryonic rat basal forebrain [269]. Also in the retina, communication within the endothelium as well as between endothelial cells and pericytes has been described, although this way of communication seems to be associated with a higher voltage loss and therefore imply a less efficient transmission [270]. By providing a low resistance, low voltage loss pathway for the spreading of a pericyte generated hyperpolarization the endothelium might connect pericytes among themselves for the coordinated regulation of vascular tone [270].

In the current study coupling could be demonstrated for skeletal muscle pericytes to HUVEC by the transfer of a fluorescent dye in micro-injection experiments. Furthermore in a functional assay, gap junction mediated conduction of a hyperpolarization between signal generating pericytes and adjacent endothelial cells could be shown. A further indication on the involvement of gap junctions came from a side effect of the membrane potential sensitive dye $DIBAC_4(3)$. Over prolonged periods of time $DIBAC_4(3)$ is able to inhibit gap junctional coupling. In the current experiments this effect was also able to inhibit dye transfer as well as the spread of an electrical hyperpolarization. Of course signal conduction as well as generation might not be a common feature of all pericytes in skeletal muscle but also not in all tissues. Pericyte isolates from human foreskin for example did not exhibit gap junctional coupling [186]. Nevertheless these experimental results support the viability of the concept,

that PC may generate a signal elicited by local environmental factors and directly relay it to endothelial cells that spread the message up- and downstream.

Western blotting revealed that pericyte-endothelial coupling was most likely mediated by channels formed by connexin 43, since Cx43 was the only vascular connexin protein that could be detected in pericyte lysates. In contrast endothelial cells also express Cx40 and Cx37 (own data and [271]).

The potential role of pericyte-endothelial gap-junctional coupling implies that an impairment of the coupling may potentially play a role in some vascular diseases. In diabetic retinopathy for example elevated levels of glucose lead to the downregulation of Cx43 expression and therefore induce an inhibition of gap junctional communication in retinal pericytes. This would in turn lead to a disruption of vascular homeostasis [272]. Similar to the vasomotor response a pericyte-generated hyperpolarization could also facilitate a calcium influx into venous endothelial cells, which induces endothelial retraction and opening of intercellular clefts [273], for example during an inflammatory reaction. There also have been reports on a gap junction mediated differentiation of porcine aortic smooth muscle cells (PASMC) by co-cultured porcine aortic endothelial cells (PAEC) that involves activation of TGF-β signaling [274].

Additionally Cx43 has been reported by Hirschi et al to play a central role in probably another, long term endothelial cell - pericyte communication. They reported that a knockout of vascular Cx43 or inhibition of gap-junctional communication blocked TGF-β activation and endothelial-induced mural cell differentiation in mice [58]. The functional relevance of this finding is still discussed controversially in the literature (e.g. Sandow and Siegl [48, 275]).

Gap junctions are mainly known for their ability to allow cells the exchange of small signaling molecules such as ions, cAMP and IP_3 across cell borders. This mechanism has been reported before for the transfer of small molecules and nucleotides through myo-endothelial junctions [184]. However, small signaling molecules and changes in membrane potential represent unspecific signals that get interpreted specifically by the cell-type they are transferred to. Transfer of miRNA would in contrast enable cells to directly exchange very specific gene-regulatory information. This process could be of use in a number of situations, such as angiogenesis and the repair of defects in the vessel wall via endothelial progenitor cells. As well it might be important in the adaptive vascular growth as well as angiogenesis in skeletal muscle under chronic exercise. Indeed, transfer of small RNA molecules has been shown already between cells: it could be shown experimentally in rat kidney cells that the gene for DNA polymerase β could be downregulated by the intercellular transfer of a synthetic siRNA in gap junction coupled cells [276]. In the current project we therefore tested whether in principle an exchange of miRNA could occur between cells through gap junctions formed by one of the vascular connexins, Cx43.

Building upon this background the potential of intercellular transfer of miRNA was analyzed in a simplified co-culture model using wild-type and Cx43 expressing HeLa cells and the miRNAs miR124 and miR15b. miR124 was chosen because it is of neuronal origin and is not endogenously expressed in HeLa cells. miR15b has been described before as a regulator of VEGF [175] and has also been proposed as a tumor marker [277]. Interestingly the transfection with miR124 was a strong and specific signal to induce a genetic program shift in HeLa cells. Two days post transfection they started to develop dendrite-like processes and entered a G0/G1 phase cell cycle arrest.

Analysis of the miRNA signal was performed following two days of co-culture of donor and detector cells. In the detector cells, the luminescence activity of a luciferase reporter plasmid was directly controlled by an miRNA recognition site in the 3' UTR and consequently proportional to the amount of a specific miRNA in the cytoplasm. As a result direct transfection of acceptor cells with synthetic miRNA led to an 80% to 90% reduction in luciferase activity suggesting proper function of the detection system. As well, direct transfection with miR15b resulted in a significant downregulation of luciferase activity in the cells transfected with the wildtype plasmid, while luciferase activity in cells transfected with the mutated plasmid remained unchanged. These data confirmed the correct operation of the detection system.

In initial miR124 experiments, co-culture of acceptor cells with connexin deficient HeLa wt cells as donors showed no significant attenuation of the luciferase signal in the acceptor cells. In contrast co-culture with stably Cx43 transfected HeLa cells that could act as miRNA donors led to a significant reduction of luciferase activity of about 30% following two days of co-culture. These data hinted towards the possibility of gap junction mediated intercellular transfer of miRNA.

However, when these experiments were repeated with a modified co-culture system omitting the cell-sorting step therefore allowing additional controls and also comprising control experiments using a binding-site mutated detection plasmid these results could not be reproduced.

Unlike in the previous experimental series, no differences were found between co-cultures with negative control donor cells and with miR124 donor cells. Especially co-cultures with coupling deficient HeLa cells and with connexin 43 expressing cells did not show differences. Additionally a stronger luciferase signal was observed in the control detector cells that had not been kept in co-culture with transfected donor cells, suggesting an unspecific effect of co-culturing. The underlying reasons for these results are so far unknown.

In control cells direct transfection with miR15b resulted in a significant downregulation of luciferase activity in the cells transfected with the wildtype plasmid, while luciferase activity in cells transfected with the mutated plasmid remained unchanged. These data confirmed the correct operation of the system. Co-culture of Hela43 detector cells containing the miR15b sensitive plasmid with miR15b transfected donor cells showed a very small attenuation of luciferase activity that did not reach statistical significance compared to detector cells without co-culture or to co-cultures with negative control transfected donor cells ($p=0.260$ and $p=0.051$, see also Table IV-1). On the other hand a trend towards higher expression levels for cells kept in co-culture with HeLa wt donor cells was visible. In acceptor cells transfected with the mutated plasmid this decrease in luciferase activity reached statistical significance ($p=0.028$ and $p=0.018$ against not co-cultured controls) again pointing to the influence of co-culturing procedures.

The reasons for these diverging and difficult to interpret results between the two experimental setups are unknown and might involve a range of different factors. First of all the stability of the synthetic miRNA intracellularly and its protein association is unknown. However these factors could be expected to have a strong influence on the availability of a specific miRNA for gap junctional transfer. It seems unlikely that miRNA molecules exist freely in the cytoplasm, but they are rather bound to proteins from the Argonaute family and other proteins [278]. Furthermore miRNA secondary structure, the current cell cycle state and cell density effects all could affect the transfer efficiency.

It is important to note that the speed of the miRNA exchange is completely unknown. The presented data were generated using co-cultures for two days but this might not be the optimum conditions. While shorter co-cultures allow less time for the transfer, longer experiments seemed impractical for reasons of cell growth. Moreover there were concerns about intracellular miRNA stability. Under physiological conditions miRNA half-life seems to be a regulatory factor for fine-tuning miRNA effects [279]. Degradation seems to be regulated by the miRNA composition outside the seed sequence. The synthetic miRNA molecules used in this study were modified by the manufacturer for increased stability and long-term effects. The consequences of these disclosed modifications for intercellular transfer are hard to judge. On the one hand increased stability could go along with stronger protein binding and therefore diminished transfer. On the other hand higher concentrations of miRNA for increased periods of time could have beneficial effects in the experiments. Last, the exchange efficiency is likely to depend on the type of connexin proteins that are expressed in the cell system. By their different pore sizes and charge characteristics they are very likely to influence the miRNA transfer efficiency [41, 280-283].

While this part of the project was still running other reports were published supporting these miRNA related findings. RNA-interference (RNAi) targeted downregulation of GFP was shown in human embryonic stem cells stably expressing GFP [284]. Similarly the transfer of RNAi was shown with shRNA against GFP in neonatal rat ventricular myocytes [285]. Katakowski et al. reported similar findings in 2010 using C. elegans miR-67 in a glioma cell model [286]. Only recently in 2011 Lim et al. reported functional transfer from bone marrow stroma to breast cancer cells implying a role in the dormancy of bone marrow metastases [287].

4. Conclusion and outlook

The main aim of this project was to establish a reproducible method for the isolation of pericytes from hamster skeletal muscle. Using a two-step approach and magnetic bead cell sorting a population of cells bearing the morphological characteristics and marker protein expression of pericytes was accomplished. The protein pattern in these cells proved to be heterogeneous in line with reports from the literature.

Furthermore, as a proof of principle, signal generation in the isolated cells could be shown to be possible via $K_V1.5$ channels. Additionally our pericytes had the ability to couple to endothelial cells via gap junctions formed by connexin 43 and transfer a hyperpolarization from the pericyte to adjacent endothelial cells. Figure V-2 summarizes the presented findings and shows the role that pericytes might play in vascular signaling. While there is still some uncertainty as to how pericytes might be stimulated in step 1, pericytes could clearly be shown to have the potential to perform steps 2 and 3.

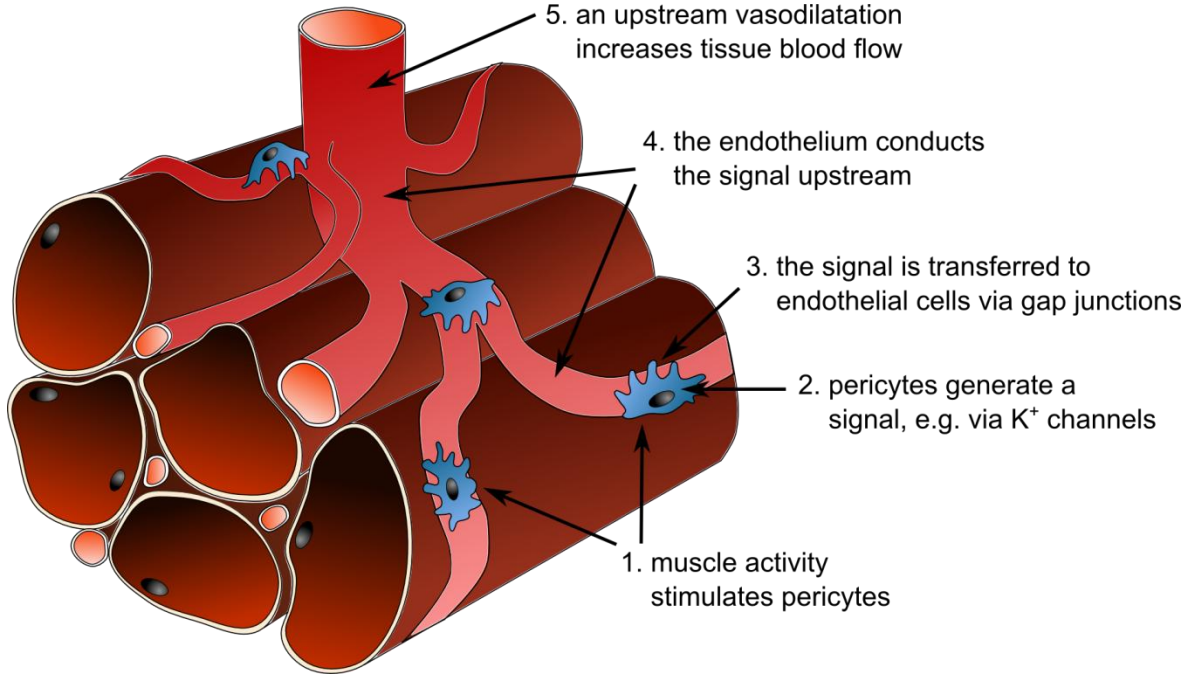

Figure V-2: Summary picture of the hypothesized steps involving pericytes in microvascular signaling in the working skeletal muscle. Image based on: [288]

Although the transfer of miRNA seemed possible in preliminary experiments these results could not be confirmed in further testing. Therefore for the transfer of miRNA no conclusive results can be reported. Still this subject should be examined further.

VI Appendix

1. Summary

In this thesis a novel method to isolate and cultivate pericytes from hamster skeletal muscle is presented. By choosing a two-step approach with magnetic-bead cell sorting for the 3G5 antigen and culture in a selective growth medium a high percentage of pericytes could be reached and their nature could be verified in subsequent characterization steps. Morphologically the cells had a typical phenotype with flat and large cell bodies and long protruding processes. Immunocytochemistry and western blotting could confirm the expression of the previously reported pericyte markers NG2, PDGFR-β, and αSMA. However, in accordance with previous reports, even the cells isolated from the same muscle and tissue, were not a uniform population.

A certain heterogeneity was also present in the functional studies investigating pericyte membrane channels by electrophysiology. In these experiments in a subset of the pericyte population the presence of the voltage sensitive potassium channel $K_V1.5$ could be demonstrated. Upon pharmacological stimulation of these channels by FFA they were able to elicit a membrane hyperpolarization and conduct it to neighboring endothelial cells via gap junctions formed by connexin 43. The expression of the $K_V1.5$ channel could also be demonstrated by immunohistochemistry in paraffin sections from hamster skeletal muscle. These findings are consistent with the hypothesis that pericytes could act as signal generators for hyperpolarization and vasodilatation in the vessel wall. The coupling with endothelial cells might relay an electric signal further along the vessel wall and lead to "EDHF mediated" dilations [48]. Interestingly in tissue sections $K_V1.5$ positive pericytes were located predominantly at vascular branchings.

We additionally studied whether gap junctions may also form a pathway for the exchange of miRNA between cells in a model co-culture system using HeLa. For the detection of the miRNA a detector system consisting of a luciferase reporter protein under control of a miR124 sensitive 3' UTR was established. Our experiments could not conclusively confirm transfer of miRNA in this system. Similar results were obtained with human miR15b.

Taken together these findings open up new possibilities for studying skeletal muscle pericyte physiology and to test novel concepts integrating the pericyte into the vascular signaling network under conditions of health and disease.

2. Zusammenfassung

In diesem Promotionsprojekt wird eine neue Methode zur Isolation und Kultivierung von Perizyten aus der Skelettmuskulatur von Hamstern vorgestellt. Durch einen zwei stufigen Ansatz mittels selektiver Isolation von Zellen mit dem 3G5 Antigen und die Kultivierung in einem selektiven Wachstumsmedium konnte in den nachfolgenden Charakterisierungsschritten ein hoher Anteil an Perizyten nachgewiesen werden. Morphologisch hatten die Zellen einen Phänotyp mit typischem flachen und großen Zellkörper und langen Fortsätzen. In der Immunhistochemie und im Western Blot konnte die Expression der bekannten Perizytenmarker NG2, PDGFR-β, und αSMA bestätigt werden. In Übereinstimmung mit der Literatur waren sowohl Morphologie, als auch die Markerexpression nicht einheitlich, sogar bei Zellen aus demselben Muskel und Gewebe. Dies ist mit der Existenz von funktionell unterschiedlichen Populationen von Perizyten vereinbar.

Eine Heterogenität der isolierten Perizyten zeigte sich auch in den funktionellen Untersuchungen der Perizytenmembran mittels Elektrophysiologie. Bei diesen Experimenten konnte in einem Teil der Perizytenpopulation der spannungsabhängige Kaliumkanal $K_V1.5$ nachgewiesen werden. Durch pharmakologische Stimulation dieses Kanals mit Flufenamsäure (FFA) konnte in den Zellen eine Hyperpolarisation der Zellmembran erzeugt werden, die über durch Connexin 43 gebildete gap junction Kanäle an benachbarte Endothelzellen weitergeleitet werden konnte. Das Vorhandensein von $K_V1.5$ konnte auch immunhistochemisch an Paraffinschnitten aus Hamstermuskel nachgewiesen werden. Diese Ergebnisse sind gut vereinbar mit der Hypothese, dass Perizyten als Signalgeneratoren für eine Hyperpolarisation der Gefäßzellen dienen und so eine Vasodilatation induzieren. Durch Kopplung von Perizyten und Endothelzellen kann ein elektrisches Signal entlang der Gefäßwand stromaufwärts eine „EDHF ähnliche“ Vasodilatation auslösen. Interessanterweise befanden sich $K_V1.5$ positive Perizyten in Gewebeschnitten bevorzugt an Aufzweigungen von Gefäßen.

Zusätzlich untersuchten wir mit Hilfe eines HeLa Ko-Kultursystemes die Möglichkeit des direkten Austausches von miRNA über gap junctions. Zur miRNA Detektion etablierten wir einen Luciferasereporters, der unter der Kontrolle einer miR124 sensitiven 3‘ UTR stand. Nach zwei Tagen Ko-Kultur ließ sich jedoch nicht schlüssig zeigen, dass ein solcher Transfer von miRNA stattfand. Dies gilt auch für zusätzliche Experimente mit der humanen miR15b.

Zusammenfassend eröffnen diese Ergebnisse neue Möglichkeiten die physiologischen Eigenschaften von Perizyten aus Skelettmuskel zu untersuchen und neue Konzepte zu testen, wie Perizyten im vaskulären Signalnetzwerk unter physiologischen Bedingungen bzw. bei Gefäßerkrankungen eingebunden sind.

3. Abbreviations

4-AP	4-Aminopyridine
A	Ampère
Ach	Acetylcholine
AGE	Advanced glycation end-products
Ago	Argonaute
APS	Ammonium persulfate
ATCC	American type culture collection
ATP	Adenosine tri-phosphate
BCA	Bicinchoninic acid
BMDC	Bone marrow-derived cell
BP	Bandpass
BSA	Bovine serum albumine
C. elegans	Caenorhabditis elegans
Ca^{++}	Calcium
cAMP	Cyclic adenosine monophosphate
CCD	Charge coupled device
CD	Cluster of differentiation
CNS	Central nervous system
CoA	Coenzyme A
COX	Cyclo-oxygenase
CR	Complement receptor
Cx	Connexin
CXCR	CXC-motive receptor
DGCR8	DiGeorge syndrome critical region 8
$DiBAC_4(3)$	Bis[1,3-dibutylbarbituric acid]trimethine oxonol
DM	Dichroic mirror
D-MEM	Dulbecco's modified Eagles medium
DMSO	Di-methyl sulphoxide
DNA	Desoxi-ribonucleic acid
DNAse	Desoxy ribonuclease
EC	Endothelial cell
EDHF	Endothelium derived hyperpolarizing factor
EDTA	Ethylenediaminetetraacetic acid
EET	Epoxyeicosatrienoic acid
EGTA	Ethylene glycol tetraacetic acid
F	Farad
FACS	Fluorescence assisted cell scanning / sorting
FCS	Fetal calf serum
FFA	Flufenamic acid
FITC	Fluorescein iso-thio cyanate
FSC	Forward scatter
g	Gram / g-force
GAPDH	Glyceraldehyde 3-phosphate dehydrogenase
GFP	Green fluorescent protein
GTP	Guanosine tri-phosphate
H_2O_2	Hydrogen-peroxide
HEPES	4-(2-hydroxyethyl)-1-piperazine-ethane-sulfonic acid
HRP	Horse radish peroxidase

HUVEC	Human umbilical vein endothelial cell
I/V	Current / voltage
IFN-γ / -α	Interferon-γ / -α
IgG	Immunoglobulin G
IgM	Immunoglobulin M
IK_{Ca}	Ca^{++} sensitive, intermediate-conductance potassium channel
IL	Interleukin
IP_3	Inositol tri-phosphate
K^+	Potassium
LAR	Luciferase assay reagent
LMU	Ludwig Maximilians Universität
LNA	N^{ω}-nitro-L-arginine
LP	Longpass
LPS	Lipopolysaccharide
m	Meter
M	Molar
MACS	Magnetic cell separation
Mg	Magnesium
MHC	Major Histo-compatibility complex
miRNA	Micro RNA
mRNA	Messenger RNA
Na^+	Sodium
NBCS	Newborn calf serum
NFκB	Nuclear factor κ
NO	Nitric oxide
NRK cells	Normal rat kidney cells
PAEC	Porcine arterial endothelial cells
PBS	Phosphate buffered saline
PC	Pericyte
PDGF	Platelet-derived growth factor
PDGFR-β	Platelet-derived growth-factor receptor β
PE	Phycoerythrin
PGI	Prostaglandin I
pH	Potential Hydrogen
PI	Propidium Iodide
PLB	Passive lysis buffer
PMN	Polymorphonuclear neutrophils
PMT	Photomultiplier tube
RIPA	Radioimmunoprecipitation assay buffer
RISC	RNA-induced silencing complex
RLU	Relative luminescence units
RNA	Ribonucleic acid
RNAi	RNA interference
RNAse	Ribonuclease
rpm	Rotations per minute
s	Second
SD	Standard deviation
SDS	Sodium dodecyl sulfate
SEM	Standard error of mean
SFM	Serum free medium

shRNA	Small hairpin RNA
siRNA	Small interfering RNA
SMC	Smooth muscle cell
SOD	Superoxide dismutase
SP	Shortpass
SSC	Side scatter
Taq	Thermophilus aquaticus
TBS	Tris buffered saline
TEA	Tetraethylammonium
TEMED	N,N,N',N'-tetramethylethylenediamine
TGF-β	Transforming growth factor beta
TNFα	Tumor necrosis factor α
TRITC	Tetramethyl Rhodamine Iso-Thiocyanate
TRP	Transient receptor potential
UTR	Untranslated region
VEGF	Vascular endothelial growth factor
VIP	Vasoactive intestinal peptide
vWF	Von Willebrand factor
wt	Wildtype
αSMA	Smooth muscle actin

4. Publications

4.1. Papers

- **Plasmalogens the neglected scavenging and regulatory species**
  Wallner S, Schmitz G
  Chem Phys Lipids. 2011 Sep;164(6):573-89

- **Isolation and functional characterization of pericytes derived from hamster skeletal muscle**
  Mogensen C, Bergner B, Wallner S, Ritter A, D'Avis S, Ninichuk O, Kameritsch P, Gloe T, Nagel W, Pohl U
  Acta Physiol (Oxf). 2011 Apr;201(4):413-26

- **The carboxyl tail of Cx43 augments p38 mediated cell migration in a gap junction independent manner**
  Behrens J, Kameritsch P, Wallner S, Pohl U, Pogoda K
  Eur J Cell Biol. 2010 Aug;89(18):828-38

- **Influence of autologous blood transfusion on natural killer and lymphokine activated killer cell activities in cancer surgery**
  Heiss MM, Fasol-Merten K, Allgayer H, Stroehlein MA, Tarabichi A, Wallner S, Eissner HI, Jauch KW, Schildberg FW
  Vox Sang. 1997;73(4):237-45

4.2. Oral presentations

- **Intercellular transfer of microRNA through Cx43 containing gap junctions**
  S. Wallner, K. Pogoda, U. Pohl
  International Gap Junction Conference Sedona, AZ 2009

4.3. Poster Presentations

- **Cells can exchange miRNA through gap junctions**
  S. Wallner, K. Pogoda1, U. Pohl
  Jahrestagung der deutschen Gesellschaft für Physiologie 2009, Giessen

- **Interleukin-8 receptors CXCR1 and CXCR2 in hamster (Mesocricetus auratus)**
  A. Ritter, S. Wallner, U. Pohl
  Jahrestagung der deutschen Gesellschaft für Physiologie 2008, Cologne

- **Gap junctional coupling between EPC and EC is mediated by Cx43/Cx43 homo- and Cx43/Cx37 hetero-channels**
  S. Wallner, K. Pogoda and U. Pohl
  Jahrestagung der deutschen Gesellschaft für Physiologie 2007, Hannover

- **Endothelial progenitor cells couple with mature endothelium via gap junctions formed by connexin 43**
  S. Wallner, K. Pogoda and U. Pohl
  GFMVB Meeting 2006, Deutsches Herzzentrum München

4.4. Grants and financial support

- EU project "Exgenesis", 6th Framework
- Friedrich-Baur-Stiftung
- DFG Deutsche Forschungsgemeinschaft

5. Acknowledgements

First and foremost, I want to express my gratitude to my supervisors Prof. Dr. Ulrich Pohl and Dr. Kristin Pogoda who provided me with the opportunity to perform the experiments and helped me grow personally and scientifically. Their expertise, understanding, and patience, added considerably to the success of the project. I hope I took their suggestions seriously.

My gratitude also goes to Brigitte Bergner, who provided invaluable advice in hamster *in vivo* experiments, cell purification and cell culture techniques, as well as to Dr. Petra Kameritsch who is an expert in microscopy and calcium signaling. Without their support this thesis would not have been possible. Part of this work is based upon experiments from Dr. Christina Mogensen whom I am very grateful for letting me build upon her data.

I also would like to thank Prof. Dr. Wolfram Nagel who performed the patch clamp experiments and gave me invaluable advice on electrophysiology and patch clamping while I was compiling the results and writing this thesis.

I especially want to thank Angela Ritter, Theres Hennig and Ramona Mettler, as well as Julian Kirsch and Fabian Kellner who started with me as colleagues and now have become friends. This is also true for Dorothea Gössel, who helped me with more things than I could list here with her high competence, but also by providing motivation and encouragement.

This thesis would not have been possible without the help, support and patience of Silvia Münzing, Ulrike Wilhelm-Forster, Sabine D'Avis, Katarzyna Stefanowski and Britta Bscheider who taught me almost all the methods I know in the lab today.

I also want to thank all the colleagues from the Walter-Brendel-Centre and the Institute of Cardiovascular Physiology and Pathophysiology, I did not mention by name, but who were there with me and helped me with all the big and small problems such a thesis implies. They all contributed significantly and made the time we spent together worthwhile.

Of course I also deeply want to thank my parents for the support they provided me through my entire life and in particular helping me through my studies.

Last, but invaluably important for me, I want to thank my friends who always provided emotional support and were there for me in the good and the bad times.

VII References

1. Koeppen, B.M., B.A. Stanton, and R.M. Berne, *Berne & Levy physiology*. 6th ed2010, Philadelphia, PA: Mosby/Elsevier. xii, 836 p.
2. Loukas, M., et al., *The cardiovascular system in the pre-Hippocratic era.* Int J Cardiol, 2007. **120**(2): p. 145-9.
3. Garber, A. and M. Linvingston, *History of the Circulatory System: discovery of the basics.* UWOMJ, 2008. **77**(2): p. 3.
4. Klinke, R. and R. Baumann, *Physiologie*, 2010, Thieme: Stuttgart [u.a.].
5. Kessel, R.G., *Basic medical histology : the biology of cells, tissues, and organs*1998, New York: Oxford University Press. ix, 550 p., 64 p. of plates.
6. Secomb, T.W. and A.R. Pries, *Information transfer in microvascular networks.* Microcirculation, 2002. **9**(5): p. 377-87.
7. Rensen, S.S., P.A. Doevendans, and G.J. van Eys, *Regulation and characteristics of vascular smooth muscle cell phenotypic diversity.* Neth Heart J, 2007. **15**(3): p. 100-8.
8. Berg, B.R., K.D. Cohen, and I.H. Sarelius, *Direct coupling between blood flow and metabolism at the capillary level in striated muscle.* Am J Physiol, 1997. **272**(6 Pt 2): p. H2693-700.
9. Davis, M.J., *Perspective: Physiological role(s) of the vascular myogenic response.* Microcirculation, 2011.
10. Johnson, P.C., *The Myogenic Response*, in *Supplement 7: Handbook of Physiology, The Cardiovascular System, Vascular Smooth Muscle*1980. p. 409-442.
11. Sharif-Naeini, R., et al., *Sensing pressure in the cardiovascular system: Gq-coupled mechanoreceptors and TRP channels.* J Mol Cell Cardiol, 2010. **48**(1): p. 83-9.
12. Schubert, R., D. Lidington, and S.S. Bolz, *The emerging role of Ca2+ sensitivity regulation in promoting myogenic vasoconstriction.* Cardiovasc Res, 2008. **77**(1): p. 8-18.
13. Hill, M.A., et al., *Arteriolar myogenic signalling mechanisms: Implications for local vascular function.* Clin Hemorheol Microcirc, 2006. **34**(1-2): p. 67-79.
14. Haga, J.H., Y.S. Li, and S. Chien, *Molecular basis of the effects of mechanical stretch on vascular smooth muscle cells.* J Biomech, 2007. **40**(5): p. 947-60.
15. Warner, T.D., *Influence of endothelial mediators on the vascular smooth muscle and circulating platelets and blood cells.* Int Angiol, 1996. **15**(2): p. 93-9.
16. de Wit, C., B. Hoepfl, and S.E. Wolfle, *Endothelial mediators and communication through vascular gap junctions.* Biol Chem, 2006. **387**(1): p. 3-9.
17. Dora, K.A., *Cell-cell communication in the vessel wall.* Vasc Med, 2001. **6**(1): p. 43-50.
18. Granger, D.N. and E. Senchenkova, *Inflammation and the microcirculation*, in *Integrated systems physiology : from molecule to function #8*2010, Morgan & Claypool Life Sciences Publishers,: San Rafael, CA.
19. de Wit, C. and T.M. Griffith, *Connexins and gap junctions in the EDHF phenomenon and conducted vasomotor responses.* Pflugers Arch, 2010. **459**(6): p. 897-914.
20. Hoepfl, B., et al., *EDHF, but not NO or prostaglandins, is critical to evoke a conducted dilation upon ACh in hamster arterioles.* Am J Physiol Heart Circ Physiol, 2002. **283**(3): p. H996-H1004.
21. de Wit, C. and S.E. Wolfle, *EDHF and gap junctions: important regulators of vascular tone within the microcirculation.* Curr Pharm Biotechnol, 2007. **8**(1): p. 11-25.
22. Maeda, S., et al., *Structure of the connexin 26 gap junction channel at 3.5 A resolution.* Nature, 2009. **458**(7238): p. 597-602.

23. Goodenough, D.A. and D.L. Paul, *Gap junctions.* Cold Spring Harb Perspect Biol, 2009. **1**(1): p. a002576.
24. Dbouk, H.A., et al., *Connexins: a myriad of functions extending beyond assembly of gap junction channels.* Cell Commun Signal, 2009. **7**: p. 4.
25. Sohl, G. and K. Willecke, *An update on connexin genes and their nomenclature in mouse and man.* Cell Commun Adhes, 2003. **10**(4-6): p. 173-80.
26. Behrens, J., et al., *The carboxyl tail of Cx43 augments p38 mediated cell migration in a gap junction-independent manner.* Eur J Cell Biol, 2010. **89**(11): p. 828-38.
27. Giepmans, B.N., *Gap junctions and connexin-interacting proteins.* Cardiovasc Res, 2004. **62**(2): p. 233-45.
28. Herve, J.C., et al., *Gap junctional complexes: from partners to functions.* Prog Biophys Mol Biol, 2007. **94**(1-2): p. 29-65.
29. Verheule, S., et al., *Characterization of gap junction channels in adult rabbit atrial and ventricular myocardium.* Circ Res, 1997. **80**(5): p. 673-81.
30. Figueroa, X.F. and B.R. Duling, *Gap junctions in the control of vascular function.* Antioxid Redox Signal, 2009. **11**(2): p. 251-66.
31. Haefliger, J.A., P. Nicod, and P. Meda, *Contribution of connexins to the function of the vascular wall.* Cardiovasc Res, 2004. **62**(2): p. 345-56.
32. Rummery, N.M., et al., *Connexin37 is the major connexin expressed in the media of caudal artery.* Arterioscler Thromb Vasc Biol, 2002. **22**(9): p. 1427-32.
33. Li, X. and J.M. Simard, *Connexin45 gap junction channels in rat cerebral vascular smooth muscle cells.* Am J Physiol Heart Circ Physiol, 2001. **281**(5): p. H1890-8.
34. van Kempen, M.J. and H.J. Jongsma, *Distribution of connexin37, connexin40 and connexin43 in the aorta and coronary artery of several mammals.* Histochem Cell Biol, 1999. **112**(6): p. 479-86.
35. Gabriels, J.E. and D.L. Paul, *Connexin43 is highly localized to sites of disturbed flow in rat aortic endothelium but connexin37 and connexin40 are more uniformly distributed.* Circ Res, 1998. **83**(6): p. 636-43.
36. Little, T.L., E.C. Beyer, and B.R. Duling, *Connexin 43 and connexin 40 gap junctional proteins are present in arteriolar smooth muscle and endothelium in vivo.* Am J Physiol, 1995. **268**(2 Pt 2): p. H729-39.
37. Severs, N.J., et al., *Immunocytochemical analysis of connexin expression in the healthy and diseased cardiovascular system.* Microsc Res Tech, 2001. **52**(3): p. 301-22.
38. Goldberg, G.S., V. Valiunas, and P.R. Brink, *Selective permeability of gap junction channels.* Biochim Biophys Acta, 2004. **1662**(1-2): p. 96-101.
39. Evans, W.H. and P.E. Martin, *Gap junctions: structure and function (Review).* Mol Membr Biol, 2002. **19**(2): p. 121-36.
40. Saez, J.C., et al., *Plasma membrane channels formed by connexins: their regulation and functions.* Physiol Rev, 2003. **83**(4): p. 1359-400.
41. Weber, P.A., et al., *The permeability of gap junction channels to probes of different size is dependent on connexin composition and permeant-pore affinities.* Biophysical Journal, 2004. **87**(2): p. 958-73.
42. Simpson, I., B. Rose, and W.R. Loewenstein, *Size limit of molecules permeating the junctional membrane channels.* Science, 1977. **195**(4275): p. 294-6.
43. Loewenstein, W.R., *Junctional intercellular communication: the cell-to-cell membrane channel.* Physiol Rev, 1981. **61**(4): p. 829-913.
44. Neijssen, J., et al., *Cross-presentation by intercellular peptide transfer through gap junctions.* Nature, 2005. **434**(7029): p. 83-8.

45. Curran, J.E. and R.I. Woodruff, *Passage of 17 kDa calmodulin through gap junctions of three vertebrate species.* Tissue Cell, 2007. **39**(5): p. 303-9.
46. Duling, B.R. and R.M. Berne, *Propagated vasodilation in the microcirculation of the hamster cheek pouch.* Circ Res, 1970. **26**(2): p. 163-70.
47. Emerson, G.G. and S.S. Segal, *Electrical coupling between endothelial cells and smooth muscle cells in hamster feed arteries: role in vasomotor control.* Circ Res, 2000. **87**(6): p. 474-9.
48. Siegl, D., et al., *Myoendothelial coupling is not prominent in arterioles within the mouse cremaster microcirculation in vivo.* Circ Res, 2005. **97**(8): p. 781-8.
49. Figueroa, X.F. and B.R. Duling, *Dissection of two Cx37-independent conducted vasodilator mechanisms by deletion of Cx40: electrotonic versus regenerative conduction.* Am J Physiol Heart Circ Physiol, 2008. **295**(5): p. H2001-7.
50. de Wit, C., *Different pathways with distinct properties conduct dilations in the microcirculation in vivo.* Cardiovasc Res, 2010. **85**(3): p. 604-13.
51. Tyml, K., et al., *Evidence for K+ channels involvement in capillary sensing and for bidirectionality in capillary communication.* Microvasc Res, 1997. **53**(3): p. 245-53.
52. Bagher, P. and S.S. Segal, *Regulation of blood flow in the microcirculation: role of conducted vasodilation.* Acta Physiol (Oxf), 2011. **202**(3): p. 271-84.
53. Segal, S.S., *Microvascular recruitment in hamster striated muscle: role for conducted vasodilation.* Am J Physiol, 1991. **261**(1 Pt 2): p. H181-9.
54. de Wit, C., et al., *Impaired conduction of vasodilation along arterioles in connexin40-deficient mice.* Circ Res, 2000. **86**(6): p. 649-55.
55. Dora, K.A., et al., *Myoendothelial gap junctions may provide the pathway for EDHF in mouse mesenteric artery.* J Vasc Res, 2003. **40**(5): p. 480-90.
56. Kruger, O., et al., *Defective vascular development in connexin 45-deficient mice.* Development, 2000. **127**(19): p. 4179-93.
57. Simon, A.M. and A.R. McWhorter, *Vascular abnormalities in mice lacking the endothelial gap junction proteins connexin37 and connexin40.* Dev Biol, 2002. **251**(2): p. 206-20.
58. Hirschi, K.K., et al., *Gap junction communication mediates transforming growth factor-beta activation and endothelial-induced mural cell differentiation.* Circ Res, 2003. **93**(5): p. 429-37.
59. Rouget, C., *Memoire sur les developpement, la structure et les proprietes physiologiques des capillaires sanguins et lymphatiques.* Arch Physiol Norm Pathol, 1873. **5**: p. 33.
60. Zimmermann, K.W., *Der feinere Bau der Blutcappillaren*1923, München,: Bergmann. 81 p.
61. Farquhar, M. and J. Hartmann, *Electron microscopy of cerebral capillaries.* Anat Rec, 1956. **124**: p. 2.
62. Ashton, N. and F. de Oliveira, *Nomenclature of pericytes. Intramural and extramural.* Br J Ophthalmol, 1966. **50**(3): p. 119-23.
63. Bondjers, C., et al., *Microarray analysis of blood microvessels from PDGF-B and PDGF-Rbeta mutant mice identifies novel markers for brain pericytes.* FASEB J, 2006. **20**(10): p. 1703-5.
64. Sims, D.E., *Diversity within pericytes.* Clin Exp Pharmacol Physiol, 2000. **27**(10): p. 842-6.
65. Nehls, V. and D. Drenckhahn, *The versatility of microvascular pericytes: from mesenchyme to smooth muscle?* Histochemistry, 1993. **99**(1): p. 1-12.
66. Nehls, V. and D. Drenckhahn, *Heterogeneity of microvascular pericytes for smooth muscle type alpha-actin.* J Cell Biol, 1991. **113**(1): p. 147-54.

67. Dellavalle, A., et al., *Pericytes of human skeletal muscle are myogenic precursors distinct from satellite cells.* Nat Cell Biol, 2007. **9**(3): p. 255-67.
68. Shepro, D. and N.M. Morel, *Pericyte physiology.* FASEB J, 1993. **7**(11): p. 1031-8.
69. Armulik, A., A. Abramsson, and C. Betsholtz, *Endothelial/pericyte interactions.* Circ Res, 2005. **97**(6): p. 512-23.
70. Mandarino, L.J., et al., *Regulation of fibronectin and laminin synthesis by retinal capillary endothelial cells and pericytes in vitro.* Exp Eye Res, 1993. **57**(5): p. 609-21.
71. Gerhardt, H. and C. Betsholtz, *Endothelial-pericyte interactions in angiogenesis.* Cell Tissue Res, 2003. **314**(1): p. 15-23.
72. Hughes, S. and T. Chan-Ling, *Characterization of smooth muscle cell and pericyte differentiation in the rat retina in vivo.* Invest Ophthalmol Vis Sci, 2004. **45**(8): p. 2795-806.
73. Bondjers, C., et al., *Transcription profiling of platelet-derived growth factor-B-deficient mouse embryos identifies RGS5 as a novel marker for pericytes and vascular smooth muscle cells.* Am J Pathol, 2003. **162**(3): p. 721-9.
74. Ozerdem, U., et al., *NG2 proteoglycan is expressed exclusively by mural cells during vascular morphogenesis.* Dev Dyn, 2001. **222**(2): p. 218-27.
75. Ozerdem, U., E. Monosov, and W.B. Stallcup, *NG2 proteoglycan expression by pericytes in pathological microvasculature.* Microvasc Res, 2002. **63**(1): p. 129-34.
76. Piquer-Gil, M., et al., *Cell fusion contributes to pericyte formation after stroke.* J Cereb Blood Flow Metab, 2009. **29**(3): p. 480-5.
77. Hamilton, N.B., D. Attwell, and C.N. Hall, *Pericyte-mediated regulation of capillary diameter: a component of neurovascular coupling in health and disease.* Front Neuroenergetics, 2010. **2**.
78. Allt, G. and J.G. Lawrenson, *Pericytes: cell biology and pathology.* Cells Tissues Organs, 2001. **169**(1): p. 1-11.
79. Sims, D.E., *The pericyte--a review.* Tissue Cell, 1986. **18**(2): p. 153-74.
80. Fernandez-Klett, F., et al., *Pericytes in capillaries are contractile in vivo, but arterioles mediate functional hyperemia in the mouse brain.* Proc Natl Acad Sci U S A, 2010. **107**(51): p. 22290-5.
81. Peppiatt, C.M., et al., *Bidirectional control of CNS capillary diameter by pericytes.* Nature, 2006. **443**(7112): p. 700-4.
82. Joyce, N.C., M.F. Haire, and G.E. Palade, *Contractile proteins in pericytes. II. Immunocytochemical evidence for the presence of two isomyosins in graded concentrations.* J Cell Biol, 1985. **100**(5): p. 1387-95.
83. Joyce, N.C., M.F. Haire, and G.E. Palade, *Contractile proteins in pericytes. I. Immunoperoxidase localization of tropomyosin.* J Cell Biol, 1985. **100**(5): p. 1379-86.
84. Balabanov, R. and P. Dore-Duffy, *Role of the CNS microvascular pericyte in the blood-brain barrier.* J Neurosci Res, 1998. **53**(6): p. 637-44.
85. Dore-Duffy, P., *Pericytes: pluripotent cells of the blood brain barrier.* Curr Pharm Des, 2008. **14**(16): p. 1581-93.
86. Edelman, D.A., et al., *Pericytes and their role in microvasculature homeostasis.* J Surg Res, 2006. **135**(2): p. 305-11.
87. Yamanishi, S., et al., *Extracellular lactate as a dynamic vasoactive signal in the rat retinal microvasculature.* Am J Physiol Heart Circ Physiol, 2006. **290**(3): p. H925-34.
88. Martin, A.R., et al., *Retinal pericytes control expression of nitric oxide synthase and endothelin-1 in microvascular endothelial cells.* Microvasc Res, 2000. **59**(1): p. 131-9.
89. Haefliger, I.O. and D.R. Anderson, *Oxygen modulation of guanylate cyclase-mediated retinal pericyte relaxations with 3-morpholino-sydnonimine and atrial natriuretic peptide.* Invest Ophthalmol Vis Sci, 1997. **38**(8): p. 1563-8.

90. Haefliger, I.O., Q. Chen, and D.R. Anderson, *Effect of oxygen on relaxation of retinal pericytes by sodium nitroprusside.* Graefes Arch Clin Exp Ophthalmol, 1997. **235**(6): p. 388-92.
91. Matsugi, T., Q. Chen, and D.R. Anderson, *Suppression of CO2-induced relaxation of bovine retinal pericytes by angiotensin II.* Invest Ophthalmol Vis Sci, 1997. **38**(3): p. 652-7.
92. Chen, Q. and D.R. Anderson, *Effect of CO2 on intracellular pH and contraction of retinal capillary pericytes.* Invest Ophthalmol Vis Sci, 1997. **38**(3): p. 643-51.
93. Matsugi, T., Q. Chen, and D.R. Anderson, *Adenosine-induced relaxation of cultured bovine retinal pericytes.* Invest Ophthalmol Vis Sci, 1997. **38**(13): p. 2695-701.
94. Crawford, C., et al., *Extracellular nucleotides affect pericyte-mediated regulation of rat in situ vasa recta diameter.* Acta Physiol (Oxf), 2011. **202**(3): p. 241-51.
95. Silldorff, E.P., M.S. Kreisberg, and T.L. Pallone, *Adenosine modulates vasomotor tone in outer medullary descending vasa recta of the rat.* J Clin Invest, 1996. **98**(1): p. 18-23.
96. Li, Q. and D.G. Puro, *Adenosine activates ATP-sensitive K(+) currents in pericytes of rat retinal microvessels: role of A1 and A2a receptors.* Brain Res, 2001. **907**(1-2): p. 93-9.
97. Hirao, M., et al., *Effects of adenosine on optic nerve head circulation in rabbits.* Exp Eye Res, 2004. **79**(5): p. 729-35.
98. Haefliger, I.O., A. Zschauer, and D.R. Anderson, *Relaxation of retinal pericyte contractile tone through the nitric oxide-cyclic guanosine monophosphate pathway.* Invest Ophthalmol Vis Sci, 1994. **35**(3): p. 991-7.
99. Kelley, C., et al., *Vasoactive hormones and cAMP affect pericyte contraction and stress fibres in vitro.* J Muscle Res Cell Motil, 1988. **9**(2): p. 184-94.
100. Markhotina, N., G.J. Liu, and D.K. Martin, *Contractility of retinal pericytes grown on silicone elastomer substrates is through a protein kinase A-mediated intracellular pathway in response to vasoactive peptides.* IET Nanobiotechnol, 2007. **1**(3): p. 44-51.
101. Dodge, A.B., H.B. Hechtman, and D. Shepro, *Microvascular endothelial-derived autacoids regulate pericyte contractility.* Cell Motil Cytoskeleton, 1991. **18**(3): p. 180-8.
102. Matsugi, T., Q. Chen, and D.R. Anderson, *Contractile responses of cultured bovine retinal pericytes to angiotensin II.* Arch Ophthalmol, 1997. **115**(10): p. 1281-5.
103. Armulik, A., G. Genove, and C. Betsholtz, *Pericytes: developmental, physiological, and pathological perspectives, problems, and promises.* Dev Cell, 2011. **21**(2): p. 193-215.
104. Chakravarthy, U. and T.A. Gardiner, *Endothelium-derived agents in pericyte function/dysfunction.* Prog Retin Eye Res, 1999. **18**(4): p. 511-27.
105. Yamagishi, S., et al., *Endothelin 1 mediates endothelial cell-dependent proliferation of vascular pericytes.* Biochem Biophys Res Commun, 1993. **191**(3): p. 840-6.
106. Hellstrom, M., et al., *Role of PDGF-B and PDGFR-beta in recruitment of vascular smooth muscle cells and pericytes during embryonic blood vessel formation in the mouse.* Development, 1999. **126**(14): p. 3047-55.
107. Egginton, S., et al., *In vivo pericyte-endothelial cell interaction during angiogenesis in adult cardiac and skeletal muscle.* Microvasc Res, 1996. **51**(2): p. 213-28.
108. Bergers, G. and S. Song, *The role of pericytes in blood-vessel formation and maintenance.* Neuro Oncol, 2005. **7**(4): p. 452-64.
109. Betsholtz, C., P. Lindblom, and H. Gerhardt, *Role of pericytes in vascular morphogenesis.* EXS, 2005(94): p. 115-25.

110. Hyldahl, R.D., et al., *Activation of nuclear factor-{kappa}B following muscle eccentric contractions in humans is localized primarily to skeletal muscle-residing pericytes.* FASEB J, 2011.
111. Yamagishi, S., et al., *Vascular endothelial growth factor acts as a pericyte mitogen under hypoxic conditions.* Lab Invest, 1999. **79**(4): p. 501-9.
112. DeRuiter, M.C., et al., *Embryonic endothelial cells transdifferentiate into mesenchymal cells expressing smooth muscle actins in vivo and in vitro.* Circ Res, 1997. **80**(4): p. 444-51.
113. Etchevers, H.C., et al., *The cephalic neural crest provides pericytes and smooth muscle cells to all blood vessels of the face and forebrain.* Development, 2001. **128**(7): p. 1059-68.
114. Rajantie, I., et al., *Adult bone marrow-derived cells recruited during angiogenesis comprise precursors for periendothelial vascular mural cells.* Blood, 2004. **104**(7): p. 2084-6.
115. Sundberg, C., et al., *Pericytes as collagen-producing cells in excessive dermal scarring.* Lab Invest, 1996. **74**(2): p. 452-66.
116. Thomas, W.E., *Brain macrophages: on the role of pericytes and perivascular cells.* Brain Res Brain Res Rev, 1999. **31**(1): p. 42-57.
117. Zhang, X., et al., *The Nell-1 growth factor stimulates bone formation by purified human perivascular cells.* Tissue Eng Part A, 2011.
118. Broadwell, R.D. and M. Salcman, *Expanding the definition of the blood-brain barrier to protein.* Proc Natl Acad Sci U S A, 1981. **78**(12): p. 7820-4.
119. Kristensson, K. and Y. Olsson, *Accumulation of protein tracers in pericytes of the central nervous system following systemic injection in immature mice.* Acta Neurol Scand, 1973. **49**(2): p. 189-94.
120. Mato, M., S. Ookawara, and K. Kurihara, *Uptake of exogenous substances and marked infoldings of the fluorescent granular pericyte in cerebral fine vessels.* Am J Anat, 1980. **157**(3): p. 329-32.
121. Mato, M., et al., *Behavior of fluorescent granular perithelium (FGP) in cerebral cortex of SHR-SP rats under some conditions.* Exp Mol Pathol, 1983. **39**(1): p. 100-9.
122. Mato, M., et al., *Uptake of fat by fluorescent granular perithelial cells in cerebral cortex after administration of fat rich chow.* Experientia, 1982. **38**(12): p. 1496-8.
123. Mato, M. and S. Ookawara, *Influences of age and vasopressin on the uptake capacity of fluorescent granular perithelial cells (FGP) of small cerebral vessels of the rat.* Am J Anat, 1981. **162**(1): p. 45-53.
124. Mato, M., et al., *An attempt to differentiate further between microglia and fluorescent granular perithelial (FGP) cells by their capacity to incorporate exogenous protein.* Am J Anat, 1985. **172**(2): p. 125-40.
125. Cancilla, P.A., et al., *The reaction of pericytes of the central nervous system to exogenous protein.* Lab Invest, 1972. **26**(4): p. 376-83.
126. Pennell, N.A. and W.J. Streit, *Tracing of fluoro-gold prelabeled microglia injected into the adult rat brain.* Glia, 1998. **23**(1): p. 84-8.
127. van Deurs, B., *Observations on the blood-brain barrier in hypertensive rats, with particular reference to phagocytic pericytes.* J Ultrastruct Res, 1976. **56**(1): p. 65-77.
128. Balabanov, R., et al., *CNS microvascular pericytes express macrophage-like function, cell surface integrin alpha M, and macrophage marker ED-2.* Microvasc Res, 1996. **52**(2): p. 127-42.
129. Dore-Duffy, P. and R. Balabanov, *The role of the CNS microvascular pericyte in leukocyte polarization of cytokine-secreting phenotype.* J Neurochem, 1998. **70**: p. S72-S72.

130. Kokovay, E., L. Li, and L.A. Cunningham, *Angiogenic recruitment of pericytes from bone marrow after stroke.* J Cereb Blood Flow Metab, 2006. **26**(4): p. 545-55.
131. Ozerdem, U. and W.B. Stallcup, *Early contribution of pericytes to angiogenic sprouting and tube formation.* Angiogenesis, 2003. **6**(3): p. 241-9.
132. Lee, R.C., R.L. Feinbaum, and V. Ambros, *The C. elegans heterochronic gene lin-4 encodes small RNAs with antisense complementarity to lin-14.* Cell, 1993. **75**(5): p. 843-54.
133. Reinhart, B.J., et al., *The 21-nucleotide let-7 RNA regulates developmental timing in Caenorhabditis elegans.* Nature, 2000. **403**(6772): p. 901-6.
134. Pasquinelli, A.E., et al., *Conservation of the sequence and temporal expression of let-7 heterochronic regulatory RNA.* Nature, 2000. **408**(6808): p. 86-9.
135. Tanzer, A. and P.F. Stadler, *Molecular evolution of a microRNA cluster.* J Mol Biol, 2004. **339**(2): p. 327-35.
136. Lee, C.T., T. Risom, and W.M. Strauss, *Evolutionary conservation of microRNA regulatory circuits: an examination of microRNA gene complexity and conserved microRNA-target interactions through metazoan phylogeny.* DNA Cell Biol, 2007. **26**(4): p. 209-18.
137. Bartel, D.P., *MicroRNAs: target recognition and regulatory functions.* Cell, 2009. **136**(2): p. 215-33.
138. He, L. and G.J. Hannon, *MicroRNAs: small RNAs with a big role in gene regulation.* Nat Rev Genet, 2004. **5**(7): p. 522-31.
139. Bentwich, I., et al., *Identification of hundreds of conserved and nonconserved human microRNAs.* Nat Genet, 2005. **37**(7): p. 766-70.
140. Lewis, B.P., C.B. Burge, and D.P. Bartel, *Conserved seed pairing, often flanked by adenosines, indicates that thousands of human genes are microRNA targets.* Cell, 2005. **120**(1): p. 15-20.
141. Friedman, R.C., et al., *Most mammalian mRNAs are conserved targets of microRNAs.* Genome Res, 2009. **19**(1): p. 92-105.
142. Lim, L.P., et al., *Microarray analysis shows that some microRNAs downregulate large numbers of target mRNAs.* Nature, 2005. **433**(7027): p. 769-73.
143. Bartel, D.P., *MicroRNAs: genomics, biogenesis, mechanism, and function.* Cell, 2004. **116**(2): p. 281-97.
144. Rodriguez, A., et al., *Identification of mammalian microRNA host genes and transcription units.* Genome Res, 2004. **14**(10A): p. 1902-10.
145. Lee, Y., et al., *MicroRNA genes are transcribed by RNA polymerase II.* EMBO J, 2004. **23**(20): p. 4051-60.
146. Zhou, X., et al., *Characterization and identification of microRNA core promoters in four model species.* PLoS Comput Biol, 2007. **3**(3): p. e37.
147. Cai, X., C.H. Hagedorn, and B.R. Cullen, *Human microRNAs are processed from capped, polyadenylated transcripts that can also function as mRNAs.* RNA, 2004. **10**(12): p. 1957-66.
148. Gregory, R.I., T.P. Chendrimada, and R. Shiekhattar, *MicroRNA biogenesis: isolation and characterization of the microprocessor complex.* Methods Mol Biol, 2006. **342**: p. 33-47.
149. Murchison, E.P. and G.J. Hannon, *miRNAs on the move: miRNA biogenesis and the RNAi machinery.* Curr Opin Cell Biol, 2004. **16**(3): p. 223-9.
150. Lund, E. and J.E. Dahlberg, *Substrate selectivity of exportin 5 and Dicer in the biogenesis of microRNAs.* Cold Spring Harb Symp Quant Biol, 2006. **71**: p. 59-66.

151. Krol, J., et al., *Structural features of microRNA (miRNA) precursors and their relevance to miRNA biogenesis and small interfering RNA/short hairpin RNA design.* J Biol Chem, 2004. **279**(40): p. 42230-9.
152. Khvorova, A., A. Reynolds, and S.D. Jayasena, *Functional siRNAs and miRNAs exhibit strand bias.* Cell, 2003. **115**(2): p. 209-16.
153. Schwarz, D.S., et al., *Asymmetry in the assembly of the RNAi enzyme complex.* Cell, 2003. **115**(2): p. 199-208.
154. Pratt, A.J. and I.J. MacRae, *The RNA-induced silencing complex: a versatile gene-silencing machine.* J Biol Chem, 2009. **284**(27): p. 17897-901.
155. Mack, G.S., *MicroRNA gets down to business.* Nat Biotechnol, 2007. **25**(6): p. 631-8.
156. Elfgang, C., et al., *Specific permeability and selective formation of gap junction channels in connexin-transfected HeLa cells.* J Cell Biol, 1995. **129**(3): p. 805-17.
157. Jaffe, E.A., et al., *Culture of human endothelial cells derived from umbilical veins. Identification by morphologic and immunologic criteria.* J Clin Invest, 1973. **52**(11): p. 2745-56.
158. Nayak, R.C., et al., *A monoclonal antibody (3G5)-defined ganglioside antigen is expressed on the cell surface of microvascular pericytes.* J Exp Med, 1988. **167**(3): p. 1003-15.
159. Andreeva, E.R., et al., *Continuous subendothelial network formed by pericyte-like cells in human vascular bed.* Tissue Cell, 1998. **30**(1): p. 127-35.
160. Birch, K.E., et al., *The immunomodulatory effects of regulatory T cells: implications for immune regulation in the skin.* Br J Dermatol, 2005. **152**(3): p. 409-17.
161. Panchuk-Voloshina, N., et al., *Alexa dyes, a series of new fluorescent dyes that yield exceptionally bright, photostable conjugates.* J Histochem Cytochem, 1999. **47**(9): p. 1179-88.
162. Berlier, J.E., et al., *Quantitative comparison of long-wavelength Alexa Fluor dyes to Cy dyes: fluorescence of the dyes and their bioconjugates.* J Histochem Cytochem, 2003. **51**(12): p. 1699-712.
163. Renart, J., J. Reiser, and G.R. Stark, *Transfer of proteins from gels to diazobenzyloxymethyl-paper and detection with antisera: a method for studying antibody specificity and antigen structure.* Proc Natl Acad Sci U S A, 1979. **76**(7): p. 3116-20.
164. Laemmli, U.K., *Cleavage of structural proteins during the assembly of the head of bacteriophage T4.* Nature, 1970. **227**(5259): p. 680-5.
165. Ashcroft, R.G. and P.A. Lopez, *Commercial high speed machines open new opportunities in high throughput flow cytometry (HTFC).* J Immunol Methods, 2000. **243**(1-2): p. 13-24.
166. Alberts, B., *Molecular biology of the cell*. 4th ed / Bruce Alberts ... [et al.] ed2002, New York: Garland Science.
167. Grissmer, S., et al., *Pharmacological characterization of five cloned voltage-gated K+ channels, types Kv1.1, 1.2, 1.3, 1.5, and 3.1, stably expressed in mammalian cell lines.* Mol Pharmacol, 1994. **45**(6): p. 1227-34.
168. Pappone, P.A. and S.C. Lee, *Alpha-adrenergic stimulation activates a calcium-sensitive chloride current in brown fat cells.* J Gen Physiol, 1995. **106**(2): p. 231-58.
169. White, M.M. and M. Aylwin, *Niflumic and flufenamic acids are potent reversible blockers of Ca2(+)-activated Cl- channels in Xenopus oocytes.* Mol Pharmacol, 1990. **37**(5): p. 720-4.
170. Kameritsch, P., et al., *Nitric oxide specifically reduces the permeability of Cx37-containing gap junctions to small molecules.* J Cell Physiol, 2005. **203**(1): p. 233-42.

171. Bolanos, J.P. and J.M. Medina, *Induction of nitric oxide synthase inhibits gap junction permeability in cultured rat astrocytes.* J Neurochem, 1996. **66**(5): p. 2091-9.
172. Yao, J., et al., *Nitric oxide-mediated regulation of connexin43 expression and gap junctional intercellular communication in mesangial cells.* J Am Soc Nephrol, 2005. **16**(1): p. 58-67.
173. Epps, D.E., M.L. Wolfe, and V. Groppi, *Characterization of the steady-state and dynamic fluorescence properties of the potential-sensitive dye bis-(1,3-dibutylbarbituric acid)trimethine oxonol (Dibac4(3)) in model systems and cells.* Chem Phys Lipids, 1994. **69**(2): p. 137-50.
174. Brauner, T., D.F. Hulser, and R.J. Strasser, *Comparative measurements of membrane potentials with microelectrodes and voltage-sensitive dyes.* Biochim Biophys Acta, 1984. **771**(2): p. 208-16.
175. Hua, Z., et al., *MiRNA-directed regulation of VEGF and other angiogenic factors under hypoxia.* PLoS One, 2006. **1**: p. e116.
176. Kuehbacher, A., C. Urbich, and S. Dimmeler, *Targeting microRNA expression to regulate angiogenesis.* Trends Pharmacol Sci, 2008. **29**(1): p. 12-5.
177. Martello, G., et al., *MicroRNA control of Nodal signalling.* Nature, 2007. **449**(7159): p. 183-8.
178. Platika, D., et al., *Neuronal traits of clonal cell lines derived by fusion of dorsal root ganglia neurons with neuroblastoma cells.* Proc Natl Acad Sci U S A, 1985. **82**(10): p. 3499-503.
179. Powers, A.C., et al., *Characterization of monoclonal antibody 3G5 and utilization of this antibody to immobilize pancreatic islet cell gangliosides in a solid phase radioassay.* Endocrinology, 1984. **114**(4): p. 1338-43.
180. Yao, J., T. Morioka, and T. Oite, *PDGF regulates gap junction communication and connexin43 phosphorylation by PI 3-kinase in mesangial cells.* Kidney Int, 2000. **57**(5): p. 1915-26.
181. Makeyev, E.V., et al., *The MicroRNA miR-124 promotes neuronal differentiation by triggering brain-specific alternative pre-mRNA splicing.* Mol Cell, 2007. **27**(3): p. 435-48.
182. Bryan, B.A. and P.A. D'Amore, *Pericyte isolation and use in endothelial/pericyte coculture models.* Methods Enzymol, 2008. **443**: p. 315-31.
183. Berrone, E., et al., *Establishment and characterization of a human retinal pericyte line: a novel tool for the study of diabetic retinopathy.* Int J Mol Med, 2009. **23**(3): p. 373-8.
184. Larson, D.M., M.P. Carson, and C.C. Haudenschild, *Junctional transfer of small molecules in cultured bovine brain microvascular endothelial cells and pericytes.* Microvasc Res, 1987. **34**(2): p. 184-99.
185. Dente, C.J., et al., *Pericytes augment the capillary barrier in in vitro cocultures.* J Surg Res, 2001. **97**(1): p. 85-91.
186. Helmbold, P., et al., *Human dermal pericytes express 3G5 ganglioside--a new approach for microvessel histology in the skin.* J Cutan Pathol, 2001. **28**(4): p. 206-10.
187. Helmbold, P., et al., *Isolation and in vitro characterization of human dermal microvascular pericytes.* Microvasc Res, 2001. **61**(2): p. 160-5.
188. von Beckerath, N., et al., *An inward rectifier and a voltage-dependent K+ current in single, cultured pericytes from bovine heart.* Cardiovasc Res, 2000. **46**(3): p. 569-78.
189. Song, S., et al., *PDGFRbeta+ perivascular progenitor cells in tumours regulate pericyte differentiation and vascular survival.* Nat Cell Biol, 2005. **7**(9): p. 870-9.

190. Murfee, W.L., T.C. Skalak, and S.M. Peirce, *Differential arterial/venous expression of NG2 proteoglycan in perivascular cells along microvessels: identifying a venule-specific phenotype.* Microcirculation, 2005. **12**(2): p. 151-60.
191. Lanner, F., M. Sohl, and F. Farnebo, *Functional arterial and venous fate is determined by graded VEGF signaling and notch status during embryonic stem cell differentiation.* Arterioscler Thromb Vasc Biol, 2007. **27**(3): p. 487-93.
192. Claxton, S. and M. Fruttiger, *Periodic Delta-like 4 expression in developing retinal arteries.* Gene Expr Patterns, 2004. **5**(1): p. 123-7.
193. Murfee, W.L., et al., *Perivascular cells along venules upregulate NG2 expression during microvascular remodeling.* Microcirculation, 2006. **13**(3): p. 261-73.
194. Chan-Ling, T., et al., *Desmin ensheathment ratio as an indicator of vessel stability: evidence in normal development and in retinopathy of prematurity.* Am J Pathol, 2004. **165**(4): p. 1301-13.
195. Newcomb, P.M. and I.M. Herman, *Pericyte growth and contractile phenotype: modulation by endothelial-synthesized matrix and comparison with aortic smooth muscle.* J Cell Physiol, 1993. **155**(2): p. 385-93.
196. Liu, Y., et al., *Hepatocyte growth factor and c-Met expression in pericytes: implications for atherosclerotic plaque development.* J Pathol, 2007. **212**(1): p. 12-9.
197. Farrington-Rock, C., et al., *Chondrogenic and adipogenic potential of microvascular pericytes.* Circulation, 2004. **110**(15): p. 2226-32.
198. Hirschi, K.K. and P.A. D'Amore, *Pericytes in the microvasculature.* Cardiovasc Res, 1996. **32**(4): p. 687-98.
199. Sundberg, C., et al., *Stable expression of angiopoietin-1 and other markers by cultured pericytes: phenotypic similarities to a subpopulation of cells in maturing vessels during later stages of angiogenesis in vivo.* Lab Invest, 2002. **82**(4): p. 387-401.
200. Stallcup, W.B., *The NG2 proteoglycan: past insights and future prospects.* J Neurocytol, 2002. **31**(6-7): p. 423-35.
201. Pugach, I.M., E.R. Andreeva, and A.N. Orekhov, *[The identification of pericyte-like cells in the subendothelium of human blood vessels].* Arkh Patol, 1999. **61**(4): p. 18-21.
202. Bostrom, K., et al., *Bone morphogenetic protein expression in human atherosclerotic lesions.* J Clin Invest, 1993. **91**(4): p. 1800-9.
203. Shi, S. and S. Gronthos, *Perivascular niche of postnatal mesenchymal stem cells in human bone marrow and dental pulp.* J Bone Miner Res, 2003. **18**(4): p. 696-704.
204. Khan, W.S., A.B. Adesida, and T.E. Hardingham, *Hypoxic conditions increase hypoxia-inducible transcription factor 2alpha and enhance chondrogenesis in stem cells from the infrapatellar fat pad of osteoarthritis patients.* Arthritis Res Ther, 2007. **9**(3): p. R55.
205. Khan, W.S., et al., *Human infrapatellar fat pad-derived stem cells express the pericyte marker 3G5 and show enhanced chondrogenesis after expansion in fibroblast growth factor-2.* Arthritis Res Ther, 2008. **10**(4): p. R74.
206. Canfield, A.E., et al., *Modulation of extracellular matrix biosynthesis by bovine retinal pericytes in vitro: effects of the substratum and cell density.* J Cell Sci, 1990. **96 (Pt 1)**: p. 159-69.
207. Capetandes, A. and M.E. Gerritsen, *Simplified methods for consistent and selective culture of bovine retinal endothelial cells and pericytes.* Invest Ophthalmol Vis Sci, 1990. **31**(9): p. 1738-44.

208. Meresse, S., et al., *Bovine brain endothelial cells express tight junctions and monoamine oxidase activity in long-term culture.* J Neurochem, 1989. **53**(5): p. 1363-71.
209. Swinscoe, J.C. and E.C. Carlson, *Capillary endothelial cells secrete a heparin-binding mitogen for pericytes.* J Cell Sci, 1992. **103 (Pt 2)**: p. 453-61.
210. Bandopadhyay, R., et al., *Contractile proteins in pericytes at the blood-brain and blood-retinal barriers.* J Neurocytol, 2001. **30**(1): p. 35-44.
211. Skalli, O., et al., *Alpha-smooth muscle actin, a differentiation marker of smooth muscle cells, is present in microfilamentous bundles of pericytes.* J Histochem Cytochem, 1989. **37**(3): p. 315-21.
212. Sundberg, C., et al., *Microvascular pericytes express platelet-derived growth factor-beta receptors in human healing wounds and colorectal adenocarcinoma.* Am J Pathol, 1993. **143**(5): p. 1377-88.
213. Ivarsson, M., et al., *Recruitment of type I collagen producing cells from the microvasculature in vitro.* Exp Cell Res, 1996. **229**(2): p. 336-49.
214. Reuterdahl, C., et al., *Characterization of platelet-derived growth factor beta-receptor expressing cells in the vasculature of human rheumatoid synovium.* Lab Invest, 1991. **64**(3): p. 321-9.
215. Guijarro-Munoz, I., et al., *The axonal repellent Slit2 inhibits pericyte migration: Potential implications in angiogenesis.* Exp Cell Res, 2012. **318**(4): p. 371-8.
216. Tomkowicz, B., et al., *Endosialin/TEM-1/CD248 regulates pericyte proliferation through PDGF receptor signaling.* Cancer Biol Ther, 2010. **9**(11): p. 908-15.
217. Lindahl, P., et al., *Pericyte loss and microaneurysm formation in PDGF-B-deficient mice.* Science, 1997. **277**(5323): p. 242-5.
218. Lamagna, C. and G. Bergers, *The bone marrow constitutes a reservoir of pericyte progenitors.* J Leukoc Biol, 2006. **80**(4): p. 677-81.
219. de Wit, C., et al., *Pentobarbital-sensitive EDHF comediates ACh-induced arteriolar dilation in the hamster microcirculation.* Am J Physiol, 1999. **276**(5 Pt 2): p. H1527-34.
220. Hungerford, J.E., W.C. Sessa, and S.S. Segal, *Vasomotor control in arterioles of the mouse cremaster muscle.* FASEB J, 2000. **14**(1): p. 197-207.
221. Huang, A., et al., *EDHF mediates flow-induced dilation in skeletal muscle arterioles of female eNOS-KO mice.* Am J Physiol Heart Circ Physiol, 2001. **280**(6): p. H2462-9.
222. Huang, A., et al., *In eNOS knockout mice skeletal muscle arteriolar dilation to acetylcholine is mediated by EDHF.* Am J Physiol Heart Circ Physiol, 2000. **278**(3): p. H762-8.
223. Koeppen, M., et al., *cGMP-dependent protein kinase mediates NO- but not acetylcholine-induced dilations in resistance vessels in vivo.* Hypertension, 2004. **44**(6): p. 952-5.
224. Bolton, T.B., R.J. Lang, and T. Takewaki, *Mechanisms of action of noradrenaline and carbachol on smooth muscle of guinea-pig anterior mesenteric artery.* J Physiol, 1984. **351**: p. 549-72.
225. Scotland, R.S., et al., *Investigation of vascular responses in endothelial nitric oxide synthase/cyclooxygenase-1 double-knockout mice: key role for endothelium-derived hyperpolarizing factor in the regulation of blood pressure in vivo.* Circulation, 2005. **111**(6): p. 796-803.
226. Huang, A., et al., *Effect of estrogen on flow-induced dilation in NO deficiency: role of prostaglandins and EDHF.* J Appl Physiol, 2001. **91**(6): p. 2561-6.
227. Liu, M.Y., et al., *Ovariectomy attenuates hyperpolarization and relaxation mediated by endothelium-derived hyperpolarizing factor in female rat mesenteric artery: a*

concomitant decrease in connexin-43 expression. J Cardiovasc Pharmacol, 2002. **40**(6): p. 938-48.
228. Nawate, S., et al., *Reciprocal changes in endothelium-derived hyperpolarizing factor- and nitric oxide-system in the mesenteric artery of adult female rats following ovariectomy.* Br J Pharmacol, 2005. **144**(2): p. 178-89.
229. Luksha, L., S. Agewall, and K. Kublickiene, *Endothelium-derived hyperpolarizing factor in vascular physiology and cardiovascular disease.* Atherosclerosis, 2009. **202**(2): p. 330-44.
230. Feletou, M. and P.M. Vanhoutte, *EDHF: new therapeutic targets?* Pharmacol Res, 2004. **49**(6): p. 565-80.
231. Grgic, I., et al., *Endothelial Ca+-activated K+ channels in normal and impaired EDHF-dilator responses--relevance to cardiovascular pathologies and drug discovery.* Br J Pharmacol, 2009. **157**(4): p. 509-26.
232. Barton, M., *Obesity and aging: determinants of endothelial cell dysfunction and atherosclerosis.* Pflugers Arch, 2010. **460**(5): p. 825-37.
233. Kohler, R., et al., *Expression and function of endothelial Ca(2+)-activated K(+) channels in human mesenteric artery: A single-cell reverse transcriptase-polymerase chain reaction and electrophysiological study in situ.* Circ Res, 2000. **87**(6): p. 496-503.
234. Eichler, I., et al., *Selective blockade of endothelial Ca2+-activated small- and intermediate-conductance K+-channels suppresses EDHF-mediated vasodilation.* Br J Pharmacol, 2003. **138**(4): p. 594-601.
235. Hinton, J.M. and P.D. Langton, *Inhibition of EDHF by two new combinations of K+-channel inhibitors in rat isolated mesenteric arteries.* Br J Pharmacol, 2003. **138**(6): p. 1031-5.
236. Burnham, M.P., et al., *Characterization of an apamin-sensitive small-conductance Ca(2+)-activated K(+) channel in porcine coronary artery endothelium: relevance to EDHF.* Br J Pharmacol, 2002. **135**(5): p. 1133-43.
237. Bychkov, R., et al., *Characterization of a charybdotoxin-sensitive intermediate conductance Ca2+-activated K+ channel in porcine coronary endothelium: relevance to EDHF.* Br J Pharmacol, 2002. **137**(8): p. 1346-54.
238. Crane, G.J., et al., *Small- and intermediate-conductance calcium-activated K+ channels provide different facets of endothelium-dependent hyperpolarization in rat mesenteric artery.* J Physiol, 2003. **553**(Pt 1): p. 183-9.
239. Gluais, P., et al., *Role of SK(Ca) and IK(Ca) in endothelium-dependent hyperpolarizations of the guinea-pig isolated carotid artery.* Br J Pharmacol, 2005. **144**(4): p. 477-85.
240. McSherry, I.N., et al., *A role for heterocellular coupling and EETs in dilation of rat cremaster arteries.* Microcirculation, 2006. **13**(2): p. 119-30.
241. Domeier, T.L. and S.S. Segal, *Electromechanical and pharmacomechanical signalling pathways for conducted vasodilatation along endothelium of hamster feed arteries.* J Physiol, 2007. **579**(Pt 1): p. 175-86.
242. Kawamura, H., et al., *ATP: a vasoactive signal in the pericyte-containing microvasculature of the rat retina.* J Physiol, 2003. **551**(Pt 3): p. 787-99.
243. Fatherazi, S. and D.L. Cook, *Specificity of tetraethylammonium and quinine for three K channels in insulin-secreting cells.* J Membr Biol, 1991. **120**(2): p. 105-14.
244. Robertson, B.E. and M.T. Nelson, *Aminopyridine inhibition and voltage dependence of K+ currents in smooth muscle cells from cerebral arteries.* Am J Physiol, 1994. **267**(6 Pt 1): p. C1589-97.

245. Okabe, K., K. Kitamura, and H. Kuriyama, *Features of 4-aminopyridine sensitive outward current observed in single smooth muscle cells from the rabbit pulmonary artery.* Pflugers Arch, 1987. **409**(6): p. 561-8.
246. Ishikawa, T., J.R. Hume, and K.D. Keef, *Modulation of K+ and Ca2+ channels by histamine H1-receptor stimulation in rabbit coronary artery cells.* J Physiol, 1993. **468**: p. 379-400.
247. Beech, D.J. and T.B. Bolton, *Two components of potassium current activated by depolarization of single smooth muscle cells from the rabbit portal vein.* J Physiol, 1989. **418**: p. 293-309.
248. Bever, C.T., Jr., *10 questions about 4-aminopyridine and the treatment of multiple sclerosis.* Neurologist, 2009. **15**(3): p. 161-2.
249. Overturf, K.E., et al., *Cloning and characterization of a Kv1.5 delayed rectifier K+ channel from vascular and visceral smooth muscles.* Am J Physiol, 1994. **267**(5 Pt 1): p. C1231-8.
250. Flower, R., et al., *Effects of anti-inflammatory drugs on prostaglandin biosynthesis.* Nat New Biol, 1972. **238**(82): p. 104-6.
251. Harks, E.G., et al., *Fenamates: a novel class of reversible gap junction blockers.* J Pharmacol Exp Ther, 2001. **298**(3): p. 1033-41.
252. Yao, J., et al., *ATP-dependent mechanism for coordination of intercellular Ca2+ signaling and renin secretion in rat juxtaglomerular cells.* Circ Res, 2003. **93**(4): p. 338-45.
253. Hill, K., et al., *Flufenamic acid is a pH-dependent antagonist of TRPM2 channels.* Neuropharmacology, 2004. **47**(3): p. 450-60.
254. Poronnik, P., M.C. Ward, and D.I. Cook, *Intracellular Ca2+ release by flufenamic acid and other blockers of the non-selective cation channel.* FEBS Lett, 1992. **296**(3): p. 245-8.
255. Ottolia, M. and L. Toro, *Potentiation of large conductance KCa channels by niflumic, flufenamic, and mefenamic acids.* Biophysical Journal, 1994. **67**(6): p. 2272-9.
256. Farrugia, G., et al., *Potassium current in circular smooth muscle of human jejunum activated by fenamates.* Am J Physiol, 1993. **265**(5 Pt 1): p. G873-9.
257. Foster, R.R., et al., *Flufenamic acid is a tool for investigating TRPC6-mediated calcium signalling in human conditionally immortalised podocytes and HEK293 cells.* Cell Calcium, 2009. **45**(4): p. 384-90.
258. Hu, H., et al., *Activation of TRPA1 channels by fenamate nonsteroidal anti-inflammatory drugs.* Pflugers Arch, 2010. **459**(4): p. 579-92.
259. Jackson, W.F., *Potassium channels in the peripheral microcirculation.* Microcirculation, 2005. **12**(1): p. 113-27.
260. Cheong, A., et al., *K(V)alpha1 channels in murine arterioles: differential cellular expression and regulation of diameter.* Am J Physiol Heart Circ Physiol, 2001. **281**(3): p. H1057-65.
261. Moore, D.H. and H. Ruska, *The fine structure of capillaries and small arteries.* J Biophys Biochem Cytol, 1957. **3**(3): p. 457-62.
262. Mather, S., et al., *Rapid endothelial cell-selective loading of connexin 40 antibody blocks endothelium-derived hyperpolarizing factor dilation in rat small mesenteric arteries.* Circ Res, 2005. **97**(4): p. 399-407.
263. Busse, R., et al., *EDHF: bringing the concepts together.* Trends Pharmacol Sci, 2002. **23**(8): p. 374-80.
264. Griffith, T.M., *Endothelium-dependent smooth muscle hyperpolarization: do gap junctions provide a unifying hypothesis?* Br J Pharmacol, 2004. **141**(6): p. 881-903.

265. Goto, K., et al., *Critical role of gap junctions in endothelium-dependent hyperpolarization in rat mesenteric arteries.* Clin Exp Pharmacol Physiol, 2002. **29**(7): p. 595-602.
266. Griffith, T.M., A.T. Chaytor, and D.H. Edwards, *The obligatory link: role of gap junctional communication in endothelium-dependent smooth muscle hyperpolarization.* Pharmacol Res, 2004. **49**(6): p. 551-64.
267. McMurdo, L., et al., *Biosynthesis of sulfidopeptide leukotrienes via the transfer of leukotriene A4 from polymorphonuclear cells to bovine retinal pericytes.* J Pharmacol Exp Ther, 1998. **285**(3): p. 1255-9.
268. Murrant, C.L. and I.H. Sarelius, *Multiple dilator pathways in skeletal muscle contraction-induced arteriolar dilations.* Am J Physiol Regul Integr Comp Physiol, 2002. **282**(4): p. R969-78.
269. Fujimoto, K., *Pericyte-endothelial gap junctions in developing rat cerebral capillaries: a fine structural study.* Anat Rec, 1995. **242**(4): p. 562-5.
270. Wu, D.M., et al., *Electrotonic transmission within pericyte-containing retinal microvessels.* Microcirculation, 2006. **13**(5): p. 353-63.
271. Yeh, H.I., et al., *Individual gap junction plaques contain multiple connexins in arterial endothelium.* Circ Res, 1998. **83**(12): p. 1248-63.
272. Li, A.F., et al., *High glucose alters connexin 43 expression and gap junction intercellular communication activity in retinal pericytes.* Invest Ophthalmol Vis Sci, 2003. **44**(12): p. 5376-82.
273. Luckhoff, A. and R. Busse, *Calcium influx into endothelial cells and formation of endothelium-derived relaxing factor is controlled by the membrane potential.* Pflugers Arch, 1990. **416**(3): p. 305-11.
274. Gairhe, S., et al., *Myoendothelial gap junctional signaling induces differentiation of pulmonary arterial smooth muscle cells.* Am J Physiol Lung Cell Mol Physiol, 2011. **301**(4): p. L527-35.
275. Sandow, S.L., et al., *Expression of homocellular and heterocellular gap junctions in hamster arterioles and feed arteries.* Cardiovasc Res, 2003. **60**(3): p. 643-53.
276. Valiunas, V., et al., *Connexin-specific cell-to-cell transfer of short interfering RNA by gap junctions.* J Physiol, 2005. **568**(Pt 2): p. 459-68.
277. Mitchell, P.S., et al., *Circulating microRNAs as stable blood-based markers for cancer detection.* Proc Natl Acad Sci U S A, 2008. **105**(30): p. 10513-8.
278. Hammell, C.M., *The microRNA-argonaute complex: a platform for mRNA modulation.* RNA Biol, 2008. **5**(3): p. 123-7.
279. Bail, S., et al., *Differential regulation of microRNA stability.* RNA, 2010. **16**(5): p. 1032-9.
280. Kanaporis, G., et al., *Gap junction channels exhibit connexin-specific permeability to cyclic nucleotides.* J Gen Physiol, 2008. **131**(4): p. 293-305.
281. Heyman, N.S., et al., *Regulation of gap junctional charge selectivity in cells coexpressing connexin 40 and connexin 43.* Am J Physiol Heart Circ Physiol, 2009. **297**(1): p. H450-9.
282. Bevans, C.G., et al., *Isoform composition of connexin channels determines selectivity among second messengers and uncharged molecules.* J Biol Chem, 1998. **273**(5): p. 2808-16.
283. Veenstra, R.D., et al., *Selectivity of connexin-specific gap junctions does not correlate with channel conductance.* Circ Res, 1995. **77**(6): p. 1156-65.
284. Wolvetang, E.J., M.F. Pera, and K.S. Zuckerman, *Gap junction mediated transport of shRNA between human embryonic stem cells.* Biochem Biophys Res Commun, 2007. **363**(3): p. 610-5.

285. Kizana, E., et al., *Gene transfer of connexin43 mutants attenuates coupling in cardiomyocytes: novel basis for modulation of cardiac conduction by gene therapy.* Circ Res, 2007. **100**(11): p. 1597-604.
286. Katakowski, M., et al., *Functional microRNA is transferred between glioma cells.* Cancer Res, 2010. **70**(21): p. 8259-63.
287. Lim, P.K., et al., *Gap junction-mediated import of microRNA from bone marrow stromal cells can elicit cell cycle quiescence in breast cancer cells.* Cancer Res, 2011. **71**(5): p. 1550-60.
288. Pannerec, A., G. Marazzi, and D. Sassoon, *Stem cells in the hood: the skeletal muscle niche.* Trends Mol Med, 2012.